UNIVERSITY OF CALIFORNIA

SANTA CRUZ

ASPECTS OF THE ECOLOGY AND SIGNIFICANCE OF MARINE DIAZOTROPHS

A dissertation submitted in partial satisfaction
of the requirements for the degree of

DOCTOR OF PHILOSOPHY

in

OCEAN SCIENCES

by

Wing Kwan Esther Mak

December 2023

The Dissertation of Wing Kwan Esther Mak is approved:

Professor Jonathan P. Zehr, Chair

Professor Raphael Kudela

Professor David Caron

Professor Eric Webb

Peter Biehl
Vice Provost and Dean of Graduate Studies

Table of Contents

Abstract

Aspects of the Ecology and Significance of Marine Diazotrophs

Wing Kwan Esther Mak

Nitrogen (N_2) fixation is an important component of the nitrogen cycle, supports primary production by supplying biologically available nitrogen, particularly in oligotrophic regions of the world's oceans where nitrogen availability often limits growth. This critical process is mediated by diazotrophs, a diverse group of organisms including both Bacteria and Archaea.

This dissertation focuses on the distribution, activity, and physiology of diazotrophs. It places a particular emphasis on the globally distributed UCYN-A/haptophyte symbiosis, which has been observed in a wide range of environments from the oligotrophic open ocean to coastal regions and colder high-latitude waters. The UCYN-A symbiosis is comprised of the N_2-fixing cyanobacterial symbiont, UCYN-A, and a photosynthetic alga (haptophyte) host, *Braarudosphaera bigelowii*. In the first chapter, the autotrophic and phagotrophic modes of nutrition of the UCYN-A/*B. bigelowii* symbiosis were investigated. The second chapter investigates the range of temperatures in which the UCYN-A/*B. bigelowii* symbiosis can grow and fix carbon and N, with a particular focus on lower temperatures representative of high-latitude waters. Chapter three reports on a study conducted during a winter cruise through the undersampled North Pacific subtropical gyre (NPSG), specifically in the often-overlooked NPSG, which analyzes the environmental

determinants influencing diazotroph distributions and abundances along a transect from Guam to the west coast of California.

In summary, this dissertation illuminates aspects of the physiology of the UCYN-A/*B. bigelowii* symbiosis, specifically its mixotrophic survival strategy and temperature responses. It also provides valuable insights into the biogeographic distributions of a variety of diazotrophs across an undersampled region of the vast Pacific Ocean. Taken together, this dissertation provides new information on the function and role of diazotrophs in open ocean N cycling.

Acknowledgments

I wish to extend my profound gratitude to my supervisor, Jonathan Zehr, for his unwavering support and insightful guidance throughout the six-year voyage of this research. His willingness to take a chance on an overseas candidate has been instrumental in my journey. His patience and dedication in mentoring a non-native English speaker, teaching me how to write, and guiding me on how to approach scientific questions thoughtfully have been invaluable. Jon provided an environment where I could freely explore my interests with guidance, support, and understanding. I am forever grateful for the opportunities I was privileged to experience under his mentorship.

Special thanks are due to Kendra Turk-Kubo, who has always been my go-to person during challenges. I have lost count of how many times I have hurried down the hallway to seek your assistance. Your readiness to help and provide emotional support has been a source of strength for me.

I am also very grateful to the members of my advisory committee, Dave Caron, Eric Webb, and Raphe Kudela, for their insightful critiques and constructive edits on this document.

I acknowledge the generous funding support provided by the Simons Foundation, which has been fundamental to the pursuit of my research.

To my current and former labmates—Katie Harding, Rosie Gradoville, Britt Henke, Tyler Coale, Anna Voznyuk, Ana Cabello, Fran Cornejo, Marine Landa, Rachel Harbeitner, Jonathan Magasin, and many others —thank you for creating a supportive and inspiring environment. The laughter and shared experiences, both on land and at sea, have been some of the most memorable aspects of my time in the lab.

I would like to express my gratitude to my parents for their love, support, and willingness to let me leave home and go to a country 7000 miles away from Hong Kong to embark on this journey. I would also like to thank Kim Kuhry, for opening her home to me for six years and treating me as a family member in Santa Cruz.

This journey has been a testament to the power of collaboration, support, and collective effort, and for this, I am thankful.

Esther Mak

November 3, 2023

Introduction

1. The N cycle and N as a nutrient

Life on Earth is comprised of diverse biomolecules, dominated by large polymeric proteins and nucleic acids. These biological molecules are formed from elements including carbon (C), nitrogen (N), phosphorus (P), oxygen (O), sulfur (S) and hydrogen (H). N is a fundamental component of nucleotides and amino acids, the building blocks of nucleic acids and proteins, respectively. Thus, the availability of N is an essential component necessary for the growth of organisms and thus plays a fundamental role in controlling ecosystem productivity on land and in the oceans.

The N cycle is a complex biogeochemical cycle that encompasses multiple oxidation-reduction chemical reactions that convert N among many different organic and inorganic forms. While the basic framework of the N cycle was outlined by Baas-Becking (1934), the last few decades have unveiled new novel pathways that have changed our understanding of this cycle (Canfield et al., 2010; Thamdrup, 2012)

Since living systems require N, the uptake and assimilation of N is a key flux in terrestrial soils and aquatic environments that incorporates inorganic N into organic forms that are biologically available to animals. Plants fulfill growth requirements by assimilating ammonium (NH_4^+) or nitrate (NO_3^-), converting the N into organic molecules such as the

amino acids and nucleotides that form proteins and nucleic acids. Animals consume plants (or animals) and metabolize the organic N for assimilation and release N, including ammonium and urea, by excretion. Upon the death of organisms, organic N compounds are converted (mineralized) back to ammonia by decomposers, in a process known as ammonification (Strock, 2008). Ammonium and nitrate can be converted to each other by specific pathways. In particular, ammonia can be converted to nitrite (NO_2^-) and subsequently nitrate through processes known as ammonia oxidation and nitrification, and both processes are performed by groups of phylogenetically limited groups of bacteria referred to as ammonia oxidizers and nitrite oxidizers (Ward et al., 2011). While ammonia can be converted to nitrate through nitrification, nitrate can also be reduced to ammonium through the dissimilatory reduction of nitrate to ammonium (DNRA) pathway (Thamdrup, 2012).

Nitrate and ammonium can ultimately be converted back to atmospheric N_2. Under anaerobic conditions, nitrate can be converted to atmospheric N_2 through denitrification, a process executed by a diverse group of largely heterotrophic bacteria (Thamdrup, 2012). and archaea (Offre et al., 2013). Meanwhile, the anammox process (anaerobic ammonium oxidation) is another pathway by which ammonium is oxidized to atmospheric N_2 gas, involving the oxidation of nitrite.

Atmospheric N_2 gas is one of the most abundant forms of N on Earth, which constitutes 78% of air. It is fixed into ammonia (and other inorganic N molecules through chemical or

biological N_2 fixation. This reaction includes the breaking of the stable triple bond within N_2 molecules, demanding a high activation energy (Howard & Rees, 1996; Newton, 2015). While this transformation is achieved chemically through the high-pressure and high-temperature Haber-Bosch process (Leigh, 2002), biologically, it's carried out by diverse specialized groups of bacteria and archaea known as diazotrophs, the N_2-fixers. N_2 fixation plays a crucial role in making the inert atmospheric N_2 bioavailable in ecosystems, and is a fundamental step in the N cycle (Postgate, 1998; Vitousek et al., 2002).

1.1 Biological N_2 fixation

Biological N_2 fixation is the reduction of N_2 to ammonium via the following reaction (Postgate, 1998):

$$N_2 + 8H^+ + 8e^- + 16\ ATP \rightarrow 2\ NH_3 + H_2 + 16\ ADP + 16Pi$$

Diazotrophs convert N_2 to ammonia using the enzyme nitrogenase (Postgate, 1998), which consists of two metalloproteins, each comprised of multiple subunits (Seefeldt et al., 2009). The nitrogenase complex is encoded by the *nif* genes, with the *nifH* gene being essential for the synthesis of the nitrogenase reductase component that is critical for enzymatic activity (Dixon & Kahn, 2004). This energy-expensive process requires 16 ATP per conversion of one N_2 molecule to two ammonia molecules, evolving one H_2 molecule

(Postgate, 1998; Postgate et al., 1982). However, some of the diazotrophs can recover the energy lost by recycling some of the H_2 directly back to the cell, using uptake hydrogenases (Wilson, Foster, et al., 2010; Wilson, Tozzi, et al., 2010).

The nitrogenase enzymes that catalyze N_2 fixation are rapidly and irreversibly inactivated by O_2 (Robson & Postgate, 1980). This is due to the oxidation of the Fe-S clusters in the Fe and MoFe proteins by O_2, which disables electron transfer and effectively inhibits nitrogenase. Paradoxically, while O_2 inhibits nitrogenase, many diazotrophs, especially cyanobacterial diazotrophs, produce O_2 as a byproduct and require it for respiration. Therefore, diazotrophs have developed various strategies to protect nitrogenase from oxidation (Berman-Frank et al., 2003; Inomura et al., 2017; Paerl et al., 2018).

1.2 The N cycle in the ocean

The marine N cycle involves many N reactions and fluxes between the sunlit surface waters (euphotic zone) and the vast stretches of the deep ocean. Within the marine environment, the cycling of N is influenced by both biological and physical processes.

Near the surface, the euphotic zone, where light penetration supports photosynthetic activity, is dominated by phytoplankton. These primary producers, akin to terrestrial plants, assimilate inorganic N forms including ammonium, urea and nitrate (Falkowski et al., 1998; Field et al., 1998). The primary sources of these inorganic N forms are terrestrial inputs,

such as rock weathering and river runoff, which bring N-rich compounds to the ocean. Other sources include N_2 fixation and atmospheric deposition. These inputs vary based on geographical locations.

Phytoplankton assimilate the inorganic N and produce organic matter, but release organic or inorganic N through excretion, lysis by viruses or senescence and during consumption by protist or zooplankton grazing. Subsequent degradation of organic matter mostly releases ammonium and urea from dead cells which are rapidly recycled within the euphotic zone (Ward, 2012; Zehr & Kudela, 2011). Microbial growth in the euphotic zone is largely supported by regenerated production (Dugdale & Goering, 1967).

As detrital particles sink out of the euphotic zone and into the deeper ocean layers, the organic matter contained within it is remineralized and releases ammonium. This ammonium is then oxidized by nitrification, resulting in increasing concentrations of nitrite and nitrate as the water ages (Ward et al., 2011). Due to the accumulation of remineralized N, the deep ocean is a reservoir of bioavailable fixed inorganic N primarily in the form of nitrate (Ward, 2012; Zehr & Kudela, 2011).

Mixing of deep ocean water with surface waters brings the nitrate (ultimately derived from the remineralization of ammonium) back to the surface through upwelling and diffusion. Ekman-driven upwelling, which occurs at specific basin boundaries and the equator, facilitate the vertical movement of deep, nitrate-rich waters to the surface. Additionally,

turbulence and diffusion at the thermocline, the transitional layer between the warmer surface and colder deep waters, also transports nitrate to the sunlit euphotic zone, making it accessible to phytoplankton.

Importantly, in certain regions of the ocean where oxygen is scarce or absent (anoxic conditions), such as oxygen minimum zones (OMZs) and sediments, fixed N removal processes such as denitrification and anammox occur (Offre et al., 2013; Thamdrup, 2012; Van de Graaf et al., 1995). These processes play a crucial role in regulating the marine nitrogen balance by converting fixed N, nitrate, and ammonium back to the atmospheric N_2 pool. DNRA also happens in anoxic environments that convert nitrate to ammonium (Thamdrup, 2012). N can also be lost through burial of organic matter in marine sediments.

The balance between sources and sinks of fixed N is critical in controlling the overall productivity of marine systems (Galloway et al., 2004; Gruber & Galloway, 2008). However, biogeochemical modelers noted an imbalance between global rates of oceanic N_2 fixation and denitrification (Gruber & Sarmiento, 1997; Michaels et al., 1996). Multiple studies to balance the marine N budget have led to varying findings, from a nearly balanced equation to a large N deficit, implying an unknown source of N_2 fixation, or underestimates of the rates of biological N_2 fixation (Codispoti, 2007; Galloway et al., 2004). Given the uncertainties, it is not clear that there is an imbalance in the N budget (Zehr & Capone, 2023).

1.3 N limitation in the open ocean

The vast expanse of the oceans, covering three-quarters of the Earth's surface, accounts for half of the photosynthetic carbon fixation on Earth, thereby playing a significant role in global carbon cycling and controlling greenhouse gases (Falkowski et al., 1998; Field et al., 1998). In many marine environments, especially the oligotrophic (nutrient-poor) regions, N is often a limiting nutrient for growth and productivity making the role of diazotrophs paramount in fueling primary productivity by contributing to the bioavailable N pool (Moore et al., 2013).

In the open ocean, stratification in the subtropics and tropics hinders vertical mixing and coupled with phytoplankton N uptake, results in low concentrations of bioavailable N at the surface. The presence of light and warm temperatures in these regions facilitates photosynthesis and growth of primary producers, who rapidly uptake and regenerate N (Dugdale & Goering, 1967). Therefore, N_2 fixation is particularly important for primary production in these oligotrophic gyres. In these regions, N_2 fixation can support up to 50% of net community production (Böttjer et al., 2017; Capone et al., 2005; Jickells et al., 2017; Karl et al., 1997).

The distribution and diversity of diazotrophs underscore their fundamental role in marine biogeochemical cycles, hinting at a broader impact on marine productivity under varying environmental conditions. Consequently, a comprehensive understanding of diazotroph

distribution, diversity, and function is indispensable for predicting how marine biogeochemical cycles and productivity may respond to changing environmental conditions.

2. Diversity of diazotrophs and their functional significance

All known diazotrophs catalyze N_2 fixation with the enzyme nitrogenase, but marine diazotroph assemblages are marked by a diversity of morphologies and lifestyles, with members ranging from free-living unicellular bacteria and filamentous species to those forming symbiotic relationships with eukaryotic phytoplankton. Early studies of marine diazotrophs predominantly utilized light or epifluorescence microscopy to visualize cyanobacterial diazotrophs, documenting the conspicuous organisms *Trichodesmium* (Ohki & Fujita, 1988) and diatom-diazotroph associations (DDAs), which encompass multiple symbiotic associations between several diatom genera and N_2-fixing bacteria.

Trichodesmium, a filamentous cyanobacterium, is a diazotroph that consists of multicellular filaments or trichomes that can form large aggregates (Webb et al., 2022). It contains gas vesicles for buoyancy (ref) and can form extensive blooms observable from space (Carpenter & Capone, 1992). Symbiotic relationships between specific types of diatoms and diazotrophic cyanobacteria are also common (DDAs), and can also form blooms in warm oligotrophic oceans (Carpenter et al., 1999). Examples include the *Richelia* (Foster et al., 2022), found as symbionts of diatoms like *Hemiaulus* spp. and

Rhizosolenia spp. *Calothrix* spp. are also observed in epiphytic symbiosis with diatoms in the *Chaetoceros* genus (Carpenter et al., 1999). *Trichodesmium* and DDAs were long considered to be the key players in marine N_2 fixation, especially in the oligotrophic oceans.

Additionally, the development and application of molecular techniques such as the polymerase chain reaction (PCR) and DNA sequencing have improved our understanding of diazotroph diversity, since they revealed microorganisms not readily visible under the microscope. Since diazotrophs share the structurally conserved nitrogenase protein encoded by the *nif* genes, primers could be designed to amplify and sequence the *nifH* gene, which encodes the identical subunits of the nitrogenase Fe protein (Zehr et al., 1998). This technique led to the discovery of new diazotrophs, their genetic diversity and their biogeographical distributions. In particular, the discovery of unicellular cyanobacterial diazotrophs, such as UCYN-A (Unicellular cyanobacteria group A), and UCYN-B (Unicellular cyanobacteria group B or *Crocosphaera watsonii*) by Zehr et al., (1998) led to the observation that they are more widely distributed than *Trichodesmium* and the DDAs (Moisander et al., 2010). This technique also led to the discovery of non-cyanobacterial diazotrophs, broadening our understanding of diversity beyond the phylum Cyanobacteria (Turk-Kubo et al., 2022; Zehr et al., 1998).

Although the unicellular UCYN-A and UCYN-B were both reported in the study by Zehr et al. (1998), they were ultimately found to be morphologically distinct. UCYN-A (*Candidatus* Atelocyanobacterium thalassa) is a unicellular cyanobacterium that lacks the

ability to fix carbon and forms a symbiotic relationship with haptophyte algae closely related to *B. bigelowii* and relatives (Thompson et al., 2014; Thompson et al., 2012). The symbiotic relationship between UCYN-A and its haptophyte host is based on their exchange of C and N (Thompson and Foster et al., 2012). On the other hand, UCYN-B, although discovered and isolated in the 1980s, was not widely appreciated until the discovery of its *nif* gene sequences (Zehr et al., 2007; Zehr et al., 2001). *C. watsonii* inhabits warm waters with temperatures between 26-30°C (Moisander et al., 2010), thus confining its distribution to oligotrophic subtropical regions. In the North Pacific Subtropical Gyre, it can reach cell numbers up to 10^7 *nifH* copies L^{-1} (Church et al., 2009; Zhang et al., 2019) and can form seasonal blooms in the late summer. *Crocosphaera* was found to contribute approximately 11% of the export production in the North Pacific Subtropical Gyre (Wilson et al., 2017).

Beyond these unicellular cyanobacterial diazotrophs (UCYN-A and UCYN-B), diverse non-cyanobacterial diazotrophs (NCDs) were found in *nifH* studies (Farnelid et al., 2011; Zehr et al., 1998). Little is known about the NCDs since there are few cultivated marine NCDs and they are largely known from DNA sequences (Bombar et al., 2016; Riemann et al., 2010). It is speculated that they may inhabit many different microniches, and have diverse physiologies, including free-living, particle-associated, or even forming symbiotic relationships (Turk-Kubo et al., 2022). The contribution of N_2 fixation has been conventionally thought to be by cyanobacterial diazotrophs, but NCD sequences have been widely reported. For example, the NCD gamma A is a γ-proteobacterium that is widespread

in tropical and subtropical surface water and is transcriptionally active (Langlois et al., 2015). Thus, the overall contribution of NCDs to nitrogen fixation in the ocean is still poorly characterized.

The application of *nifH* PCR amplification techniques expanded our understanding of the biogeography of diazotrophs. Although *Trichodesmium*, *Crocosphaera*, and DDAs were initially found in oligotrophic gyres and tropical waters, the UCYN-A symbiosis and NCDs are more widely distributed and have been recovered in regions including the open ocean, but also temperate coastal systems and polar regions (Shao et al., 2023; Turk-Kubo et al., 2022). One of the key subjects of this thesis, UCYN-A, plays a substantial role in contributing fixed N_2 to marine environments in a variety of locations and different conditions (as reported by (Church et al., 2009; Goebel et al., 2007; Martínez-Pérez et al., 2016; Montoya et al., 2004; Turk et al., 2011). UCYN-A has also been observed to be as abundant or even more abundant than other cyanobacterial diazotrophs in tropical or subtropical oceans (Foster et al., 2007; Kong et al., 2011), and is also globally abundant in coastal regions (Cabello et al., 2020; Mulholland et al., 2012; Turk-Kubo et al., 2021) and cold, high-latitude water such as the Arctic (Harding et al., 2018; Shiozaki et al., 2020). Since UCYN-A is so important as a marine diazotroph, it is crucial to study the physiology of this diazotroph.

3. Unique nature of UCYN-A and its physiology

UCYN-A (*Candidatus* Atelocyanobacterium thalassa) is an unusual unicellular cyanobacterium.

UCYN-A has a small (1.44-1.49 Mb) metabolically reduced genome that lacks many major pathways (Bombar et al., 2014; Tripp et al., 2010). For example, it is not able to fix carbon, since it lacks the carbon-fixing RubisCO, and also lacks genes for photosystem II and thus cannot perform oxygenic photosynthesis. Other metabolic pathways are also absent including the entire tricarboxylic acid (TCA) cycle. The symbiotic relationship between UCYN-A and its haptophyte host hinges on the exchange of fixed C (from the haptophyte) and fixed N (from UCYN-A) (Tripp et al., 2010; Zehr et al., 2017) but likely includes other metabolic interdependencies (Sarkar et al., 2021).

There are multiple sublineages of UCYN-A. Phylogenetic examination of UCYN-A *nifH* gene sequences has led to the classification of at least six sublineages, several of which have been demonstrated to associate with distinct, but closely related hosts of differing sizes, occupying diverse geographic regions (Bombar et al., 2014; Farnelid et al., 2016; Turk-Kubo et al., 2017). UCYN-A1 is the smallest sublineage and populates the open ocean (ca. 2 µm, Thompson et al. (2014)). In contrast, UCYN-A2, which is larger than UCYN-A1 (ca. 5 µm), is also associated with a larger haptophyte host, *B. bigelowii* (Hagino et al., 2013) and is more abundant in coastal waters (Turk-Kubo et al., 2017). UCYN-A1 has yet to be cultivated since its discovery through nitrogenase gene amplification. Only recently the coastal UCYN-A2/*B. bigelowii* symbiosis has been successfully maintained in unialgal culture. This advancement opened new avenues for

determining the biological characteristics using laboratory techniques not previously possible to apply to uncultivated natural populations.

The UCYN-A2 host, *B. bigelowii* has two flagella and a haptonema - a thread-like organelle capable of capturing and transporting food particles (Hagino et al., 2013; Kawachi et al., 1991). Haptophytes have been documented as bacterial grazers, accounting for 9-27% of bacterivory in ecosystems such as a coastal Mediterranean site (Unrein et al., 2014). Furthermore, the potential phagotrophic activity of *B. bigelowii* has been implicated by various studies. For instance, an experiment introducing ^{13}C-labeled *Synechococcus* and *Prochlorococcus* to a microbial community at Station ALOHA recovered sequences of both UCYN-A1 and UCYN-A2 hosts through DNA stable isotope probing (DNA-SIP), indicating possible grazing on the labeled cyanobacteria (Frias-Lopez et al., 2009). Krupke et al. (2015) further provided putative evidence of the phagotrophic nature of UCYN-A1 host cells by observing an unidentified structure, potentially a consumed prey organism, within the UCYN-A1 host cell using nanoscale secondary ion mass spectrometry (nanoSIMS). Despite these findings, the specific extent and role of phagotrophy in *B. bigelowii* remains enigmatic. **Chapter 1** aimed to illuminate the phagotrophic capabilities of *B. bigelowii*, aiming to determine if *B. bigelowii* was phagotrophic and the degree to which its phagotrophy contributes to its nutrition.

4. Environmental controls on diazotroph physiology and distribution

4.1 Nutrient availability

Nitrogen (N), phosphorus (P), and iron (Fe) are significant nutrients in marine ecosystems often limiting primary productivity as well as diazotrophy (Falkowski et al., 1998). Although N is often the limiting nutrient in the ocean, P is also a crucial factor in determining diazotroph abundances and activity (Sañudo-Wilhelmy et al., 2001). Not only is P a component of essential biomolecules, such as nucleic acids (DNA and RNA) and phospholipids that constitute cell membranes, diazotrophs are thought to have an elevated requirement for phosphorus as N_2 fixation requires a significant amount of ATP, which contains phosphorus (Postgate et al., 1982). Thus diazotrophs may be at a competitive advantage for available P compared to their non-diazotrophic counterparts (Ward et al., 2013).

Dissolved inorganic P is a source of P; however, since its concentrations vary significantly in the ocean (Björkman & Karl, 2003), diazotrophs have adopted various strategies, including high-affinity scavenging for extracellular inorganic phosphate, utilizing organic P compounds, and lowering cellular P requirement by element substitution (Dyhrman & Haley, 2006b; Pereira et al., 2019; Van Mooy et al., 2009). While *Trichodesmium* can harness both phosphonates and phosphoesters (Dyhrman et al., 2006), *Crocosphaera* restricts its metabolism to phosphoesters (Dyhrman & Haley, 2006a). Little is known about

the UCYN-A symbiosis organic P-metabolism; genomic analysis hints at the symbiont's inability to utilize organic P compounds (Tripp et al., 2010).

Fe is important for primary producers (Behrenfeld & Kolber, 1999) but is particularly important for diazotrophs since the nitrogenase enzyme contains 38 Fe atoms per enzyme complex (Whittaker et al., 2011). Fe is required in the photosynthetic process in the electron transport chain ferredoxin, cytochromes, and both photosystems I and II for photosynthetic cyanobacterial diazotrophs. Although Fe input in the ocean includes atmospheric dust, upwelling, fluvial inputs, and hydrothermal vents, it is often considered limiting due to the low solubility of Fe in oxygenated seawater (Liu & Millero, 2002). Diazotrophs have evolved mechanisms to address Fe-limitation. For example, *Crocosphaera* allocates Fe between photosystems and nitrogenase in response to the diel cycle, underscoring the intricate adaptations diazotrophs have evolved to navigate the challenges posed by Fe availability (Saito et al., 2011).

The interactions of N, P, and Fe are important in influencing the growth and activity of diazotrophs, with their collective influence transcending the impact of a single nutrient factor. The concept of nutrient colimitation is where the growth of organism, such as diazotrophs is regulated by the interplay of multiple nutrients (Mills et al., 2004). For example, according to the Redfield ratio, marine phytoplankton require N and P in a specific ratio to fulfill their cellular requirements. This principle lays the groundwork for understanding how the ratio of N:P available in the ocean, coupled with their absolute

concentrations, can influence the distribution of N_2-fixers (Ward et al., 2013). Building on this, the resource ratio theory suggests that organisms best suited to a particular N:P ratio may have survival advantages over others, providing a lens through which to predict the distribution of diazotrophs across varying marine environments. Beyond the N and P dynamic, the interaction of Fe with P is noteworthy. Contrary to a direct alleviation of P limitation by Fe, Fe-deficient conditions can prompt diazotrophs to utilize P more efficiently due to diminished cellular P quotas. This phenomenon can be observed in some marine diazotrophs, further underscoring the nuanced nutrient interplay influencing diazotroph distribution (Garcia et al., 2015). This complex interplay of N, P, and Fe, and its impact on diazotroph ecology needs further exploration through empirical observations and modeling studies to bridge the gap between theoretical predictions and real-world observations, aiming for a more holistic understanding of diazotroph ecology in the marine nutrient landscape.

4.2 Light dependency

Light can play a crucial role in N_2 fixation by using light energy to provide photosynthate, ATP, and reductant. This process is critical for most cyanobacterial diazotrophs, which require direct light energy for N_2 fixation. In the oligotrophic open ocean, there is sufficient energy for photosynthesis to depths of greater than 100-150 m, either available directly (harvested by cyanobacteria) or indirectly (heterotrophs fed by photosynthate). However,

despite the known significance of light, the specific depth profiles of N_2 fixation for different cyanobacteria are not yet well-understood (Church et al., 2009).

Also, some non-cyanobacterial diazotrophs may depend on light energy indirectly. Although some of these microorganisms may utilize mechanisms such as rhodopsin or bacteriochlorophyll-based energy generation from light, others may rely on photosynthate derived from a photoautotroph (Benavides et al., 2018).

4.3 Oxygen sensitivity

N_2 fixation is highly sensitive to inhibition by O_2 (Robson & Postgate, 1980). However, diazotrophs also need oxygen for cellular respiration to obtain energy, and cyanobacterial diazotrophs generate O_2 as a byproduct. Thus, diazotrophs must maintain a delicate balance of intracellular oxygen concentration to support these processes. To avoid the inactivation of nitrogenase by O_2, diazotrophs have evolved different strategies to segregate N_2 fixation from O_2 in space, time, or a combination of both (Fay, 1992).

Lowering the intracellular O_2 concentration allows N_2 fixation to proceed while preserving sufficient O_2 levels to sustain energy generation through respiration (Bergman et al., 1997; Fay, 1992; Gallon, 1992). Some cyanobacterial diazotrophs employ a temporal segregation strategy by separating photosynthesis (an O_2-producing process) and N_2 fixation (an oxygen-sensitive process) activities, such as in the unicellular cyanobacterial diazotrophs

Crocosphaera and *Cyanothece*, as these organisms fix N_2 at night and perform photosynthesis during the day, following a diel cycle (Colón-López et al., 1997; Shi et al., 2010). This approach helps them counteract the problem of O_2 inactivation while still enabling them to use the fixed carbon from photosynthesis to fuel their nighttime nitrogen fixation.

The UCYN-A symbiosis can fix N_2 during the day because they have lost the genes for photosystem II (PSII) and, therefore, do not evolve O_2 during the day. However, none of these strategies would prevent ambient O_2 from diffusing across membranes in a fully oxic environment such as the photic ocean. A recent study pointed out the presence of a class of lipids, called hopanoids, in the membranes of non-heterocyst-forming cyanobacterial diazotrophs that might act as O_2 diffusion barriers to regulate the oxygen that could enter the intracellular space from the environment (Cornejo-Castillo & Zehr, 2019). Therefore, this mechanism could control the O_2 concentration in the intracellular environment of N_2-fixing cyanobacteria to avoid the inactivation of nitrogenase enzymes (Cornejo-Castillo & Zehr, 2019).

4.4 Temperature influence

Temperature regulates the enzymatic activity of nitrogenase by dictating the rates of molecular reactions and interactions. Moreover, temperature also impacts O_2 gas solubility.

In particular, O_2 gas solubility is depressed above a water temperature of 25°C, conferring an advantage to certain diazotrophs living in warmer waters (Stal, 2009).

Despite diazotrophs all containing nitrogenase, they may occupy different thermal niches due to their varying physiologies. Both *Trichodesmium* and *Crocosphaera* inhabit tropical and subtropical regions. *Trichodesmium* has been observed to thrive at temperatures ranging from 20-35°C, with an optimum at 26-27°C (Boyd et al., 2013; Breitbarth et al., 2007; Fu et al., 2014). Similarly, *Crocosphaera* exhibits a narrower thermal range than *Trichodesmium*, from 24-32°C, with an optimum at approximately 30°C (Fu et al., 2014; Webb et al., 2009). *Cyanothece* sp. BG043511 demonstrated growth in a laboratory study within the range of 14-38°C, and the peak nitrogen fixation rates were documented at around 30°C (Brauer et al., 2013).

The thermal niche for UCYN-A has been more challenging to decipher since it has remained uncultured until very recently. Nonetheless, field surveys have offered insights into its temperature responses. Moisander et al. (2010) and Tang and Cassar (2019) proposed a polynomial model for UCYN-A against temperature, indicating an increasing abundance with temperature until approximately 24°C, followed by a decrease at higher temperatures, with a sudden drop-off at 30°C. With UCYN-A found in colder, high-latitude waters (such as the Arctic Ocean, Antarctic Ocean, and Danish Straits (Bentzon-Tilia et al., 2015; Harding et al., 2018; Shiozaki et al., 2020) and coastal regions, its growth temperature range is hypothesized to be broader than that of other N_2 fixers, yet information

about the thermal niche of UCYN-A is still lacking. The thermal niche of diazotrophs is important for parameterizing biogeochemical ocean models, such as the ECCO-Darwin model (Carroll et al., 2020). In **Chapter 2**, this is addressed by investigating the temperature range of the UCYN-A2/*B. bigelowii* culture, including at low temperatures such as 6°C.

5. Need for study on diazotrophs in understudied regions

The expansive central ocean gyres in the tropics and subtropics, across the Pacific, Atlantic, and Indian oceans, have been recognized as diazotroph habitats, because of the characteristically low fixed N concentrations. Within the North Pacific subtropical gyre (NPSG), insights into N_2 fixation originate primarily from Station ALOHA and its surrounding waters (Böttjer et al., 2017; Turk-Kubo et al., 2023). Nonetheless, the inferences drawn from a single station does not encapsulate the complexity of the NPSG, given its variance of biogeochemical provinces, each showing different hydrological properties and phytoplanktonic composition (Hofmann Elizondo et al., 2021; Kavanaugh et al., 2014; Reygondeau et al., 2013).

Beyond Station ALOHA, diazotroph distributions have been observed to extend into the western Pacific and Kuroshio current region (Cheung et al., 2017; Shiozaki et al., 2018), throughout the gyre (Church et al., 2008; Kitajima et al., 2009) and to the transition zone (Gradoville et al., 2020; Shiozaki et al., 2017). A recently published diazotroph database

underscores the spatial knowledge gap in the western NPSG, particularly in remote open ocean expanses beyond the Kuroshio regions and the western Pacific close to land (Shao et al., 2023). This region, a likely diazotroph environment, has only been sampled with a few data points, which limits accuracy when attempting to formulate N budgets and modeling efforts. The limited sampling in such regions generally hampers our comprehensive understanding of biogeochemical processes.

In addition to relatively sparse datasets, the existing data is biased towards spring and summer seasons, obscuring our comprehension of N_2 fixation patterns and diazotroph abundances during winter months. While summer-orientated studies at Station ALOHA showed elevated N_2 fixation rates (Böttjer et al., 2017; Dore et al., 2002; Turk-Kubo et al., 2023), extrapolating these findings to the expansive and varied NPSG, particularly through winter, is speculative. This underscores a pronounced knowledge gap concerning spatial-temporal dynamics across the basin, including the transition zones and the notably underexplored western Pacific region. In **Chapter 3**, we describe diazotroph abundances and activities along a transect from Guam to San Francisco in the winter season and across the undersampled western Pacific, passing through different regions with distinct biogeochemical characteristics, significantly contributing to filling the existing data gap in the western NPSG.

6. Aims of the thesis

This thesis aims to investigate the distribution, activity, and physiology of unicellular cyanobacterial diazotrophs. The first two chapters focus on the globally prevalent UCYN-A/*B. bigelowii* symbiosis.

In Chapter 1, the potential mixotrophic lifestyle of the UCYN-A/*B. bigelowii* symbiosis is investigated using experiments designed to ascertain their phagotrophic activity.

In Chapter 2, the physiology of the UCYN-A/*B. bigelowii* symbiosis is investigated under various temperatures, since temperature is a major factor controlling the growth of microorganisms. This chapter details the diazotroph's growth and activity responses to an array of temperatures, including those in colder environments where other typical marine diazotrophs are absent.

In Chapter 3, the distribution and activity of diazotrophs in the undersampled region of the low-latitude North Pacific subtropical gyre is described during the winter season. This chapter shows the transition of the diazotroph assemblages across several oceanic regions and crossing gradients in environmental conditions.

To conclude, this thesis broadens our understanding of the UCYN-A/B. bigelowii symbiosis by providing critical physiological measurements and revealing important

aspects of its nutritional mode. This research not only clarifies the nuances of individual diazotrophs but also aligns with a more expansive scientific goal. The oceanographic survey of the under-researched North Pacific bestows new measurements and insights regarding the diazotroph assemblies and their activity rates across different biogeochemical zones. Recognizing that N often limits primary productivity in vast oceanic regions, these investigations offer a newfound understanding into the biology of the globally widespread UCYN-A/B. bigelowii symbiosis under varying conditions and its change in growth activities in specific areas and future climate scenarios. By enhancing our knowledge of diazotrophs and the marine N cycle, we are better positioned to fine-tune N budget assessments, optimize modeling efforts, and anticipate climate-driven shifts within these systems.

References

Baas-Becking, L. (1934). Geobiologie of inleiding tot de milieukunde. WP van Stockum and Zoon NV, The Hague, The Netherlands. *Cited from*, 14-24.

Behrenfeld, M. J., & Kolber, Z. S. (1999). Widespread Iron Limitation of Phytoplankton in the South Pacific Ocean. *science*, *283*(5403), 840-843. https://doi.org/doi:10.1126/science.283.5403.840

Benavides, M., Shoemaker, K. M., Moisander, P. H., Niggemann, J., Dittmar, T., Duhamel, S., Grosso, O., Pujo-Pay, M., Hélias-Nunige, S., Fumenia, A., & Bonnet, S. (2018). Aphotic N_2 fixation along an oligotrophic to ultraoligotrophic transect in the western tropical South Pacific Ocean. *Biogeosciences*, *15*(10), 3107-3119. https://doi.org/10.5194/bg-15-3107-2018

Bentzon-Tilia, M., Traving, S. J., Mantikci, M., Knudsen-Leerbeck, H., Hansen, J. L. S., Markager, S., & Riemann, L. (2015). Significant N_2 fixation by heterotrophs, photoheterotrophs and heterocystous cyanobacteria in two temperate estuaries. *The ISME Journal*, *9*(2), 273-285.

Bergman, B., Gallon, J. R., Rai, A. N., & Stal, L. J. (1997). N2 Fixation by non-heterocystous cyanobacteria. *FEMS Microbiology Reviews*, *19*(3), 139-185. https://doi.org/https://doi.org/10.1016/S0168-6445(96)00028-9

Berman-Frank, I., Lundgren, P., & Falkowski, P. (2003). Nitrogen fixation and photosynthetic oxygen evolution in cyanobacteria. *Research in microbiology*, *154*(3), 157-164.

Björkman, K. M., & Karl, D. M. (2003). Bioavailability of dissolved organic phosphorus in the euphotic zone at Station ALOHA, North Pacific Subtropical Gyre. *Limnology and Oceanography*, *48*(3), 1049-1057. https://doi.org/https://doi.org/10.4319/lo.2003.48.3.1049

Bombar, D., Heller, P., Sanchez-Baracaldo, P., Carter, B. J., & Zehr, J. P. (2014). Comparative genomics reveals surprising divergence of two closely related strains of uncultivated UCYN-A cyanobacteria. *8*(12), 2530-2542. https://doi.org/10.1038/ismej.2014.167

Bombar, D., Paerl, R. W., & Riemann, L. (2016). Marine non-cyanobacterial diazotrophs: moving beyond molecular detection. *Trends in Microbiology*, *24*(11), 916-927.

Böttjer, D., Dore, J. E., Karl, D. M., Letelier, R. M., Mahaffey, C., Wilson, S. T., Zehr, J., & Church, M. J. (2017). Temporal variability of nitrogen fixation and particulate nitrogen export at Station ALOHA. *Limnology and Oceanography*, *62*(1), 200-216. https://doi.org/10.1002/lno.10386

Boyd, P. W., Rynearson, T. A., Armstrong, E. A., Fu, F., Hayashi, K., Hu, Z., Hutchins, D. A., Kudela, R. M., Litchman, E., & Mulholland, M. R. (2013). Marine phytoplankton temperature versus growth responses from polar to tropical waters–outcome of a scientific community-wide study. *PLoS ONE*, *8*(5), e63091.

Brauer, V. S., Stomp, M., Rosso, C., van Beusekom, S. A., Emmerich, B., Stal, L. J., & Huisman, J. (2013). Low temperature delays timing and enhances the cost of nitrogen fixation in the unicellular cyanobacterium *Cyanothece*. *The ISME journal*, *7*(11), 2105-2115.

Breitbarth, E., Oschlies, A., & LaRoche, J. (2007). Physiological constraints on the global distribution of *Trichodesmium* effect of temperature on diazotrophy. *Biogeosciences*, *4*(1), 53-61. https://doi.org/10.5194/bg-4-53-2007

Cabello, A. M., Turk-Kubo, K. A., Hayashi, K., Jacobs, L., Kudela, R. M., & Zehr, J. P. (2020). Unexpected presence of the nitrogen-fixing symbiotic cyanobacterium UCYN-A in Monterey Bay, California. *J Phycol*, *56*(6), 1521-1533. https://doi.org/10.1111/jpy.13045

Canfield, D. E., Glazer, A. N., & Falkowski, P. G. (2010). The Evolution and Future of Earth's Nitrogen Cycle. *Science*, *330*(6001), 192-196. https://doi.org/doi:10.1126/science.1186120

Capone, D. G., Burns, J. A., Montoya, J. P., Subramaniam, A., Mahaffey, C., Gunderson, T., Michaels, A. F., & Carpenter, E. J. (2005). Nitrogen fixation by *Trichodesmium* spp.: An important source of new nitrogen to the tropical and subtropical North Atlantic Ocean. *Global Biogeochemical Cycles*, *19*(2), n/a-n/a. https://doi.org/10.1029/2004gb002331

Carpenter, E. J., & Capone, D. G. (1992). Nitrogen fixation in *Trichodesmium* blooms. In *Marine pelagic cyanobacteria: Trichodesmium and other diazotrophs* (pp. 211-217). Springer.

Carpenter, E. J., Montoya, J. P., Burns, J., Mulholland, M. R., Subramaniam, A., & Capone, D. G. (1999). Extensive bloom of a N_2-fixing diatom/cyanobacterial association in the tropical Atlantic Ocean. *Marine Ecology Progress Series*, *185*, 273-283.

Carroll, D., Menemenlis, D., Adkins, J., Bowman, K., Brix, H., Dutkiewicz, S., Fenty, I., Gierach, M., Hill, C., & Jahn, O. (2020). The ECCO-Darwin data-assimilative global ocean biogeochemistry model: Estimates of seasonal to multidecadal surface ocean pCO_2 and air-sea CO2 flux. *Journal of Advances in Modeling Earth Systems*, *12*(10), e2019MS001888.

Cheung, S., Suzuki, K., Saito, H., Umezawa, Y., Xia, X., & Liu, H. (2017). Highly heterogeneous diazotroph communities in the Kuroshio Current and the Tokara Strait, Japan. *PLoS ONE*, *12*(10), e0186875.

Church, M. J., Björkman, K. M., Karl, D. M., Saito, M. A., & Zehr, J. P. (2008). Regional distributions of nitrogen-fixing bacteria in the Pacific Ocean. *Limnology and Oceanography*, *53*(1), 63-77. https://doi.org/https://doi.org/10.4319/lo.2008.53.1.0063

Church, M. J., Mahaffey, C., Letelier, R. M., Lukas, R., Zehr, J. P., & Karl, D. M. (2009). Physical forcing of nitrogen fixation and diazotroph community structure in the North Pacific subtropical gyre. *23*(2), n/a-n/a. https://doi.org/10.1029/2008gb003418

Codispoti, L. (2007). An oceanic fixed nitrogen sink exceeding 400 Tg N a^{-1} vs the concept of homeostasis in the fixed-nitrogen inventory. *Biogeosciences*, *4*(2), 233-253.

Colón-López, M. S., Sherman, D. M., & Sherman, L. A. (1997). Transcriptional and translational regulation of nitrogenase in light-dark-and continuous-light-grown cultures of the unicellular cyanobacterium *Cyanothece* sp. strain ATCC 51142. *Journal of Bacteriology*, *179*(13), 4319-4327.

Cornejo-Castillo, F. M., & Zehr, J. P. (2019). Hopanoid lipids may facilitate aerobic nitrogen fixation in the ocean. *Proc Natl Acad Sci U S A*, *116*(37), 18269-18271. https://doi.org/10.1073/pnas.1908165116

Dixon, R., & Kahn, D. (2004). Genetic regulation of biological nitrogen fixation. *Nat Rev Microbiol*, *2*(8), 621-631. https://doi.org/10.1038/nrmicro954

Dore, J. E., Brum, J. R., Tupas, L. M., & Karl, D. M. (2002). Seasonal and interannual variability in sources of nitrogen supporting export in the oligotrophic subtropical North Pacific Ocean. *Limnology and Oceanography*, *47*(6), 1595-1607. https://doi.org/https://doi.org/10.4319/lo.2002.47.6.1595

Dugdale, R. C., & Goering, J. J. (1967). Uptake of new and regenerated forms of nitrogen in primary productivity. *Limnology and Oceanography*, *12*(2), 196-206. https://doi.org/https://doi.org/10.4319/lo.1967.12.2.0196

Dyhrman, S. T., Chappell, P. D., Haley, S. T., Moffett, J. W., Orchard, E. D., Waterbury, J. B., & Webb, E. A. (2006). Phosphonate utilization by the globally important marine diazotroph *Trichodesmium*. *Nature*, *439*(7072), 68-71. https://doi.org/10.1038/nature04203

Dyhrman, S. T., & Haley, S. T. (2006a). Phosphorus scavenging in the unicellular marine diazotroph *Crocosphaera watsonii*. *Appl Environ Microbiol*, *72*(2), 1452-1458. https://doi.org/10.1128/aem.72.2.1452-1458.2006

Dyhrman, S. T., & Haley, S. T. (2006b). Phosphorus Scavenging in the Unicellular Marine Diazotroph *Crocosphaera watsonii*. *Applied and Environmental Microbiology*, *72*(2), 1452-1458. https://doi.org/10.1128/aem.72.2.1452-1458.2006

Falkowski, Barber, R. T., & Smetacek, V. (1998). Biogeochemical Controls and Feedbacks on Ocean Primary Production. *Science*, *281*(5374), 200-206. https://doi.org/doi:10.1126/science.281.5374.200

Farnelid, H., Andersson, A. F., Bertilsson, S., Al-Soud, W. A., Hansen, L. H., Sørensen, S., Steward, G. F., Hagström, Å., & Riemann, L. (2011). Nitrogenase gene amplicons from global marine surface waters are dominated by genes of non-cyanobacteria. *PLoS ONE*, *6*(4), e19223.

Farnelid, H., Turk-Kubo, K., Muñoz-Marín, M., & Zehr, J. (2016). New insights into the ecology of the globally significant uncultured nitrogen-fixing symbiont UCYN-A. *Aquatic Microbial Ecology*, *77*(3), 125-138. https://doi.org/10.3354/ame01794

Fay, P. (1992). Oxygen relations of nitrogen fixation in cyanobacteria. *Microbiol Rev*, *56*(2), 340-373. https://doi.org/10.1128/mr.56.2.340-373.1992

Field, C. B., Behrenfeld, M. J., Randerson, J. T., & Falkowski, P. (1998). Primary Production of the Biosphere: Integrating Terrestrial and Oceanic Components. *Science*, *281*(5374), 237-240. https://doi.org/doi:10.1126/science.281.5374.237

Foster, R. A., Subramaniam, A., Mahaffey, C., Carpenter, E. J., Capone, D. G., & Zehr, J. P. (2007). Influence of the Amazon River plume on distributions of free-living and symbiotic cyanobacteria in the western tropical north Atlantic Ocean. *Limnology and Oceanography*, *52*(2), 517-532. https://doi.org/https://doi.org/10.4319/lo.2007.52.2.0517

Foster, R. A., Villareal, T. A., Lundin, D., Waterbury, J. B., Webb, E. A., & Zehr, J. P. (2022). *Richelia*. In *Bergey's Manual of Systematics of Archaea and Bacteria* (pp. 1-17). https://doi.org/https://doi.org/10.1002/9781118960608.gbm01520

Frias-Lopez, J., Thompson, A., Waldbauer, J., & Chisholm, S. W. (2009). Use of stable isotope-labelled cells to identify active grazers of picocyanobacteria in ocean surface waters. *Environmental Microbiology*, *11*(2), 512-525.

Fu, F.-X., Yu, E., Garcia, N. S., Gale, J., Luo, Y., Webb, E. A., & Hutchins, D. A. (2014). Differing responses of marine N_2 fixers to warming and consequences for future diazotroph community structure. *Aquatic Microbial Ecology*, *72*(1), 33-46.

Gallon, J. (1992). Reconciling the incompatible: nitrogen fixation and oxygen. *New phytologist*, *122*, 571-609.

Galloway, J. N., Dentener, F. J., Capone, D. G., Boyer, E. W., Howarth, R. W., Seitzinger, S. P., Asner, G. P., Cleveland, C. C., Green, P., & Holland, E. A. (2004). Nitrogen cycles: past, present, and future. *Biogeochemistry*, *70*, 153-226.

Garcia, N. S., Fu, F., Sedwick, P. N., & Hutchins, D. A. (2015). Iron deficiency increases growth and nitrogen-fixation rates of phosphorus-deficient marine cyanobacteria. *ISME j*, *9*(1), 238-245. https://doi.org/10.1038/ismej.2014.104

Goebel, N. L., Edwards, C. A., Church, M. J., & Zehr, J. P. (2007). Modeled contributions of three types of diazotrophs to nitrogen fixation at Station ALOHA. *The ISME journal*, *1*(7), 606-619. https://doi.org/10.1038/ismej.2007.80

Gradoville, M. R., Farnelid, H., White, A. E., Turk-Kubo, K. A., Stewart, B., Ribalet, F., Ferrón, S., Pinedo-Gonzalez, P., Armbrust, E. V., Karl, D. M., John, S., & Zehr, J.

P. (2020). Latitudinal constraints on the abundance and activity of the cyanobacterium UCYN-A and other marine diazotrophs in the North Pacific. *Limnology and Oceanography*. https://doi.org/10.1002/lno.11423

Gruber, N., & Galloway, J. N. (2008). An Earth-system perspective of the global nitrogen cycle. *Nature*, *451*(7176), 293-296. https://doi.org/10.1038/nature06592

Gruber, N., & Sarmiento, J. L. (1997). Global patterns of marine nitrogen fixation and denitrification. *Global Biogeochemical Cycles*, *11*(2), 235-266. https://doi.org/https://doi.org/10.1029/97GB00077

Hagino, K., Onuma, R., Kawachi, M., & Horiguchi, T. (2013). Discovery of an Endosymbiotic Nitrogen-Fixing Cyanobacterium UCYN-A in *Braarudosphaera bigelowii* (*Prymnesiophyceae*). *8*(12), e81749. https://doi.org/10.1371/journal.pone.0081749

Harding, K., Turk-Kubo, K. A., Sipler, R. E., Mills, M. M., Bronk, D. A., & Zehr, J. P. (2018). Symbiotic unicellular cyanobacteria fix nitrogen in the Arctic Ocean. *Proceedings of the National Academy of Sciences*, *115*(52), 13371-13375. https://doi.org/10.1073/pnas.1813658115

Hofmann Elizondo, U., Righetti, D., Benedetti, F., & Vogt, M. (2021). Biome partitioning of the global ocean based on phytoplankton biogeography. *Progress in Oceanography*, *194*, 102530. https://doi.org/https://doi.org/10.1016/j.pocean.2021.102530

Howard, J. B., & Rees, D. C. (1996). Structural Basis of Biological Nitrogen Fixation. *Chem Rev*, *96*(7), 2965-2982. https://doi.org/10.1021/cr9500545

Inomura, K., Bragg, J., & Follows, M. J. (2017). A quantitative analysis of the direct and indirect costs of nitrogen fixation: a model based on *Azotobacter vinelandii*. *The ISME journal*, *11*(1), 166-175.

Jickells, T. D., Buitenhuis, E., Altieri, K., Baker, A. R., Capone, D., Duce, R. A., Dentener, F., Fennel, K., Kanakidou, M., LaRoche, J., Lee, K., Liss, P., Middelburg, J. J., Moore, J. K., Okin, G., Oschlies, A., Sarin, M., Seitzinger, S., Sharples, J., . . . Zamora, L. M. (2017). A reevaluation of the magnitude and impacts of anthropogenic atmospheric nitrogen inputs on the ocean. *Global Biogeochemical Cycles*, *31*(2), 289-305. https://doi.org/https://doi.org/10.1002/2016GB005586

Karl, D., Letelier, R., Tupas, L., Dore, J., Christian, J., & Hebel, D. (1997). The role of nitrogen fixation in biogeochemical cycling in the subtropical North Pacific Ocean. *Nature*, *388*(6642), 533-538. https://doi.org/10.1038/41474

Kavanaugh, M. T., Hales, B., Saraceno, M., Spitz, Y. H., White, A. E., & Letelier, R. M. (2014). Hierarchical and dynamic seascapes: A quantitative framework for scaling pelagic biogeochemistry and ecology. *Progress in Oceanography*, *120*, 291-304. https://doi.org/https://doi.org/10.1016/j.pocean.2013.10.013

Kawachi, M., Inouye, I., Maeda, O., & Chihara, M. (1991). The haptonema as a food-capturing device: observations on *Chrysochromulina hirta* (*Prymnesiophyceae*). *Phycologia*, *30*(6), 563-573. https://doi.org/10.2216/i0031-8884-30-6-563.1

Kitajima, S., Furuya, K., Hashihama, F., Takeda, S., & Kanda, J. (2009). Latitudinal distribution of diazotrophs and their nitrogen fixation in the tropical and subtropical western North Pacific. *Limnology and Oceanography*, *54*(2), 537-547.

Kong, L., Jing, H., Kataoka, T., Sun, J., & Liu, H. (2011). Phylogenetic diversity and spatio-temporal distribution of nitrogenase genes (*nifH*) in the northern South China Sea. *Aquatic Microbial Ecology*, *65*(1), 15-27.

Krupke, A., Mohr, W., Laroche, J., Fuchs, B. M., Amann, R. I., & Kuypers, M. M. (2015). The effect of nutrients on carbon and nitrogen fixation by the UCYN-A–haptophyte symbiosis. *The ISME journal*, *9*(7), 1635-1647. https://doi.org/10.1038/ismej.2014.253

Langlois, R., Großkopf, T., Mills, M., Takeda, S., & LaRoche, J. (2015). Widespread Distribution and Expression of Gamma A (UMB), an Uncultured, Diazotrophic, γ-Proteobacterial *nifH* Phylotype. *PLoS ONE*, *10*(6), e0128912. https://doi.org/10.1371/journal.pone.0128912

Leigh, G. J. (2002). *Nitrogen fixation at the millennium*. Elsevier.

Liu, X., & Millero, F. J. (2002). The solubility of iron in seawater. *Marine Chemistry*, *77*(1), 43-54. https://doi.org/https://doi.org/10.1016/S0304-4203(01)00074-3

Martínez-Pérez, C., Mohr, W., Löscher, C. R., Dekaezemacker, J., Littmann, S., Yilmaz, P., Lehnen, N., Fuchs, B. M., Lavik, G., Schmitz, R. A., Laroche, J., & Kuypers, M. M. M. (2016). The small unicellular diazotrophic symbiont, UCYN-A, is a key player in the marine nitrogen cycle. *Nature Microbiology*, *1*(11), 16163. https://doi.org/10.1038/nmicrobiol.2016.163

Michaels, A. F., Olson, D., Sarmiento, J. L., Ammerman, J. W., Fanning, K., Jahnke, R., Knap, A. H., Lipschultz, F., & Prospero, J. M. (1996). Inputs, losses and

transformations of nitrogen and phosphorus in the pelagic North Atlantic Ocean. *Biogeochemistry*, *35*(1), 181-226. https://doi.org/10.1007/BF02179827

Mills, M. M., Ridame, C., Davey, M., La Roche, J., & Geider, R. J. (2004). Iron and phosphorus co-limit nitrogen fixation in the eastern tropical North Atlantic. *Nature*, *429*(6989), 292-294. https://doi.org/10.1038/nature02550

Moisander, P. H., Beinart, R. A., Hewson, I., White, A. E., Johnson, K. S., Carlson, C. A., Montoya, J. P., & Zehr, J. P. (2010). Unicellular Cyanobacterial Distributions Broaden the Oceanic N_2 Fixation Domain. *Science*, *327*(5972), 1512-1514. https://doi.org/10.1126/science.1185468

Montoya, J. P., Holl, C. M., Zehr, J. P., Hansen, A., Villareal, T. A., & Capone, D. G. (2004). High rates of N_2 fixation by unicellular diazotrophs in the oligotrophic Pacific Ocean. *Nature*, *430*(7003), 1027-1032. https://doi.org/10.1038/nature02824

Moore, C., Mills, M., Arrigo, K., Berman-Frank, I., Bopp, L., Boyd, P., Galbraith, E., Geider, R., Guieu, C., & Jaccard, S. (2013). Processes and patterns of oceanic nutrient limitation. *Nature Geoscience*, *6*(9), 701-710.

Mulholland, M., Bernhardt, P., Blanco-Garcia, J., Mannino, A., Hyde, K., Mondragon, E., Turk, K., Moisander, P., & Zehr, J. (2012). Rates of dinitrogen fixation and the abundance of diazotrophs in North American coastal waters between Cape Hatteras and Georges Bank. *Limnology and Oceanography*, *57*(4), 1067-1083.

Newton, W. E. (2015). Recent Advances in Understanding Nitrogenases and How They Work. In *Biological Nitrogen Fixation* (pp. 5-20). https://doi.org/https://doi.org/10.1002/9781119053095.ch2

Offre, P., Spang, A., & Schleper, C. (2013). Archaea in biogeochemical cycles. *Annual Review of Microbiology*, *67*, 437-457.

Ohki, K., & Fujita, Y. (1988). Aerobic nitrogenase activity measured as acetylene reduction in the marine non-heterocystous cyanobacterium *Trichodesmium* spp. grown under artificial conditions. *Marine Biology*, *98*, 111-114.

Paerl, R. W., Hansen, T. N., Henriksen, N. N., Olesen, A. K., & Riemann, L. (2018). N-fixation and related O_2 constraints on model marine diazotroph *Pseudomonas stutzeri* BAL361. *Aquatic Microbial Ecology*, *81*(2), 125-136.

Pereira, N., Shilova, I. N., & Zehr, J. P. (2019). Use of the high-affinity phosphate transporter gene, *pstS*, as an indicator for phosphorus stress in the marine diazotroph *Crocosphaera watsonii* (Chroococcales, Cyanobacteria). *J Phycol*, *55*(4), 752-761. https://doi.org/10.1111/jpy.12863

Postgate, J. (1998). *Nitrogen fixation*. Cambridge University Press.

Postgate, J. R., Stewart, W. D. P., & Rosswall, T. (1982). Biological nitrogen fixation: fundamentals. *Philosophical Transactions of the Royal Society of London. B, Biological Sciences*, *296*(1082), 375-385. https://doi.org/doi:10.1098/rstb.1982.0013

Reygondeau, G., Longhurst, A., Martinez, E., Beaugrand, G., Antoine, D., & Maury, O. (2013). Dynamic biogeochemical provinces in the global ocean. *Global Biogeochemical Cycles*, *27*(4), 1046-1058.

Riemann, L., Farnelid, H., & Steward, G. F. (2010). Nitrogenase genes in non-cyanobacterial plankton: prevalence, diversity and regulation in marine waters.

Aquatic Microbial Ecology, *61*(3), 235-247. https://www.int-res.com/abstracts/ame/v61/n3/p235-247/

Robson, R. L., & Postgate, J. R. (1980). Oxygen and hydrogen in biological nitrogen fixation. *Annual Reviews in Microbiology*, *34*(1), 183-207.

Saito, M. A., Bertrand, E. M., Dutkiewicz, S., Bulygin, V. V., Moran, D. M., Monteiro, F. M., Follows, M. J., Valois, F. W., & Waterbury, J. B. (2011). Iron conservation by reduction of metalloenzyme inventories in the marine diazotroph *Crocosphaera watsonii*. *Proceedings of the National Academy of Sciences*, *108*(6), 2184-2189. https://doi.org/doi:10.1073/pnas.1006943108

Sañudo-Wilhelmy, S. A., Kustka, A. B., Gobler, C. J., Hutchins, D. A., Yang, M., Lwiza, K., Burns, J., Capone, D. G., Raven, J. A., & Carpenter, E. J. (2001). Phosphorus limitation of nitrogen fixation by *Trichodesmium* in the central Atlantic Ocean. *Nature*, *411*(6833), 66-69. https://doi.org/10.1038/35075041

Sarkar, D., Landa, M., Bandyopadhyay, A., Pakrasi, H. B., Zehr, J. P., & Maranas, C. D. (2021). Elucidation of trophic interactions in an unusual single-cell nitrogen-fixing symbiosis using metabolic modeling. *PLoS Comput Biol*, *17*(5), e1008983. https://doi.org/10.1371/journal.pcbi.1008983

Seefeldt, L. C., Hoffman, B. M., & Dean, D. R. (2009). Mechanism of Mo-Dependent Nitrogenase. *Annual Review of Biochemistry*, *78*(1), 701-722. https://doi.org/10.1146/annurev.biochem.78.070907.103812

Shao, Z., Xu, Y., Wang, H., Luo, W., Wang, L., Huang, Y., Agawin, N. S. R., Ahmed, A., Benavides, M., Bentzon-Tilia, M., Berman-Frank, I., Berthelot, H., Biegala, I. C.,

Bif, M. B., Bode, A., Bonnet, S., Bronk, D. A., Brown, M. V., Campbell, L., . . . Luo, Y. W. (2023). Global oceanic diazotroph database version 2 and elevated estimate of global oceanic N_2 fixation. *Earth Syst. Sci. Data*, *15*(8), 3673-3709. https://doi.org/10.5194/essd-15-3673-2023

Shi, T., Ilikchyan, I., Rabouille, S., & Zehr, J. P. (2010). Genome-wide analysis of diel gene expression in the unicellular N_2-fixing cyanobacterium *Crocosphaera watsonii* WH 8501. *The ISME journal*, *4*(5), 621-632.

Shiozaki, T., Bombar, D., Riemann, L., Hashihama, F., Takeda, S., Yamaguchi, T., Ehama, M., Hamasaki, K., & Furuya, K. (2017). Basin scale variability of active diazotrophs and nitrogen fixation in the North Pacific, from the tropics to the subarctic Bering Sea. *Global Biogeochemical Cycles*, *31*(6), 996-1009.

Shiozaki, T., Fujiwara, A., Inomura, K., Hirose, Y., Hashihama, F., & Harada, N. (2020). Biological nitrogen fixation detected under Antarctic sea ice. *Nature Geoscience*, *13*(11), 729-732.

Shiozaki, T., Kondo, Y., Yuasa, D., & Takeda, S. (2018). Distribution of major diazotrophs in the surface water of the Kuroshio from northeastern Taiwan to south of mainland Japan. *Journal of Plankton Research*, *40*(4), 407-419. https://doi.org/10.1093/plankt/fby027

Stal, L. J. (2009). Is the distribution of nitrogen-fixing cyanobacteria in the oceans related to temperature? *Environ Microbiol*, *11*(7), 1632-1645. https://doi.org/10.1111/j.1758-2229.2009.00016.x

Strock, J. (2008). Ammonification. In *Encyclopedia of ecology, five-volume set* (pp. 162-165). Elsevier Inc.

Tang, W., & Cassar, N. (2019). Data-driven modeling of the distribution of diazotrophs in the global ocean. *Geophysical Research Letters*, *46*(21), 12258-12269.

Thamdrup, B. (2012). New pathways and processes in the global nitrogen cycle. *Annual Review of Ecology, Evolution, and Systematics*, *43*, 407-428.

Thompson, A., Carter, B. J., Turk-Kubo, K., Malfatti, F., Azam, F., & Zehr, J. P. (2014). Genetic diversity of the unicellular nitrogen-fixing cyanobacteria UCYN-A and its prymnesiophyte host. *Environmental Microbiology*, *16*(10), 3238-3249. https://doi.org/10.1111/1462-2920.12490

Thompson, A. W., Foster, R. A., Krupke, A., Carter, B. J., Musat, N., Vaulot, D., Kuypers, M. M. M., & Zehr, J. P. (2012). Unicellular Cyanobacterium Symbiotic with a Single-Celled Eukaryotic Alga. *Science*, *337*(6101), 1546-1550. https://doi.org/10.1126/science.1222700

Tripp, H. J., Bench, S. R., Turk, K. A., Foster, R. A., Desany, B. A., Niazi, F., Affourtit, J. P., & Zehr, J. P. (2010). Metabolic streamlining in an open-ocean nitrogen-fixing cyanobacterium. *464*(7285), 90-94. https://doi.org/10.1038/nature08786

Turk, K., Rees, A. P., Zehr, J. P., Pereira, N., Swift, P., Shelley, R., Lohan, M., Woodward, E. M. S., & Gilbert, J. (2011). Nitrogen fixation and nitrogenase (*nifH*) expression in tropical waters of the eastern North Atlantic. *The ISME journal*, *5*(7), 1201-1212. https://doi.org/10.1038/ismej.2010.205

Turk-Kubo, K. A., Farnelid, H. M., Shilova, I. N., Henke, B., & Zehr, J. P. (2017). Distinct ecological niches of marine symbiotic N_2-fixing cyanobacterium Candidatus *Atelocyanobacterium thalassa* sublineages. *Journal of Phycology*, *53*(2), 451-461. https://doi.org/10.1111/jpy.12505

Turk-Kubo, K. A., Gradoville, M. R., Cheung, S., Cornejo-Castillo, F., Harding, K. J., Morando, M., Mills, M., & Zehr, J. P. (2022). Non-cyanobacterial diazotrophs: Global diversity, distribution, ecophysiology, and activity in marine waters. *FEMS Microbiol Rev*. https://doi.org/10.1093/femsre/fuac046

Turk-Kubo, K. A., Henke, B. A., Gradoville, M. R., Magasin, J. D., Church, M. J., & Zehr, J. P. (2023). Seasonal and spatial patterns in diazotroph community composition at Station ALOHA. *Frontiers in Marine Science*, *10*, 1130158.

Turk-Kubo, K. A., Mills, M. M., Arrigo, K. R., van Dijken, G., Henke, B. A., Stewart, B., Wilson, S. T., & Zehr, J. P. (2021). UCYN-A/haptophyte symbioses dominate N_2 fixation in the Southern California Current System. *ISME Communications*, *1*(1), 1-13.

Unrein, F., Gasol, J. M., Not, F., Forn, I., & Massana, R. (2014). Mixotrophic haptophytes are key bacterial grazers in oligotrophic coastal waters. *The ISME journal*, *8*(1), 164.

Van de Graaf, A. A., Mulder, A., de Bruijn, P., Jetten, M., Robertson, L. A., & Kuenen, J. G. (1995). Anaerobic oxidation of ammonium is a biologically mediated process. *Applied and Environmental Microbiology*, *61*(4), 1246-1251.

Van Mooy, B. A. S., Fredricks, H. F., Pedler, B. E., Dyhrman, S. T., Karl, D. M., Koblížek, M., Lomas, M. W., Mincer, T. J., Moore, L. R., Moutin, T., Rappé, M. S., & Webb, E. A. (2009). Phytoplankton in the ocean use non-phosphorus lipids in response to phosphorus scarcity. *458*(7234), 69-72. https://doi.org/10.1038/nature07659

Vitousek, P. M., Cassman, K., Cleveland, C., Crews, T., Field, C. B., Grimm, N. B., Howarth, R. W., Marino, R., Martinelli, L., Rastetter, E. B., & Sprent, J. I. (2002). Towards an ecological understanding of biological nitrogen fixation. *Biogeochemistry*, *57*(1), 1-45. https://doi.org/10.1023/A:1015798428743

Ward, B. (2012). The global nitrogen cycle. *Fundamentals of geobiology*, 36-48.

Ward, B. A., Dutkiewicz, S., Moore, C. M., & Follows, M. J. (2013). Iron, phosphorus, and nitrogen supply ratios define the biogeography of nitrogen fixation. *Limnology and Oceanography*, *58*(6), 2059-2075.

Ward, B. B., Arp, D. J., & Klotz, M. G. (2011). *Nitrification*. American Society for Microbiology Press.

Webb, E. A., Ehrenreich, I. M., Brown, S. L., Valois, F. W., & Waterbury, J. B. (2009). Phenotypic and genotypic characterization of multiple strains of the diazotrophic cyanobacterium, *Crocosphaera watsonii*, isolated from the open ocean. *11*(2), 338-348. https://doi.org/10.1111/j.1462-2920.2008.01771.x

Webb, E. A., Foster, R. A., Villareal, T., Waterbury, J. B., & Zehr, J. P. (2022). *Trichodesmium*. In *Bergey's Manual of Systematics of Archaea and Bacteria* (pp. 1-12). https://doi.org/https://doi.org/10.1002/9781118960608.gbm00448.pub2

Whittaker, S., Bidle, K. D., Kustka, A. B., & Falkowski, P. G. (2011). Quantification of nitrogenase in *Trichodesmium* IMS 101: implications for iron limitation of nitrogen fixation in the ocean. *Environ Microbiol Rep*, *3*(1), 54-58. https://doi.org/10.1111/j.1758-2229.2010.00187.x

Wilson, Foster, R. A., Zehr, J. P., & Karl, D. M. (2010). Hydrogen production by *Trichodesmium erythraeum Cyanothece* sp. and *Crocosphaera watsonii*. *Aquatic Microbial Ecology*, *59*(2), 197-206.

Wilson, Tozzi, S., Foster, R. A., Ilikchyan, I., Kolber, Z. S., Zehr, J. P., & Karl, D. M. (2010). Hydrogen Cycling by the Unicellular Marine Diazotroph *Crocosphaera watsonii* Strain WH8501. *76*(20), 6797-6803. https://doi.org/10.1128/aem.01202-10

Wilson, S. T., Aylward, F. O., Ribalet, F., Barone, B., Casey, J. R., Connell, P. E., Eppley, J. M., Ferrón, S., Fitzsimmons, J. N., Hayes, C. T., Romano, A. E., Turk-Kubo, K. A., Vislova, A., Armbrust, E. V., Caron, D. A., Church, M. J., Zehr, J. P., Karl, D. M., & Delong, E. F. (2017). Coordinated regulation of growth, activity and transcription in natural populations of the unicellular nitrogen-fixing cyanobacterium *Crocosphaera*. *Nature Microbiology*, *2*(9), 17118. https://doi.org/10.1038/nmicrobiol.2017.118

Zehr, J. P., Bench, S. R., Mondragon, E. A., McCarren, J., & DeLong, E. F. (2007). Low genomic diversity in tropical oceanic N_2-fixing cyanobacteria. *Proceedings of the National Academy of Sciences*, *104*(45), 17807-17812. https://doi.org/doi:10.1073/pnas.0701017104

Zehr, J. P., & Capone, D. G. (2023). Unsolved mysteries in marine nitrogen fixation. *Trends Microbiol*. https://doi.org/10.1016/j.tim.2023.08.004

Zehr, J. P., & Kudela, R. M. (2011). Nitrogen Cycle of the Open Ocean: From Genes to Ecosystems. *Annual Review of Marine Science*, *3*(1), 197-225. https://doi.org/10.1146/annurev-marine-120709-142819

Zehr, J. P., Mellon, M. T., & Zani, S. (1998). New nitrogen-fixing microorganisms detected in oligotrophic oceans by amplification of nitrogenase (*nifH*) genes. *Appl. Environ. Microbiol.*, *64*(9), 3444-3450.

Zehr, J. P., Shilova, I. N., Farnelid, H. M., Muñoz-Marín, M. D. C., & Turk-Kubo, K. A. (2017). Unusual marine unicellular symbiosis with the nitrogen-fixing cyanobacterium UCYN-A. *Nature Microbiology*, *2*(1), 16214. https://doi.org/10.1038/nmicrobiol.2016.214

Zehr, J. P., Waterbury, J. B., Turner, P. J., Montoya, J. P., Omoregie, E., Steward, G. F., Hansen, A., & Karl, D. M. (2001). Unicellular cyanobacteria fix N_2 in the subtropical North Pacific Ocean. *Nature*, *412*(6847), 635-638. https://doi.org/10.1038/35088063

Zhang, R., Zhang, D., Chen, M., Jiang, Z., Wang, C., Zheng, M., Qiu, Y., & Huang, J. (2019). N_2 fixation rate and diazotroph community structure in the western tropical North Pacific Ocean. *Acta Oceanologica Sinica*, *38*(12), 26-34. https://doi.org/10.1007/s13131-019-1513-4

Chapter 1: Phagotrophy in the UCYN-A2/*Braarudosphaera bigelowii* symbiosis

Authors: Wing Kwan Esther Mak[1] (wimak@ucsc.edu), Kendra Turk-Kubo[1] (kturk@ucsc.edu), David A. Caron[2](dcaron@usc.edu), Rachel Harbeitner[1] (rharbeit@ucsc.edu), Jonathan Magasin[1] (jmagasin@gmail.com), Tyler Coale[1] (tcoale@ucsc.edu) , Kyoko Hagino[3] (kyokohagino@kochi-u.ac.jp), Yoshihito Takano[3] (takadino@gmail.com), Tomohiro Nishimura[4,5](nishimura_tomohiro49@fra.go.jp), Masao Adachi[4](madachi@kochi-u.ac.jp), and Jonathan P Zehr[1] (zehrj@ucsc.edu)

[1] Department of Ocean Sciences, University of California, Santa Cruz, CA, USA

[2] Department of Biological Sciences, University of Southern California, Los Angeles, CA, USA

[3] Marine Core Research Institute, Kochi University, Nankoku, Kochi, Japan

[4] Faculty of Agriculture and Marine Science, Kochi University, Nankoku, Kochi, Japan

[5] Fisheries Technology Institute, Japan Fisheries Research and Education Agency, Hatsukaichi, Hiroshima, Japan

Abstract

Biological nitrogen fixation provides fixed nitrogen for microbes living in the oligotrophic open ocean. UCYN-A2, the globally distributed marine unicellular cyanobacterial diazotroph, lives in symbiosis with a haptophyte host, *Braarudosphaera bigelowii* which is based on the exchange of fixed carbon for fixed nitrogen. Indirect evidence suggested that *B. bigelowii* might be a mixotrophic (phagotrophic) phototrophic flagellate, prior to the discovery that it harbored an N_2-fixing symbiont. The goal of this study was to determine if *B. bigelowii* can graze on bacteria using several independent approaches. The results showed that *B. bigelowii* grazed on the co-occurring bacteria at a rate of 5–7 cells/h/*B. bigelowii* cell and that the overall grazing rate was significantly higher at nighttime than daytime. Data from 16S rRNA gene amplicon sequencing suggested that *B. bigelowii* preferentially grazed on certain bacterial 16S genotypes. In addition, Lysotracker™ staining of the symbiosis suggested active digestive activities inside the *B. bigelowii* cell. Carbon and nitrogen fixation measurements revealed that the carbon demand of the host could not be fulfilled by photosynthesis alone, implying supplementation by heterotrophy. These independent lines of evidence together revealed that the UCYN-A2/*B. bigelowii* symbiosis is phagotrophic, and that the protist may rely on mixotrophic metabolism as a supplementary carbon or energy source at different times of the day.

Introduction

Phytoplankton are photosynthetic protists or cyanobacteria that are responsible for approximately half of the Earth's carbon fixation (Field et al., 1998) and form the base of the marine food web (Stoecker et al., 2017). Mixotrophy increases the efficiency of trophic transfer, and thus enhances the rate of nutrient retention in the system (Fischer et al., 2017; Mitra et al., 2014; Ward & Follows, 2016). This nutritional strategy can alleviate low nutrient conditions, as phagotrophic organisms have the capacity to exploit prey. Many phytoplankton are mixotrophs that combine photosynthetic (autotrophic) and heterotrophic modes of nutrition, including phagotrophy (engulfing prey or particulate organic carbon) and osmotrophy (deriving energy from dissolved organic carbon as source of nutrients that may be unavailable to strict autotrophs) (Edwards, 2019; Rothhaupt, 1996). For example, the haptophyte *Prymnesium parvum* uses phagotrophy during phosphate-limiting conditions (Nygaard & Tobiesen, 1993). In resource-limited environments, having access to two types of food sources provides a competitive advantage, increasing the chances of survival.

Haptophytes are among the groups of phytoplankton that have the ability to adopt a mixotrophic mode of nutrition (Unrein et al. 2014). They are one of the most widely distributed primary producers and can account for 30–50% of the total chlorophyll-a biomass in the oceans (Liu et al. 2009). A notable example is the haptophyte

Braarudosphaera bigelowii, which forms a symbiotic relationship with a nitrogen-fixing cyanobacterium, UCYN-A (*Candidatus* Atelocyanobacterium thalassa). The UCYN-A cyanobacterium, which is globally distributed (Farnelid et al. 2016; Martínez-Pérez et al. 2016; Tang and Cassar 2019), has a metabolically streamlined genome and lacks photosynthetic capabilities, including oxygenic photosynthesis and carbon fixation. Instead, it fixes nitrogen and provides to its haptophyte partner in exchange for fixed carbon (Zehr et al. 2008; Tripp et al. 2010). Both UCYN-A and *B. bigelowii* are classified into several genotypes; UCYN-A1 dominates the open ocean, whereas UCYN-A2, which forms a symbiotic relationship with *B. bigelowii* (18S genotype III), is the prevalent form in coastal regions (Turk-Kubo et al., 2017).

Previous studies suggested that the haptophyte *B. bigelowii* is also a phagotroph that grazes on bacteria. In the study by Frias-Lopez et al. (2009),^{13}C-labeled *Synechococcus* and *Prochlorococcus* were fed to an *in situ* microbial community at station ALOHA, which is located in the North Pacific Ocean. A DNA stable isotope probing technique (DNA-SIP) was used to identify grazers. The recovered sequences showed a high similarity to two closely related sequences (97.7 – 99.7% nt identity to gb|KF771254) for UCYN-A2 and to eleven closely related sequences (97.8 – 99.2% nt identity to gb|JX291836) for UCYN-A1 based on the 18S rRNA DNA region. In another study, Krupke et al. (2015) used nanoscale secondary ion mass spectrometry (nanoSIMS) and observed an unknown structure within the UCYN-A1 haptophyte symbiosis which could have been an engulfed prey.

Despite the discovery of the globally important nitrogen fixer two decades ago, the UCYN-A symbiosis was not isolated in culture until 2018 when *B. bigelowii* genotype III, containing UCYN-A2, was isolated from the coastal waters of the Sea of Japan (Loconte et al. in prep). In the whole transcriptome analysis of the haptophyte, *B. bigelowii,* using the predictive model by Burns et al. (2018), a high likelihood of phagotrophic behavior was indicated, with phagocyte prediction scores reaching 0.95 (Suzuki et al., 2021). The availability of the *B. bigelowii*/UCYN-A2 culture allowed us to design experiments to directly characterize physiology, including phagotrophy. This study evaluated the mode of nutrition of the UCYN-A2/*B. bigelowii* symbiosis by assessing the relative contribution of phagotrophy and phototrophy during growth. Dilution experiments were also used to measure grazing rates on the bacteria in the culture, and stains were used to visualize the food vacuole and assess digestive activity. Carbon and nitrogen fixation rates were also measured. Taken together, this study provides direct evidence that *B. bigelowii* is a phagotroph, which is important ecologically and offers insights into the physiological adaptations of *B. bigelowii* as a mixotrophic organism.

Experimental Procedures

Culture Isolation

Sea surface water sample (10 liter) was collected at Furue Port, Nagasaki, Japan (33°21'58.7"N 129°31'03.7"E) on May 1, 2018. The sample was pre-filtered through a

plankton net with 50µm opening (Sefar Inc. DIN-110, Swiss) in order to remove large planktons, and then concentrated to ca. 50ml using a plankton net with 1µm opening (Sefar Inc. NY1-HD, Swiss). The concentrated seawater sample was examined under an inverted light microscope (Olympus CKX41, Japan). A small portion of the concentrated seawater, which contained several motile cells of *B. bigelowii* and some unidentified phytoplanktons, was collected using a capillary in the inverted light microscope, placed into a culture well with 10% f/2 medium (Guillard & Ryther, 1962) and ca. 0.1% of filtered gelidium jelly extract (GJE) (Nishimura et al. 2020) and incubated in light-dark cycle consisting of 12h of light and 12h of darkness at 18˚C for two weeks to make a preculture sample. *Braarudosphaera bigelowii* and other unidentified phytoplankton cells grew together in the preculture sample. Ca. 50µl of preculture sample was collected and moved into new f/2 medium with GJE extract (1%) (1 ml) once a week. From the precultured samples, *B. bigelowii* cells were re-isolated using capillaries under the inverted light microscope. Each isolate was rinsed with sterile seawater by pipetting under the inverted light microscope, and was grown in f/2 medium with 1% GJE extract under the same conditions. One of the isolates grew in culture strains, and labelled as FR-21. The strain was identified through genotyping analysis. The host was identified through 18S rRNA primers as *B. bigelowii* genotype III, and the symbiont was identified through nitrogenase *nifH* primers as UCYN-A2 (Hagino et al., 2013). Strain FR-21 was deposited to the National Institute for Environmental Studies (NIES) Japan as NIES-4399, and was shared with the University of California, Santa Cruz for this study. The strain was identified through genotyping analysis.

The host was identified through 18S rRNA primers, and the symbiont was identified through nitrogenase nifH primers.

Culture Conditions

The cultures of strain FR-21 (NIES-4399) were maintained at a light intensity of 60 μmol photons $m^{-2}s^{-1}$ with a light-dark cycle of 12h:12h at 18℃. For maintenance, the cultures were transferred periodically with the modified seawater based-f/2 media described above. The seawater medium, with a salinity of 34 ppt, was based on water collected from 150 m and 200 m depths in Monterey Bay, California, USA (36°44'49.2"N 122°01'19.2"W). The culture was not axenic.

Diel bacterial grazing rates determined by dilution experiments

Mortality of the co-occurring bacterial assemblage due to the grazing by the UCYN-A2*/B. bigelowii* symbiosis (Strain FR-21, NIES-4399) was measured using the dilution method (Landry et al., 1995) in two replicate experiments. The diluent was prepared by filtering the UCYN-A2*/B. bigelowii* symbiosis culture through a 0.2 μm Supor® Membrane (Pall Corp, Port Washington, NY, United States), and then combined in different proportions (20, 60 and 100%) with unfiltered culture to create a gradient in grazing pressure. Each

dilution level consisted of three replicate bottles, each of which contains a volume of 25 mL. The experiments were initiated at the beginning of the dark cycle and incubated for 24 hours, following the same conditions as those used for culturing, including media, light and temperature.

Samples (2 mL) for cell counts were collected at T_0 (start of dark cycle), T_{12} (start of light cycle) and T_{24} (end of light cycle), fixed immediately with glutaraldehyde (Electron Microscopy Sciences, Hatfield, PA, United States) for a final concentration of 0.25% v/v, and incubated in the dark at room temperature for 15 min and stored at -80°C until analysis. Cell counts were obtained using a BD Influx cell sorter with a 488 nm Sapphire laser (Coherent, Santa Clara, CA, United States). All samples were diluted 10-fold with sterile culture media to achieve the linear range of the cytometer, then filtered through a CellTrics® filter with 30 μm pore-size mesh (Partec, Swedesboro, NJ, United States). The UCYN-A2/*B. bigelowii* symbiosis (grazer) was identified and gated based on the *B. bigelowii* chlorophyll-*a* fluorescence (red fluorescence) and forward scatter (FSC; a proxy for cell size). Data was triggered on the FSC channel and events were counted for 5 min.

A subset of flow cytometry samples were also stained with SYBR® Green I Nucleic Acid Stain (Lonza Group, Basel, Switzerland). After incubation in the dark for 15 minutes, the stained bacteria within the samples were subsequently identified and counted based on the 531 nm wavelength fluorescence (green fluorescence) and FSC. Data was triggered on the 531 channel and events were counted for 1 min (Marie et al., 1999). The bacteria population

was gated into high nucleic acid bacteria (HNA) and low nucleic acid bacteria (LNA) based on 531 nm fluorescence and side scatter (SSC). The data was processed using Flowjo 10.8.0 (Tree Star, Inc., Ashland, OR, United States).

To calculate mortality (m) and growth rates (μ) of the bacteria, HNA and LNA were plotted against the proportion of unfiltered culture (i.e., 20, 60 and 100% dilution level), which corresponds to the relative grazing pressure. Linear regression was employed, and the negative slope from the linear regression is the mortality rate (m), while the y-intercept represents the bacterial growth rate (μ) when the grazer is theoretically absent (Landry et al., 1998). The significance of the linear regression results was assessed using p-values, indicating the level of statistical significance of the relationships between variables.

Measuring differential grazing of different co-occurring bacteria

Samples were subsampled from the dilution experiment to characterize the bacterial community composition by amplification and sequencing of the 16S rRNA gene. Two milliliter samples were filtered through 0.2 μm pore-size 25 mm diameter Supor filters (Pall Corp, Port Washington, NY, United States) in sterile Swinnex® holders (Millipore). The filters were transferred into 2.0 mL bead beating tubes that contained 0.1 and 0.5 mm diameter sterile glass beads (BioSpec Products, Bartsville, OK, United States), and stored in -80°C until further analysis. DNA was extracted using a protocol of freeze-thaw, bead-beating and proteinase K digestion (Moisander et al., 2008) and then followed by the

Qiacube® (Qiagen, Germantown, MD, United States) automated on-column DNA extraction and clean-up protocol using the DNeasy Plant Mini kit (Qiagen).

To identify and quantify the bacterial community composition, the V3/V4 hypervariable region of the 16S rRNA gene was amplified using the universal primers Bakt_341F and Bakt_805R (Herlemann et al., 2011) with common sequence linkers (Moonsamy et al., 2013). The PCR amplification began with an initial denaturation step at 95°C for 5 min, followed by cycling at 95°C for 40 sec, 53°C for 40 sec, and 72°C for 60 sec for 30 cycles. The process concluded with a final elongation step at 72°C for 7 min. Libraries were prepared and paired-end reads were sequenced using an Illumina MiSeq at the Genomics and Microbiome Core Facility at Rush University Medical Center (Green et al., 2015). All reads were processed through quality control, denoised, merged and chimera-checked using DADA2 pipeline and formed amplicon sequence variants (ASV) (Callahan et al., 2016). Taxonomy was assigned using the Silva reference database (Quast et al., 2012). The R package phyloseq (McMurdie & Holmes, 2013) was used to analyze community composition and DESeq2 (Love et al., 2014) was used to calculate differential change of the community composition of each treatment between the time points.

Staining UCYN-A2/*B. bigelowii* symbiosis with Lysotracker™ Green

Lysotracker ™ Green DND-26 (Thermo Fisher Scientific, Waltham, MA, United States), a cell-permeable green dye that stains acidic intracellular compartments (Sintes & Del

Giorgio, 2010), was used to stain the UCYN-A2/*B. bigelowii* symbiosis. A stock solution of 1mM Lysotracker™ Green DND-26 was diluted 1:20000 to stain 1mL samples from the live symbiosis culture. The UCYN-A2/*B. bigelowii* symbiosis culture was grown to a concentration of 10^6 cells/mL, and then sampled at day and night time points. The cells were analyzed immediately without any fixation by epifluorescence microscopy (Axio Imager 2, Zeiss, Dublin, CA, United States) at 630X magnification and analyzed using Zeiss ZEN Digital Imaging for Light Microscopy software. Chlorophyll signal was exited using red fluorescence. The stained UCYN-A2/*B. bigelowii* symbiosis was also analyzed using flow cytometry, based on 531 nm fluorescence and forward scatter (FSC1). As a control, the UCYN-A2/*B. bigelowii* symbiosis without staining were also analyzed using the same cytometry method.

Growth rate, C fixation and N_2 fixation rate measurements

The UCYN-A2/B. bigelowii symbiosis culture was cultivated under consistent conditions, including the same media, light intensity of 60 μmol photons m^{-2} s^{-1}, and a temperature of 18°C, maintained for more than 10 generations. The culture was diluted to the same starting concentration every three days to maintain exponential phase while subsampled for growth rate, C and N_2 fixation rates at each transfer. To measure the growth rate, 0.5mL of the culture was sampled daily in three replicate culture bottles at the same time of day, fixed immediately with glutaraldehyde (Electron Microscopy Sciences, Hatfield, PA, United

States) at a final concentration of 0.25% v/v, then incubated at room temperature in the dark for 15 min. Fixed samples were then flash frozen at -80°C until further analysis.

All samples were diluted 10-fold with 0.2 μm filtered culture media to achieve the linear range of the cytometer, and the UCYN-A2/*B. bigelowii* symbiosis cells were identified and counted based on the *B. bigelowii* chl *a* fluorescence and forward scatter (FSC), events were counted for 5 min as described in the previous section. Steady state growth rates (μ) were calculated from linear regressions of ln (cell concentration) versus time.

Bulk C and N_2 fixation rates were measured by the ^{13}C and $^{15}N_2$ tracer method of Montoya et al. (1996), amended by Mohr et al. (2010) and Wilson et al. (2012). $^{15}N_2$ enriched seawater was prepared following the procedure described by Klawonn et al. (2015). Eight milliliters of $^{15}N_2$ gas (99 atom %, Cambridge Scientific) were injected into 250 mL of 0.2 μm pore-size filtered culture medium, vortexed for 5 minutes and stabilized at room temperature for at least 24h. $^{15}N_2$ enriched seawater was then transferred to 25 mL crimp-sealed glass serum bottles. Three bottles were then collected from the entire batch of $^{15}N_2$ enriched seawater to be used for later evaluation of the initial atom % of N_2. This analysis was performed using Membrane Inlet Mass Spectrometry (MIMS), following the method outlined by Ferrón et al. (2016).

To start the incubation, 1 mL of $^{15}N_2$ enriched seawater and 300 μL of 59 mM ^{13}C -labeled bicarbonate (final concentration: 1.17mmol/L 99 atom% $NaH^{13}CO_3$, Cambridge Isotope

Laboratories) were added to 14 mL of the UCYN-A2/*B. bigelowii* symbiosis culture in 15 mL serum bottles, crimp-sealed and incubated at the 18°C for 24 hours. The T_0 $\delta^{13}PC$ /$\delta^{15}PN$ natural abundance samples were prepared by adding 1mL of filtered medium to 14mL of the UCYN-A2/*B. bigelowii* symbiosis culture. After 24h, each incubation was filtered onto pre-combusted 25 mm diameter glass fiber filters (GF/F, Whatman) and frozen and stored at -80°C.

The filters were then dried at 60°C for 24 h, followed by acid fumigation with hydrochloric acid for 48 h, and then pelleted into tin capsules. Particulate C, particulate N, and isotopic composition ($\delta^{13}C$, $\delta^{15}N$) were analyzed using a CE Instruments NC2500 elemental analyzer coupled to a Thermo Scientific DELTAplus XP isotope ratio mass spectrometer via a Thermo-Scientific Conflo III at the University of California Santa Cruz Stable Isotope Laboratory. N_2 fixation rates were calculated from the following equation (Montoya, Voss et al. 1996):

$$N_2\ fixation\ rate(fmol\ cell^{-1}\ d^{-1}) = \frac{A_{PN} - A_{PN_0}}{A_{N_2} - A_{PN_0}} * \frac{[PN]}{\Delta t} * \frac{1}{cell}$$

where A_{PN} and A_{PN0} are the fractional ^{15}N enrichment (in units of atom %) after and before the incubation, respectively. [PN] is the particulate nitrogen concentration at the end of the incubation period, is the duration of incubation in units of hours, and A_{N2} is the fractional

^{15}N-enrichment of the N_2 source pool, determined by MIMS. To calculate the N_2 fixation rate per cell, the bulk rate was then divided by cell count, determined by flow cytometry. Limits of detection (LOD) and minimum quantifiable rates (MQR) were calculated as in Gradoville et al. (2017).

Similarly, C fixation rates were determined by the following equation:

$$C\ fixation\ rate(fmol\ cell^{-1}\ d^{-1}) = \frac{A_{PC} - A_{PC_0}}{A_{CO_2} - A_{PC_0}} * \frac{[PC]}{\Delta t} * \frac{1}{cell}$$

where the terms A_{PC} , A_{PC0}, and [PC] corresponds to the values of carbon in this equation. The concentration of total inorganic carbon (DIC) was determined using a Shimadzu TOC-VCSH. Inorganic carbon A_{CO2} was measured by injection of a sample into 25 wt% H_3PO_4 in the reaction vessel, evolving CO_2.

Calculations of C and N sources and demand

C and N requirements were calculated using the C and N content per cell, growth rate, and the C and N_2 fixation rate per cell. The cellular C and N content was measured through the isotopic analysis of ^{13}C and ^{15}N, as described in the preceding section, using elemental analysis. The total C and N content of each sample was measured and subsequently divided by the number of cells quantified via flow cytometry. C and N requirements per day were

calculated by C and N content/cell multiplied by (1- exp μ). Percentage biomass contributed by C and N_2 fixation was calculated by the C and N_2 fixation rates/cell/day divided by the C and N requirement per day.

C uptake from grazing was estimated from the bacteria cell sizes, volume: biomass ratio, grazing rates and trophic efficiency. The dimensions of 12 bacteria were measured using epifluorescence microscopy (Axio Imager 2, Zeiss, Dublin, CA, United States) at 630X magnification, and the width and length of each cell were determined using Zeiss ZEN Digital Imaging for Light Microscopy software. This involved capturing images of the cells and using the software to measure the width and length of each cell at the cross section. These measurements were then used to calculate the biovolume using the formula:

$$Volume = \pi \times W^2 \times (\frac{L}{4} - \frac{W}{6})$$

where W is the width at the cross section and L is the length (Hillebrand et al., 1999).

The biovolume was then converted to C biomass using the equation:

$$m = 197\, x\, V^{0.46}$$

where m is the C biomass and V is the volume (Cermak et al., 2017), and the minimum and maximum C was then estimated by multiplying the grazing rate per day and a conservative trophic transfer efficiency of 10%–30% (Priyadarshi et al., 2019). Percentage biomass by grazing was calculated by the C and N uptake rate/d from grazing divided by C requirement per day.

Results

The results of the dilution experiments show that the UCYN-A2/*B. bigelowii* symbiosis was actively grazing on the co-occuring bacteria in the culture. The three-point dilution experiments were repeated twice and all treatments were done in triplicate. The slope of the growth rate plotted against different dilution levels ranged from -0.6 to -0.7/d, indicating the 24 h grazing rate of the symbiosis on the co-occurring bacteria population was 0.6–0.7/d (Figure 1a). This indicates the bacteria were being grazed at a rate of 6–7 cells/haptophyte/hour. The intrinsic growth rate (μ_0), determined using the y-intercept of the linear regression, which is the growth rate of bacteria where no grazer is present theoretically, was 0.6–0.8/d (Figure 1d).

In order to compare grazing in the 12 h daytime period to the 12 h nighttime period, subsamples for cell counts were taken at the end of the light and dark cycles. The 12 h nighttime grazing rate ranged from 1.0–1.1 /d ($p=0.009$) (Figure 1c), which is equivalent to approximately 8 cells per hour, but there were no statistically significant grazing rates detected in the 12 h daytime period (Figure 1b). The 12 h nighttime intrinsic growth rate was 1.0–1.2/d ($p=0.009$) (Figure 1f), however, the daytime intrinsic growth rate was not statistically significant from the linear regression (Figure 1e).

The composition of the bacteria assemblage was determined to detect whether the host exhibits differential grazing on the co-occurring bacterial species. The most abundant ASV

at T_0 was in the orders Flavobacteriales (39.5%), followed by Alteromonadales (16.9%), and Rhodobacterales (15.1%). The relative abundances of some strains increased from T_0 to T_{24} under the reduced grazing pressure in the 20% bottles, suggesting that these strains may be differentially grazed. These strains included the orders Chitinophagales, Rhodospirillales, Flavobacteriales and Opitutales. The log2-fold change was 0.61–1.96 (Figure 2). No changes were observed throughout the incubation in the 100% bottles, where grazing pressure was high. These changes may be attributed to differential grazing, differential bacterial growth, or a combination of both factors.

The host was observed under the microscope after staining with Lysotracker- DND-26 to determine the digestive activity of the food vacuole. The vacuole surrounding the symbionts and the nucleus fluoresced green under 504/511 nm excitation/emission after staining. The brightest signal originated from the compartment closest to the symbiont, but it also stained the compartment at the flagella side of the cell (Figure 3). The results were supported with flow cytometry enumeration of lysotracker-stained cells, which showed that approximately 90% of the host cells had green fluorescence. No signal was observed in the same green fluorescing region in the unstained UCYN-A2/*B. bigelowii* symbiosis culture (Figure 4). The results indicate that there was recent digestive activity in the feeding vacuole that caused acidic conditions in the food vacuole.

The UCYN-A2/*B.bigelowii* C and N_2 fixation and growth rates were measured to determine whether autotrophy was sufficient for the growth requirements. The growth rate of the

symbiosis under cultured condition averaged 0.44 ± 0.03 /d. The C fixation rate was 1393 ± 298 fmol C/cell/d and the C content was 4256 ± 206 fmol C/cell. The percentage of total per cell C content obtained from C fixation was estimated to be 60 ± 16%. The N_2 fixation rate was 160 ± 20 fmol N/cell/d and the N content was 489 ± 27 fmol N/cell (Figure 5). The percentage of total per cell N content obtained from N_2 fixation was estimated to be 60 ± 11%. The average co-cultivated bacteria biomass per cell was estimated to be ca. 76 fg C/cell, with the interquartile range as 23 fg C/cell. Measured grazing rates were 6.1–7.1/h (or 146 cells/d, assuming constant grazing rates throughout a diel cycle), and using a very conservative or trophic transfer efficiency from 10%–30%, grazing contributes between 4.0%–19% of the C biomass requirement (Table 6).

Discussion

Phagotrophy in the UCYN-A2/*B. bigelowii* symbiosis may provide an ecological advantage

Our results provide multiple lines of evidence that support the hypothesis that the UCYN-A2/*B. bigelowii* symbiosis is capable of phagotrophy. Results from the dilution experiments demonstrate the haptophyte's ability to engage in grazing on prey cells, which is further supported by the lysotracker staining revealing the presence of an active food vacuole for digestion. It should be noted that while lysotracker is commonly used to specifically label acidic food vacuoles, it is possible that it may also stain other acidic structures. Nonetheless, presence of lysotracker-labeled compartments and the measured grazing rates supports the phagotrophic activity of UCYN-A2/*B. bigelowii* symbiosis. The C and N budget analysis reveals that the rates of photosynthesis and N_2 fixation alone are insufficient to sustain the daily growth rates, indicating the reliance on an external nutritional source. The ability to utilize a phagotrophic mode of nutrition may confer an ecological advantage in different environmental conditions.

UCYN-A/*B. bigelowii* symbioses are some of the most abundant and widespread marine diazotrophs. Unlike other N_2-fixers that are typically associated with the oligotrophic open ocean conditions, the symbiosis can be found in the open ocean, temperate coastal regions, brackish water, and even cold high-latitude waters (Bentzon-Tilia et al., 2015; Cheung et

al., 2020; Harding et al., 2018; Shiozaki et al., 2020), and even actively transcribing *nifH* in coastal sediments (Brown & Jenkins, 2014). Based on our findings, it is plausible to interpret that the utilization of different nutritional modes may confer a distinct ecological advantage, enabling it to inhabit regions of the ocean with varying environmental properties. The ability to obtain fixed N from the symbiont is a potential ecological advantage in oligotrophic ocean regions, and the photosynthetic capability allows the symbiont to harvest light energy from the euphotic zone. In regions where light is limited, such as in high latitude waters (which are seasonally-light limited), coastal waters and sediments, and the lower euphotic zone, the phagotrophic capability of the symbiosis may provide a means to acquire supplementary energy from grazing. The phagotropic lifestyle allows the UCYN-A/*B. bigelowii* symbiosis to adapt to various ocean regimes, potentially explaining its presence in oligotrophic open ocean, coastal, and high latitude regions.

The UCYN-A2/*B. bigelowii* symbiosis selectively grazed certain bacterial strains, resulting in an increase of abundances of certain strains when grazing pressure was decreased. Specifically, Chitinophagales, Rhodospirillales, Flavobacteriales and Opitutales exhibit enhanced abundance under reduced grazing pressure. Of the four orders that were preferentially grazed, three orders- Chitinophagales, Flavobacteriales and Opitutales were classified as copiotrophs capable of degrading diverse organic compounds, such as chitin and cellulose (Rosenberg et al., 2014), fermenting carbohydrates (Chin et al., 2001), and breaking down phosphoric acid monoesters to phosphate (Rosenberg et al., 2014). It should be noted that our culturing conditions might have enriched for copiotrophs due to the

excess added C source (GJE extract). As a result, the observed copiotrophs here may not necessarily represent the bacterial population that exists in the marine environments where the UCYN-A2/B. bigelowii symbiosis is found. Due to their ability to utilize different substrates, copiotrophs tend to grow at higher growth rates and reach higher abundances, thereby supporting a larger and more diverse population of grazers in the environment. An alternative speculation is that the production of simple compounds by copiotrophs serves as a food source for grazers, thus making them more attractive to grazers. The underlying mechanisms driving these observed changes could involve differential grazing, distinct patterns of bacterial growth, or a combination of these factors.

Carbon and nitrogen requirements for growth may be supported by grazing

Our findings indicate that phagotrophy is important to supplement energy in the symbiosis under these culture conditions. In nutrient-replete conditions where the culture is maintained, the estimated C and N requirements for symbiosis growth could not be met solely by C and N_2 fixation. Only 60 ± 16% of the total C quota and 60 ± 11% of the total N quota needed to sustain the measured growth rates were supplied by CO_2 and N_2 fixation. This suggests that the symbiosis needed external C and N sources to maintain growth. While it is difficult to accurately estimate the trophic efficiency, using the conservative estimates of both trophic efficiency and bacterial biomass, grazing could account for 4.0 % to 19% of the host's carbon requirements.

Similarly, N_2 fixation could supply only 60 ± 11% of the UCYN-A2/*B. bigelowii* symbiosis N requirement, which suggests there is another N source. A recent transcriptome study of *B. bigelowii* revealed the absence of many transcripts relating to utilization of common N substrates, such as nitrate, nitrite, formamide, glutamate, glutamine, cyanate and urea (Suzuki et al., 2021). Although this could be due to the nature of the transcriptomic study which may be missing some information due to the lack of the complete genome, another reason could be that the host cells were not utilizing these N sources in spite of their presence in the growth medium. An environmental study of the UCYN-A host by Mills et al. (2020) using nanoSIMS showed that the host could not take up nitrate as a N source, but could take up some ammonium. This result was also supported by the transcriptomic study that showed that the ammonium transporters were expressed (Suzuki et al., 2021). However, ammonium transporter gene expressed could be due to the need of the host to acquire ammonium from the symbiont, which produce ammonium as a product of N_2 fixation. Suzuki et al. suggested some co-occurring bacteria were capable of reducing nitrate to ammonium, and the ammonium transporter gene in the host could be expressed to uptake of ammonium by diffusion, or by grazing (Suzuki et al., 2021). Our experimental results also agreed with the metatranscriptomic-based analysis by Suzuki et al. (2021) that the host was predicted to be highly likely a phagotroph.

The UCYN-A/*B.bigelowii* symbiosis was shown to have the highest grazing rates during the night and cease grazing during the day. The reason of nocturnal grazing remains highly speculative. An interpretation drawn from these findings suggests that the symbiosis, by

incorporating carbon and nitrogen through photosynthesis and N_2 fixation during the daytime, could engage in night grazing to replenish carbon and nitrogen levels along with other essential nutrients. This nocturnal grazing pattern might align more effectively with the cell's energy dynamics, allocating ATP and reductants primarily for nitrogen fixation during the day. On the other hand, cell division (Landa et al., 2021), grazing, and digestion activities predominantly occur during the nighttime. Jones (1997) classified mixotrophy into four categories, according to the degree of phagotrophy and phototrophy in different kinds of mixotrophs. Group A predominantly uses phagotrophy, while groups B, C, and D rely primarily on phototrophy as their main mode of nutrition. In group B, the ingestion rates are inversely proportional to light intensity, whereas group C uses phagotrophy to acquire essential nutrients, and thus grazing rates are proportional to light intensity, resulting in feeding during the daytime. Group D represents an extreme case where ingestion of prey only occurs during prolonged periods of darkness (Jones, 1997). The UCYN-A/*B.bigelowii* symbiosis exhibits characteristics that are most similar to group B mixotrophs. *B.bigelowii* mainly obtains its C through photosynthesis. A majority of C needed for growth (64 ±11%) is obtained through phototrophy indicating it is the primary mode of nutrition. Grazing occurs at night when light is absent, suggesting that the main goal of feeding is to supplement energy as an alternative carbon source. However, the UCYN-A/*B.bigelowii* symbiosis could not grow axenically (Hagino, personal communication)., which suggests the possibility nutrition through feeding is necessary An example of this group is the haptophyte *Chrysochromulina brevifilum*, where ingestion rates are inversely proportional to light intensity and grazing is utilized to supplement

energy in conditions of limited light availability, thus allowing for optimal growth (Hansen & Hjorth, 2002). The UCYN-A/*B.bigelowii* symbiosis exhibits a similar mixotrophic lifestyle but with diazotrophic capabilities, allowing it to thrive in a variety of oceanic environments, and making it a unique and important organism in marine ecosystems.

Conclusions

Our study provides evidence that the UCYN-A2/*B.bigelowii* symbiosis is a phagotroph, by measuring grazing rates of the symbiosis on co-occurring bacteria in dilution experiments. The results indicate the host is a nighttime grazer, and likely uses grazing for supplemental nutrition at night. The host demonstrated preferential grazing towards certain groups of copiotrophs, and maintained an active food vacuole for digestion. Taken together, our study provides novel insights on how the UCYN-A2/*B.bigelowii symbiosis* switches between different mode of nutrition to maintain its C and N requirement in varying environment conditions, that may explain its broad environmental distribution and persistence in light-limited habitats, which have implications for better understanding the ecological role of this important player in marine ecosystems.

Acknowledgments

We gratefully acknowledge Stefan Green and his staff (Univeristy of Illinois, Chicago) for sequencing consultation, Colin Carney (University of California, Santa Cruz) for the stable isotope analysis, Angelicque White and Carolina Funkey (University of Hawaii, Manoa) for the MIMS analysis, and Anna V. Voznyuk (University of California, Santa Cruz) for processing flow cytometry samples. We greatly appreciate Mary Rose Gradoville (University of California, Santa Cruz) and Ondřej Prasil (Czech Academy of Sciences) for helpful discussions. We would like to acknowledge the financial support provided by Simons Foundations under award ID 824082 to J.P. Z.

Author Contributions

EM designed the study, conducted experiments, collected and analyzed data, and wrote the manuscript. KTK conceived and designed the study, contributed to the experimental design, and critically reviewed and edited the manuscript. RH, JM and TC contributed to data collection, and interpretation, and reviewed and edited the manuscript. KH established and provided the culture strains for this study. YT carried out the sampling of seawater in Nagasaki and provided assistance in the establishment and maintenance of the culture strain. TN and MA designed and provided the media recipe and unpublished medium. JPZ designed the study, supervised the project, secured funding, and provided critical feedback throughout the study and manuscript preparation. All authors reviewed the final version of the manuscript and approved it for publication.

References

Bentzon-Tilia, M., Traving, S. J., Mantikci, M., Knudsen-Leerbeck, H., Hansen, J. L. S., Markager, S., & Riemann, L. (2015). Significant N_2 fixation by heterotrophs, photoheterotrophs and heterocystous cyanobacteria in two temperate estuaries. *The ISME journal*, *9*(2), 273-285. https://doi.org/10.1038/ismej.2014.119

Brown, S. M., & Jenkins, B. D. (2014). Profiling gene expression to distinguish the likely active diazotrophs from a sea of genetic potential in marine sediments. *Environmental Microbiology*, *16*(10), 3128-3142. https://doi.org/https://doi.org/10.1111/1462-2920.12403

Burns, J. A., Pittis, A. A., & Kim, E. (2018). Gene-based predictive models of trophic modes suggest Asgard archaea are not phagocytotic. *Nature Ecology & Evolution*, *2*(4), 697-704. https://doi.org/10.1038/s41559-018-0477-7

Callahan, B. J., McMurdie, P. J., Rosen, M. J., Han, A. W., Johnson, A. J. A., & Holmes, S. P. (2016). DADA2: High-resolution sample inference from Illumina amplicon data. *Nature methods*, *13*(7), 581-583.

Cermak, N., Becker, J. W., Knudsen, S. M., Chisholm, S. W., Manalis, S. R., & Polz, M. F. (2017). Direct single-cell biomass estimates for marine bacteria via Archimedes' principle. *The ISME journal*, *11*(3), 825-828.

Cheung, S., Nitanai, R., Tsurumoto, C., Endo, H., Nakaoka, S. i., Cheah, W., Lorda, J. F., Xia, X., Liu, H., & Suzuki, K. (2020). Physical forcing controls the basin-scale

occurrence of nitrogen-fixing organisms in the North Pacific Ocean. *Global Biogeochemical Cycles*, *34*(9), e2019GB006452.

Chin, K. J., Liesack, W., & Janssen, P. H. (2001). *Opitutus terrae* gen. nov., sp. nov., to accommodate novel strains of the division

'Verrucomicrobia' isolated from rice paddy soil. *International Journal of Systematic and Evolutionary Microbiology*, *51*(6), 1965-1968. https://doi.org/https://doi.org/10.1099/00207713-51-6-1965

Edwards, K. F. (2019). Mixotrophy in nanoflagellates across environmental gradients in the ocean. *Proceedings of the National Academy of Sciences*, *116*(13), 6211-6220. https://doi.org/10.1073/pnas.1814860116

Field, C. B., Behrenfeld, M. J., Randerson, J. T., & Falkowski, P. (1998). Primary Production of the Biosphere: Integrating Terrestrial and Oceanic Components. *Science*, *281*(5374), 237-240. https://doi.org/doi:10.1126/science.281.5374.237

Fischer, R., Giebel, H. A., Hillebrand, H., & Ptacnik, R. (2017). Importance of mixotrophic bacterivory can be predicted by light and loss rates. *Oikos*, *126*(5), 713-722.

Frias-Lopez, J., Thompson, A., Waldbauer, J., & Chisholm, S. W. (2009). Use of stable isotope-labelled cells to identify active grazers of picocyanobacteria in ocean surface waters. *Environmental Microbiology*, *11*(2), 512-525.

Green, S. J., Venkatramanan, R., & Naqib, A. (2015). Deconstructing the polymerase chain reaction: understanding and correcting bias associated with primer degeneracies and primer-template mismatches. *PLoS ONE*, *10*(5), e0128122.

Guillard, R. R., & Ryther, J. H. (1962). Studies of marine planktonic diatoms: I. *Cyclotella nana Hustedt*, and *Detonula confervacea* (Cleve) *Gran*. *Canadian journal of microbiology*, *8*(2), 229-239.

Hagino, K., Onuma, R., Kawachi, M., & Horiguchi, T. (2013). Discovery of an Endosymbiotic Nitrogen-Fixing Cyanobacterium UCYN-A in *Braarudosphaera bigelowii* (*Prymnesiophyceae*). *8*(12), e81749. https://doi.org/10.1371/journal.pone.0081749

Hansen, P., & Hjorth, M. (2002). Growth and grazing responses of *Chrysochromulina ericina* (*Prymnesiophyceae*): the role of irradiance, prey concentration and pH. *Marine Biology*, *141*, 975-983.

Harding, K., Turk-Kubo, K. A., Sipler, R. E., Mills, M. M., Bronk, D. A., & Zehr, J. P. (2018). Symbiotic unicellular cyanobacteria fix nitrogen in the Arctic Ocean. *Proceedings of the National Academy of Sciences*, *115*(52), 13371-13375. https://doi.org/10.1073/pnas.1813658115

Herlemann, D. P., Labrenz, M., Jürgens, K., Bertilsson, S., Waniek, J. J., & Andersson, A. F. (2011). Transitions in bacterial communities along the 2000 km salinity gradient of the Baltic Sea. *The ISME journal*, *5*(10), 1571-1579.

Hillebrand, H., Dürselen, C.-D., Kirschtel, D., Pollingher, U., & Zohary, T. (1999). Biovolume Calculation for Pelagic and Benthic Microalgae. *Journal of Phycology*, *35*(2), 403-424. https://doi.org/https://doi.org/10.1046/j.1529-8817.1999.3520403.x

Jones, H. (1997). A classification of mixotrophic protists based on their behaviour. *Freshwater Biology*, *37*(1), 35-43.

Klawonn, I., Bonaglia, S., Brüchert, V., & Ploug, H. (2015). Aerobic and anaerobic nitrogen transformation processes in N_2-fixing cyanobacterial aggregates. *The ISME journal*, *9*(6), 1456-1466.

Krupke, A., Mohr, W., Laroche, J., Fuchs, B. M., Amann, R. I., & Kuypers, M. M. (2015). The effect of nutrients on carbon and nitrogen fixation by the UCYN-A–haptophyte symbiosis. *The ISME journal*, *9*(7), 1635-1647. https://doi.org/10.1038/ismej.2014.253

Landa, M., Turk-Kubo, K. A., Cornejo-Castillo, F. M., Henke, B. A., & Zehr, J. P. (2021). Critical Role of Light in the Growth and Activity of the Marine N_2-Fixing UCYN-A Symbiosis [Original Research]. *Frontiers in Microbiology*, *12*. https://doi.org/10.3389/fmicb.2021.666739

Landry, M., Kirshtein, J., & Constantinou, J. (1995). A refined dilution technique for measuring the community grazing impact of microzooplankton, with experimental tests in the central equatorial Pacific. *Marine ecology progress series. Oldendorf*, *120*(1), 53-63.

Landry, M. R., Brown, S. L., Campbell, L., Constantinou, J., & Liu, H. (1998). Spatial patterns in phytoplankton growth and microzooplankton grazing in the Arabian Sea during monsoon forcing. *Deep Sea Research Part II: Topical Studies in Oceanography*, *45*(10-11), 2353-2368.

Love, M. I., Huber, W., & Anders, S. (2014). Moderated estimation of fold change and dispersion for RNA-seq data with DESeq2. *Genome biology*, *15*(12), 1-21.

Marie, D., Partensky, F., Vaulot, D., & Brussaard, C. (1999). Enumeration of Phytoplankton, Bacteria, and Viruses in Marine Samples. *Current Protocols in Cytometry*, *10*(1), 11.11.11-11.11.15. https://doi.org/https://doi.org/10.1002/0471142956.cy1111s10

McMurdie, P. J., & Holmes, S. (2013). phyloseq: an R package for reproducible interactive analysis and graphics of microbiome census data. *PLoS ONE*, *8*(4), e61217.

Mitra, A., Flynn, K. J., Burkholder, J. M., Berge, T., Calbet, A., Raven, J. A., Granéli, E., Glibert, P. M., Hansen, P. J., Stoecker, D. K., Thingstad, F., Tillmann, U., Våge, S., Wilken, S., & Zubkov, M. V. (2014). The role of mixotrophic protists in the biological carbon pump. *Biogeosciences*, *11*(4), 995-1005. https://doi.org/10.5194/bg-11-995-2014

Mohr, W., Intermaggio, M. P., & Laroche, J. (2010). Diel rhythm of nitrogen and carbon metabolism in the unicellular, diazotrophic cyanobacterium *Crocosphaera watsonii* WH8501. *12*(2), 412-421. https://doi.org/10.1111/j.1462-2920.2009.02078.x

Moisander, P. H., Beinart, R. A., Voss, M., & Zehr, J. P. (2008). Diversity and abundance of diazotrophic microorganisms in the South China Sea during intermonsoon. *The ISME journal*, *2*(9), 954-967.

Montoya, J. P., Voss, M., Kahler, P., & Capone, D. G. (1996). A simple, high-precision, high-sensitivity tracer assay for N_2 fixation. *Applied and Environmental Microbiology*, *62*(3), 986-993.

Moonsamy, P., Williams, T., Bonella, P., Holcomb, C., Höglund, B., Hillman, G., Goodridge, D., Turenchalk, G., Blake, L., & Daigle, D. (2013). High throughput HLA genotyping using 454 sequencing and the Fluidigm Access Array™ system for simplified amplicon library preparation. *Tissue antigens*, *81*(3), 141-149.

Nygaard, K., & Tobiesen, A. (1993). Bacterivory in algae: A survival strategy during nutrient limitation. *38*(2), 273-279. https://doi.org/10.4319/lo.1993.38.2.0273

Priyadarshi, A., Smith, S. L., Mandal, S., Tanaka, M., & Yamazaki, H. (2019). Micro-scale patchiness enhances trophic transfer efficiency and potential plankton biodiversity. *Scientific Reports*, *9*(1), 17243. https://doi.org/10.1038/s41598-019-53592-6

Quast, C., Pruesse, E., Yilmaz, P., Gerken, J., Schweer, T., Yarza, P., Peplies, J., & Glöckner, F. O. (2012). The SILVA ribosomal RNA gene database project: improved data processing and web-based tools. *Nucleic acids research*, *41*(D1), D590-D596.

Rosenberg, E., DeLong, E. F., Lory, S., Stackebrandt, E., & Thompson, F. (2014). The prokaryotes: other major lineages of Bacteria and the Archaea.

Rothhaupt, K. O. (1996). Laboratorary Experiments with a Mixotrophic *Chrysophyte* and Obligately Phagotrophic and Photographic Competitors. *77*(3), 716. https://doi.org/10.2307/2265496

Shiozaki, T., Fujiwara, A., Inomura, K., Hirose, Y., Hashihama, F., & Harada, N. (2020). Biological nitrogen fixation detected under Antarctic sea ice. *Nature Geoscience*, *13*(11), 729-732.

Sintes, E., & Del Giorgio, P. A. (2010). Community heterogeneity and single-cell digestive activity of estuarine heterotrophic nanoflagellates assessed using lysotracker and flow cytometry. *Environmental Microbiology*, *12*(7), 1913-1925.

Stoecker, D. K., Hansen, P. J., Caron, D. A., & Mitra, A. (2017). Mixotrophy in the marine plankton. *Annual Review of Marine Science*, *9*, 311-335.

Suzuki, S., Kawachi, M., Tsukakoshi, C., Nakamura, A., Hagino, K., Inouye, I., & Ishida, K. I. (2021). Unstable Relationship Between *Braarudosphaera bigelowii* (= *Chrysochromulina parkeae*) and Its Nitrogen-Fixing Endosymbiont. *Front Plant Sci*, *12*, 749895. https://doi.org/10.3389/fpls.2021.749895

Turk-Kubo, K. A., Farnelid, H. M., Shilova, I. N., Henke, B., & Zehr, J. P. (2017). Distinct ecological niches of marine symbiotic N_2-fixing cyanobacterium *Candidatus Atelocyanobacterium thalassa* sublineages. *Journal of Phycology*, *53*(2), 451-461. https://doi.org/10.1111/jpy.12505

Ward, B. A., & Follows, M. J. (2016). Marine mixotrophy increases trophic transfer efficiency, mean organism size, and vertical carbon flux. *Proceedings of the National Academy of Sciences*, *113*(11), 2958-2963. https://doi.org/10.1073/pnas.1517118113

Wilson, S. T., Böttjer, D., Church, M. J., & Karl, D. M. (2012). Comparative assessment of nitrogen fixation methodologies, conducted in the oligotrophic North Pacific Ocean. *Appl Environ Microbiol*, *78*(18), 6516-6523. https://doi.org/10.1128/aem.01146-12

Tables and figures

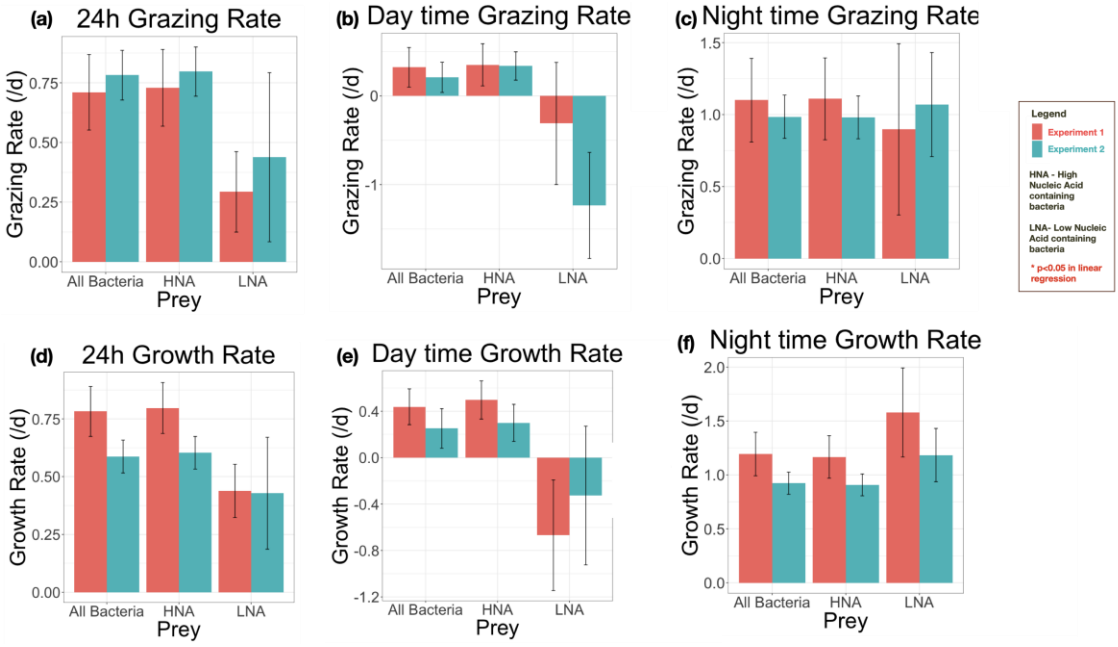

Figure 1. Grazing rates and growth rates plotted against co-cultivated bacterial prey. Red and blue bars represent two replicate experiments. Figure 1a and 1d represents 24h total grazing and growth rates, while Figure 1b, 1c, 1e and 1f represents daytime or nighttime grazing or growth rates. All 24h and nighttime grazing rates were statistically significant ($p<0.05$). HNA – high nucleic acid-containing bacteria; LNA – low nucleic acid-containing bacteria.

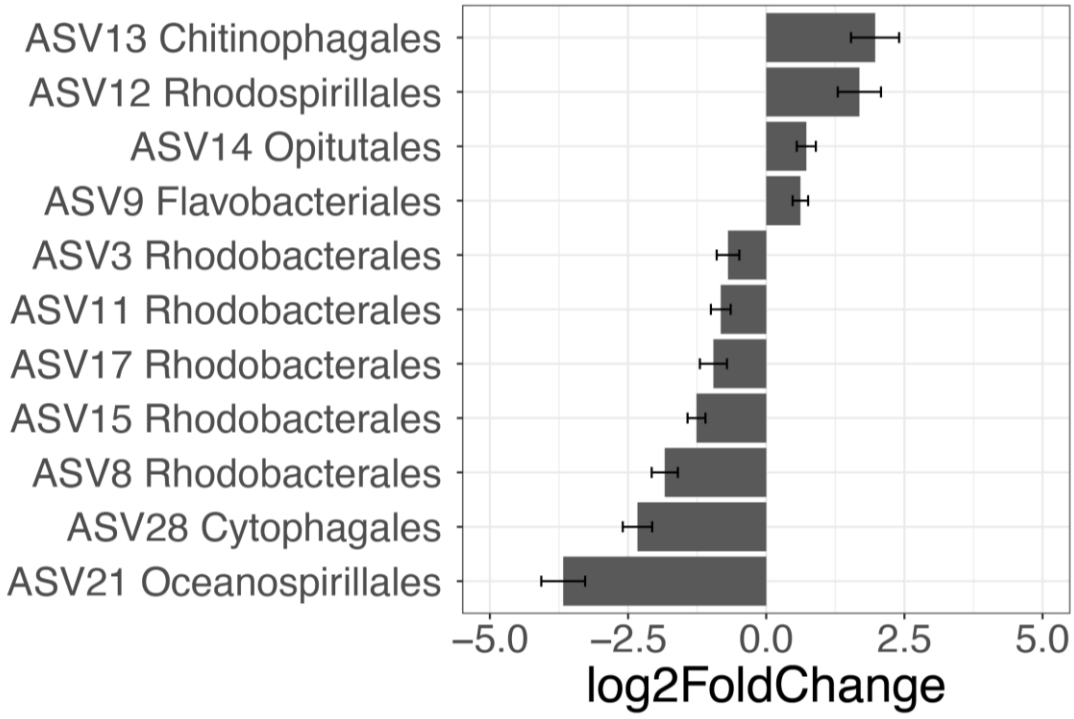

Figure 2. Changes in the relative abundances of ASVs that showed differential changes in the 20% treatment within 24h.

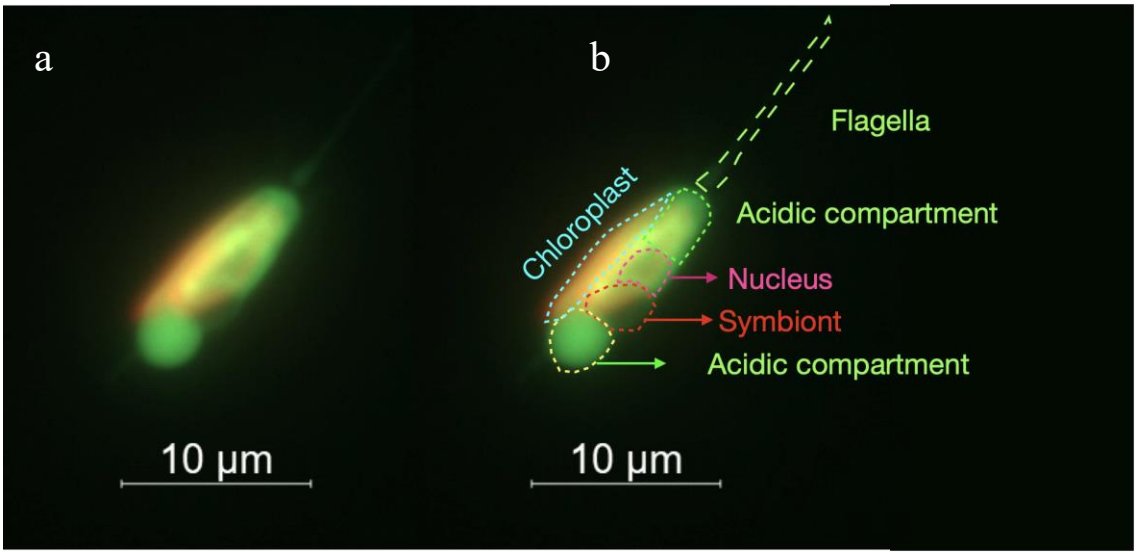

Figure 3. Fluorescent microscopy image of UCYN-A/*B.bigelowii* symbiosis after treatment with Lysotracker DND-26. The green fluorescence signal indicates acidic subcellular regions stained with Lysotracker DND-26, and chloroplasts are exited using red fluorescence. Figures 3a and 3b show images of the same cell, with Figure 3b labeled to highlight different components of the cell.

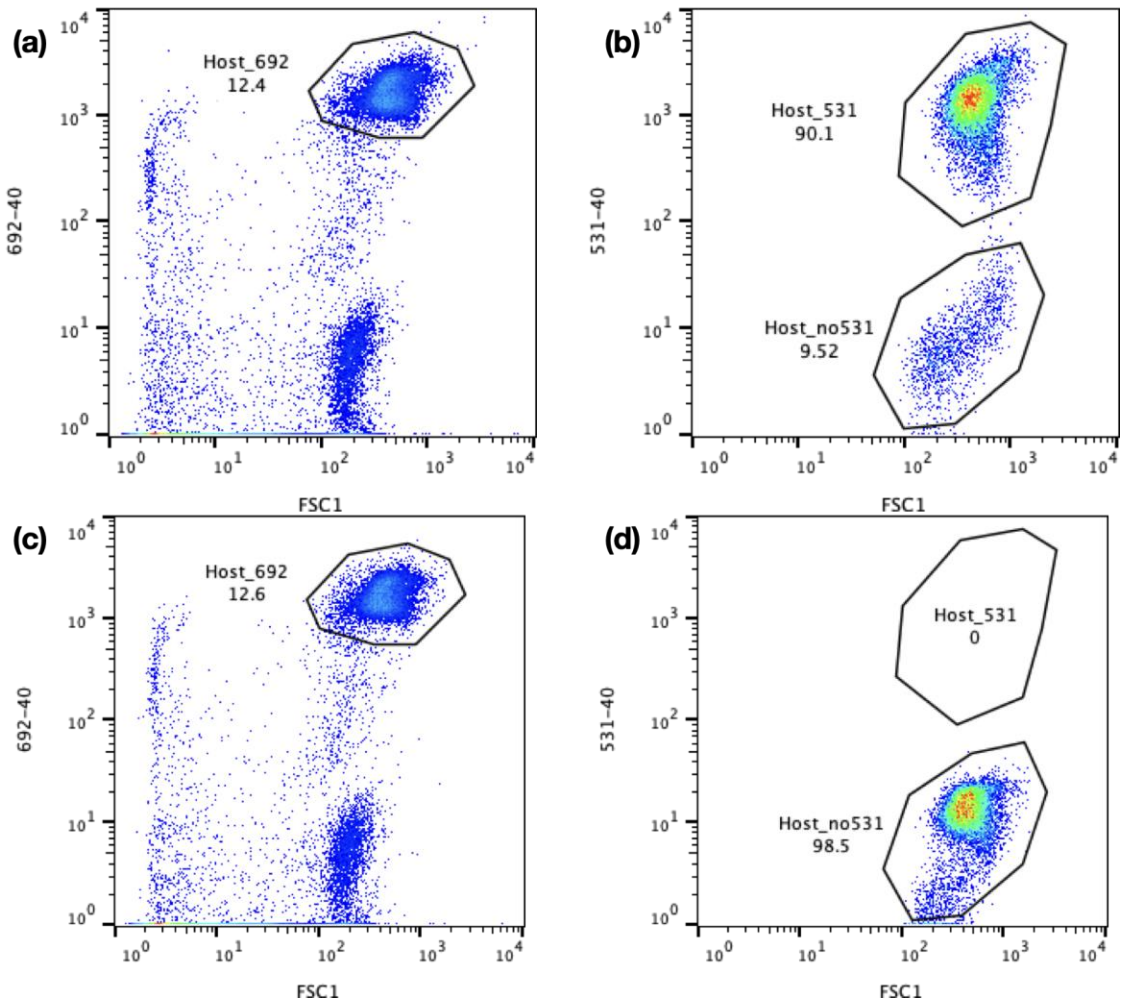

Figure 4. Cytograph depicting UCYN-A/B. bigelowii symbiosis stained with Lysotracker DND-26. Panels (a) and (b) display the staining of Lysotracker DND-26 at the host chlorophyll signal in the 692 nm channel and Lysotracker DND-26 staining in the 531 nm channel, respectively. Panels (c) and (d) serve as negative controls, showing the presence of host chlorophyll signals in the 692 nm channel and the absence of Lysotracker staining in the 531 nm channel, respectively.

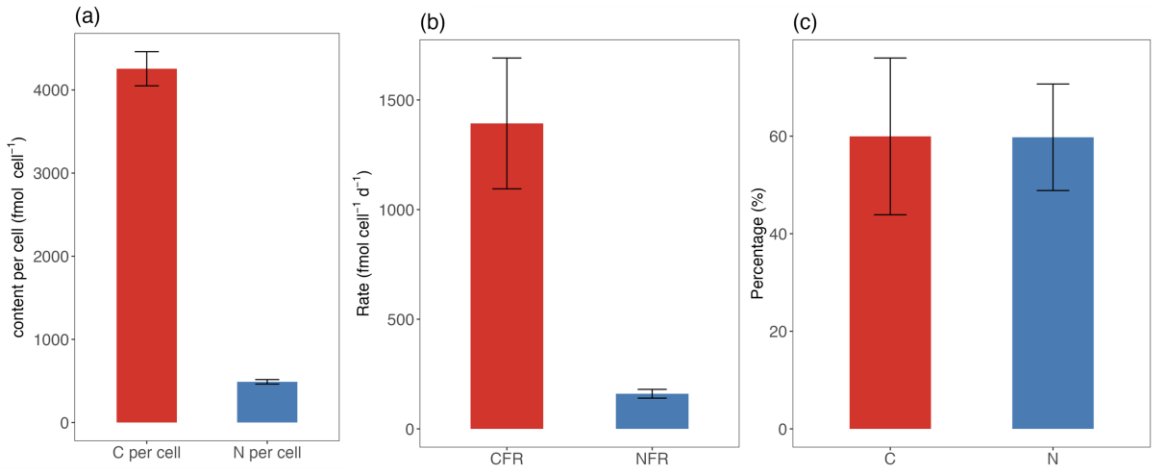

Figure 5. Summary of cellular growth, fixation rates, and elemental content for the UCYN-A2/B. bigelowii symbiosis. Panel (a) illustrates the carbon and nitrogen fixation rates per cell. Panel (b) quantifies the carbon and nitrogen content per cell. Panel (c) depicts the percentage of cellular biomass attributable to carbon and nitrogen fixation.

Table 6: Potential Grazing Contribution to Daily Growth Rate Requirement. The lower and upper estimates of cell length and width were determined using the lower quartile and upper quartile of the measured cells. Volumes were calculated following the methods outlined by Hillebrand et al. (1999). Biovolume was converted to biomass using the equation from Cermak et al. (2017), and the percentage of biomass from grazing was calculated based on trophic efficiency (Priyadarshi et al. 2019).

Estimates	**Lower estimate**	**Higher estimate**
Length (L) (μm)	2.36	2.73
Width (W) (μm)	0.228	0.296
Volume (μm^3)	0.0900	0.174
Biomass (fg C/cell)	9530	15100
Trophic Efficiency (%)	10	30
% biomass from grazing (%)	4.0	19

Supplementary table 1. Table showing the grazing rates per grazer calculated from two dilution experiments.

Supplementary table 1a. Table showing the grazing rates (Experiment 1)

	Total Bacteria	HNA	LNA
Bacteria μ with grazer	0.11	0.12	0.01
Bacteria μ with grazer	0.12	0.12	0.04
Bacteria μ with grazer	0.12	0.14	-0.05
Bacteria μ without grazer	1.25	1.27	0.94
Duration	24h	24h	24h
Grazer concentration mean	1.6E05	1.6E05	1.6E05
Bacteria concentration mean	2.4E07	2.2E07	2.0E06
Ingestion Rate (cells/grazer/h)	7.16	6.61	0.49
Ingestion Rate (cells/grazer/h)	7.12	6.59	0.47
Ingestion Rate (cells/grazer/h)	7.09	6.51	0.52
Mean	7.12	6.57	0.49
Stdev	0.03	0.05	0.02

Supplementary table 1b. Table showing the grazing rates (Experiment 2)

	Total Bacteria	HNA	LNA
Bacteria μ with grazer	0.16	0.16	0.04
Bacteria μ with grazer	0.16	0.7	0.11
Bacteria μ with grazer	0.17	0.16	0.41
Bacteria μ without grazer	0.78	0.80	0.44
Duration	24h	24h	24h
Grazer concentration mean	3.8E05	3.8E05	3.8E05
Bacteria concentration mean	9.0E07	8.6E07	4.4E06
Ingestion Rate (cells/grazer/h)	6.18	5.97	0.19
Ingestion Rate (cells/grazer/h)	6.09	5.91	0.16
Ingestion Rate (cells/grazer/h)	6.03	6.02	0.01
Mean	6.10	5.97	0.12
Stdev	0.07	0.05	0.09

Chapter 2: Temperature Constraints on the Growth, Carbon Fixation, and Nitrogen Fixation of the UCYN-A2/*Braarudosphaera bigelowii* symbiosis

Authors: Wing Kwan Esther Mak[1] (wimak@ucsc.edu), Kendra Turk-Kubo[1] (kturk@ucsc.edu), Anna V Voznyuk [1] (avoznyuk@ucsc.edu), Mary Rose Gradoville[1,2] (rgradoville@critfc.org), Kyoko Hagino[3] (kyokohagino@kochi-u.ac.jp), Jonathan P Zehr[1] (zehrj@ucsc.edu)

[1] Department of Ocean Sciences, University of California, Santa Cruz, CA, USA

[2] Columbia River Inter-Tribal Fish Commission, Portland, OR, USA

[3] Center for Advanced Marine Core Research, Kochi University, Kochi, Japan

Abstract

Dinitrogen (N_2)-fixing microorganisms play a crucial role in supplying nitrogen (N) to the oceans by converting atmospheric N_2 into bioavailable N. While N_2 fixation was traditionally thought to be limited to warm oligotrophic ocean waters, the symbiotic association between the N_2-fixing UCYN-A cyanobacterium and specific haptophytes, including *Braarudosphaera bigelowii* and relatives (UCYN-A symbiosis), has been found in many ocean environments, such as temperate coastal and cold polar waters. This study investigated the growth and activity of the only UCYN-A symbiosis in culture, the UCYN-A2/*B. bigelowii* symbiosis, in response to a range of temperatures in order to predict its global distribution and ecology. Incubation experiments were conducted with the UCYN-A2/*B. bigelowii* symbiosis isolate to determine growth rates, carbon (C) and N_2 fixation rates, and cell sizes across a temperature range of 6°C to 26°C. Growth rates were maximum in the range between 10°C and 22°C and lower at 6°C and 26°C. The size of both partners of the symbiosis decreased with temperature. The growth and activity across a wide range of temperatures helps to explain the wide geographic distribution in coastal waters, warm oligotrophic waters, and cooler temperate zones. This study provides the first growth and activity measurements from an isolate of the UCYN-A symbiosis, which contributes to a better understanding of the optimal temperature ranges for N_2 fixation in the UCYN-A symbiosis, providing vital information needed to parameterize the activity of the UCYN-A symbiosis in ecosystem models.

Introduction

Nitrogen (N) is a limiting nutrient that constrains primary productivity in the majority of the oceans (Falkowski et al., 1998; Moore et al., 2013). Important sources of N to the euphotic zones include upwelling and vertical mixing, as well as biological dinitrogen (N_2) fixation. The latter plays a substantial role in some regions, supporting over half of the export production, particularly in areas like the North Pacific Subtropical Gyre (Böttjer et al., 2017; Capone et al., 2005; Jickells et al., 2017; Karl et al., 1997).

Most marine N_2 fixation studies focused on the filamentous cyanobacterium *Trichodesmium* and the diatom cyanobacterial symbiont *Richelia* in warm ocean waters (>20°C) (Breitbarth et al., 2007), until the discovery of diverse N_2-fixing species, including the symbiotic unicellular cyanobacterial N_2-fixer *Candidatus* Atelocyanobacterium thalassa (UCYN-A), the unicellular cyanobacterium *Crocosphaera watsonii* (UCYN-B) , and diverse non-cyanobacteria (Waterbury & Rippka, 1989; Zehr et al., 1998). Since then, N_2-fixers have been found in a variety of oceanic habitats, and are not strictly confined to warm waters. In particular, UCYN-A has been detected in tropical and temperate waters in every major ocean basin (Farnelid et al., 2016; Martínez-Pérez et al., 2016; Shiozaki et al., 2015; Tang & Cassar, 2019), in nearshore coastal waters as well as the open ocean (Cabello et al., 2020; Mulholland et al., 2012; Turk-Kubo et al., 2021), and cold high latitude waters (Harding et al., 2018; Shiozaki et al., 2020).

UCYN-A are a group of very closely related unicellular cyanobacterial strains, that are metabolically reduced and symbiotic with specific haptophyte hosts comprised of *B. bigelowii* and closely related species/strains (herein referred to collectively as the UCYN_A symbiosis). UCYN-A fixes N_2 that is rapidly assimilated by the haptophyte in return for fixed carbon (Thompson et al., 2012). UCYN-A has a small genome that lacks many metabolic pathways including photosystem II and the TCA cycle (Tripp et al., 2010; Zehr et al., 2008), and is predicted to be highly dependent on its host for many metabolites (Sarkar et al., 2021). While it is known that there is an exchange of C and N between the partners (Thompson et al., 2012), the specific chemical forms remain unclear (Mills et al., 2020; Sarkar et al., 2021).

At least six sublineages of the UCYN-A symbiosis have been identified using quantitative PCR (qPCR)- and fluorescent in situ hybridization (FISH)-based methods (Thompson et al., 2014; Turk-Kubo et al., 2017). These sublineages include the smaller UCYN-A1 (~1 μm) in symbiosis with a small haptophyte (~2 μm), and UCYN-A2 (~2-3 μm) associated with a larger haptophyte, identified as *Braarudosphaera bigelowii* (~7-10 μm) (Bombar et al., 2014; Hagino et al., 2013; Thompson et al., 2014; Zehr & Bombar, 2015). Each of these sublineages has distinct genomic characteristics and niches (Bombar et al., 2014; Farnelid et al., 2016). The UCYN-A1 symbiosis is typically abundant in the oligotrophic open ocean, while the UCYN-A2 symbiosis is generally associated with coastally-influenced waters (Hagino et al., 2013; Turk-Kubo et al., 2017), although it has also been detected in the open ocean (Gradoville et al., 2020; Martínez-Pérez et al., 2016).

The contribution of the UCYN-A symbiosis to the oceanic N budget may be particularly important given its wide distribution throughout marine environments. However, little is known about how UCYN-A grows in cold and temperate waters, while other cyanobacterial N_2-fixers predominantly inhabit warmer regions. A compilation of global marine cyanobacterial N_2-fixer abundance data by Tang and Cassar (2019) showed that the empirical optimal temperature for *Trichodesmium* and UCYN-B is ~26-30°C, consistent with laboratory culture studies (Breitbarth et al., 2007; Fu et al., 2014) and their high abundances in the subtropical ocean gyres. In contrast, environmental data indicates that the UCYN-A symbiosis has its highest abundance in waters around ~24°C, however it is also the only marine cyanobacterial N_2-fixer that has been demonstrated to fix N_2 at temperatures below 4°C (Harding et al., 2018), suggesting broad temperature adaptation.

To better understand the influence of temperature on the growth and activity of the UCYN-A symbiosis, culture experiments were performed under temperature-controlled conditions ranging from 6-26°C. We conducted experiments with the UCYN-A2/*B. bigelowii symbiosis*, a recently cultivated coastal sublineage, henceforth referred to as 'the UCYN-A2/*B. bigelowii* symbiosis'. We hypothesized that the growth and activity of the UCYN-A2/*B. bigelowii* symbiosis would increase with temperatures typical of oligotrophic surface waters, yet could also grow at temperatures as low as 4°C typical of the Arctic region, where UCYN-A has been found (Harding et al., 2018). The effects of temperature on growth and cell physiology were determined by measuring growth rates (by cell count

and chlorophyll concentration), C and N_2 fixation rates, cell size, and elemental (C, N) content across the full temperature range used.

Methods

Cultivation and growth conditions

Ten-liters of sea surface water was collected from Furue Port, Nagasaki, Japan at 33°21'58.7"N 129°31'03.7"E on May 1, 2018. To eliminate large plankton, the sample was first passed through a 50 μm mesh plankton net, and cells were concentrated to approximately 50 mL with a 1 μm mesh net. The seawater samples were analyzed under an inverted light microscope (Olympus CKX41, Japan). A subsample of the concentrated seawater, containing *B. bigelowii* cells and other unknown types of phytoplankton was isolated with a capillary tube under the microscope and placed into a culture well with 10% F/2 medium and ca. 0.1% of GJ extract (Nishimura et al., 2020). It was then incubated under a light-dark cycle (12h light -12h dark) at 18˚C for two weeks to obtain a preculture. *B. bigelowii* and various other phytoplankton species both co-existed in this initial culture. Fifty μL of this cultured sample was transferred weekly into fresh media. From these cultured samples, *B. bigelowii* cells were isolated with capillaries, washed, and cultivated in the same medium. One particular isolate, named FR-21, successfully survived and grew. This isolate, FR-21, is accessible at Japan's National Institute for Environmental Studies as NIES-4399.

The FR-21 culture was maintained at a light intensity of 60 μmol photons $m^{-2}s^{-1}$ with a light-dark cycle of 12h:12h in a temperature-controlled incubator. For maintenance, the

culture was transferred periodically with modified seawater based-F/2 media (Guillard & Ryther, 1962) as described above. The seawater medium was based on water collected from 150 m and 200 m depths in Monterey Bay, California, USA (36°44'49.2"N 122°01'19.2"W).

Experimental Design

Temperature experiment 1

The goal of experiment 1 was to determine the duration of the exponential growth phase in the culture at different temperatures. For logistical reasons, primarily due to limited incubator availability, the experimental temperature treatments were divided into two sets. The UCYN-A2/*B. bigelowii* symbiosis culture was grown at 18°C, 22°C and 26°C for the first set of experiments, followed by 6°C, 10°C, 14°C, and 22°C in the second set of experiments. Constant temperatures were maintained using water baths equipped with internal circulators to ensure uniform temperature. Cultures were grown under cool white fluorescent light, provided by 20-Watt 2 ft Linear T12 Philips fluorescent tubes, characterized by a color temperature of 4100K, which produces a balanced, neutral white light. The light intensity was maintained at 60 $\pm$ 3 μmol photons m^{-2} s^{-1}, measured using a Quantum Scalar Laboratory (QSL) Radiometer (QSL-2100) using immersed settings. After at least 10 generations of growth, triplicate flasks of culture from each temperature were sampled and diluted to a starting concentration of approximately 8 $\times 10^4$ cells mL^{-1} in a

volume of 100 mL in a Corning® 75 cm^2 U-shaped canted neck cell culture flask. The cultures were grown for 18-23 days and were subsampled daily. The positions of the triplicate flasks were rotated daily to ensure equivalent light intensity. Subsamples for flow cytometry were taken by removing 1 mL of culture from each flask and fixing immediately with glutaraldehyde (Electron Microscopy Sciences, Hatfield, PA, United States) to a final concentration of 0.25% v/v, then incubating in the dark for 15 min and freezing at -80°C until further analysis.

Temperature experiment 2

After determining the duration of exponential growth phase, Experiment 2 aimed to measure the growth and activities during the exponential phase. In this experiment, the UCYN-A2/*B. bigelowii* symbiosis culture was grown at 18°C, 22°C and 26°C for the first set of experiments, followed by 6°C, 10°C, 14°C, and 22°C for the second set of experiments. The cultures were grown under 60 μmol photons $m^{-2}s^{-1}$ light intensity, and were diluted to the same starting concentration (8×10^4 cells mL^{-1}). In contrast to Experiment 1, the culture was regularly diluted to the initial concentration every 3-4 days, with this procedure repeated three times consecutively. Thus, the exponential phase was maintained over a total period of 9-12 days. The cultures were subsampled daily for flow cytometry (1 mL, as described above) and chlorophyll *a* concentration (0.95 mL). At each transfer, the culture was sampled for microscopy (0.5 mL). Additionally, 30 mL of the

culture was incubated in glass vials at the respective temperatures to measure C and N_2 fixation rates.

Flow cytometry analysis

Cell counts were measured using a BD Influx cell sorter with a 488 nm Sapphire laser (Coherent, Santa Clara, CA, United States). All samples were diluted 10-fold with 0.2 µm pore-size filtered culture media to achieve the linear range of the cytometer, then filtered through a CellTrics® filter with 30 µm pore-size mesh (Partec, Swedesboro, NJ, United States). The cells were identified and counted based on chlorophyll fluorescence (red florescence) and forward scatter (FSC; a proxy for cell size). Data were triggered on the FSC channel and events were counted for 5 min. The data was processed using Flowjo 10.8.0 (Tree Star, Inc., Ashland, OR, United States). Growth rates were calculated using the formula:

$$\mu = \ln(\frac{t_f}{t_0}) \div t$$

where t_f is the final cell concentration at the end of exponential growth period, t_0 denotes the initial cell concentration at the start, t is the duration of the period (x-x days).

Chlorophyll concentration

Culture samples from each flask (1 mL) were filtered through a Whatman GF/F filter (Cytiva, Marlborough, MA, USA) and were extracted with 90% acetone (HPLC grade, Fisher scientific, USA) overnight in the dark at 4°C. Chlorophyll concentrations were measured using a Turner Fluorometer TD-700 (Turner Designs, Inc., San Jose, CA) as described in Welschmeyer (1994).

C fixation, N_2 fixation, and C- and N-specific growth rate measurements

The C and N_2 fixation rates were determined using the ^{13}C technique and the $^{15}N_2$ tracer approach of Montoya et al. (1996), modified by Mohr et al. (2010) and Wilson et al. (2012). The preparation of $^{15}N_2$ enriched seawater followed the protocol outlined by Klawonn et al. (2015). Eight mL of $^{15}N_2$ gas (99 atom %, Cambridge Scientific) were introduced into 250 mL polycarbonate bottle of 0.2 μm pore-size filtered culture medium, vortexed for 5 minutes, and allowed to equilibrate at room temperature for over 24 hours. This enriched seawater was then transferred to 27 mL crimp-sealed glass serum vials, leaving no headspace. Three subsamples of the $^{15}N_2$ enriched seawater were stored for analysis of the initial atom % of N_2 using Membrane Inlet Mass Spectrometry (MIMS) (Ferrón et al., 2016), yielding atom $\%^{15}N_2$ values 42.7 ±1.4%.

For the rate measurement incubations, 1 mL of $^{15}N_2$ enriched seawater and 300 µL of 59 mM ^{13}C -labeled bicarbonate (99 atom% $NaH^{13}CO_3$, Cambridge Isotope Laboratories) were combined with 14 mL of the UCYN-A2/*B. bigelowii* symbiosis culture in 15 mL serum vials, crimp-sealed, and incubated at the designated temperatures for 24 hours. Time zero samples of $\delta^{13}C$ and $\delta^{15}N$ of the natural abundance particulate N (PN) and particulate C (PC) were prepared by adding 1 mL of filtered medium to 14 mL of the UCYN-A2/*B. bigelowii* symbiosis culture. After 24 hours, each incubation was filtered through pre-combusted 25 mm glass fiber filters (GF/F, Whatman) and stored at -80°C. Subsequently, filters were dried at 60°C for 24 hours, acid-fumed using 5 mL 12N hydrochloric acid for 48 hours, and then pressed into tin capsules. The samples were analyzed at the University of California Santa Cruz Stable Isotope Laboratory for particulate C, particulate N, and isotopic composition ($\delta^{13}C$, $\delta^{15}N$) using a CE Instruments NC2500 elemental analyzer connected to a Thermo Scientific DELTAplus XP isotope ratio mass spectrometer through a universal continuous flow interface Thermo-Scientific Conflo III. N_2 fixation rates were calculated using the equation from Montoya et al. (1996):

$$N_2\ fixation\ rate(fmol\ cell^{-1}\ d^{-1}) = \frac{A_{PN} - A_{PN_0}}{A_{N_2} - A_{PN_0}} * \frac{[PN]}{\Delta t} * \frac{1}{cell}$$

where A_{PN} and A_{PN0} represent the fractional ^{15}N enrichment (in atom %) after and before incubation, respectively; [PN] denotes the particulate N concentration at the end of the

incubation period; Δt represents the incubation duration in hours; and A_{N2} refers to the fractional ^{15}N -enrichment of the N_2 source pool, as determined by MIMS. The N_2 fixation rate per cell was calculated by dividing the bulk rate by the cell count, as determined by flow cytometry. The limits of detection (LOD) and minimum quantifiable rates (MQR) were computed according to Gradoville et al. (2017). Similarly, C fixation rates were determined by the following equation:

$$C\ fixation\ rate(fmol\ cell^{-1}\ d^{-1}) = \frac{A_{PC} - A_{PC_0}}{A_{CO_2} - A_{PC_0}} * \frac{[PC]}{\Delta t} * \frac{1}{cell}$$

where A_{PC} corresponds to the fractional ^{13}C enrichment, expressed in atom percentage, after the incubation period, while A_{PC0} represents the same prior to incubation. The symbol [PC] represents the particulate C concentration at the end of the incubation. A_{CO_2}refers to the fractional ^{13}C enrichment of the bicarbonate source pool.

The C and N specific growth rates were calculated by the equation:

$$N\ specific\ growth\ rate(\ d^{-1}) = \frac{A_{PN} - A_{PN_0}}{A_{N_2} - A_{PN_0}} * \frac{1}{\Delta t}$$

$$C\ specific\ growth\ rate(\ d^{-1}) = \frac{A_{PC} - A_{PC_0}}{A_{CO_2} - A_{PC_0}} * \frac{1}{\Delta t}$$

Microscopy

Samples (0.5 mL) of the culture were collected for microscopy and fixed with 37% formaldehyde at a final concentration of 2% overnight, then filtered through 0.6 µm pore-size polycarbonate filters (Millipore Isopore, EMD Millipore, Billerica, MA, USA) backed with 0.8 µm pore-size cellulose acetate filters (Sterlitech Corp. Kent, WA, USA), Finally, the samples were frozen at -80°C until the time of further analysis. The filters were stained with DAPI by ProLong Diamond Antifade Mountant with DAPI (Thermo Fisher, Waltham, Massachusetts, USA) for 24 hours, then were examined by epifluorescence microscopy (Axio Imager 2, Zeiss, Dublin, CA, United States) at 630X magnification under blue light, and images were captured with Zeiss ZEN Digital Imaging for Light Microscopy software. Length and width of 30 cells per temperature treatment were measured with the image analysis software Fiji (Schindelin et al., 2012; Schneider et al., 2012). The volume of the UCYN-A2/*B. bigelowii* symbiosis cells were calculated with the spheroid formula:

$$Volume\ = \frac{\pi}{6} \times d^2 \times h$$

where d is the diameter at the apical section and h is height.

The volume of the symbiont is calculated by the sphere formula:

$$Volume = \frac{\pi}{6} \times d^3$$

where d is the diameter at the cross section (Hillebrand et al., 1999).

Dunn test statistics

The Shapiro-Wilk test was employed to test the normality of the data. Subsequently, the Barnett test was utilized to check the equality of variances across groups. The Kruskal-Wallis test was performed to determine if there were any significant differences among the groups, followed by the Dunn test, which was corrected for multiple comparisons using the Bonferroni method, to determine the pairwise differences among the temperature groups. All statistical analyses were performed using R version 4.3.1 in RStudio version 2023.06.1+524 (R Core Team, 2021; RStudio Team, 2021). The significance level for all statistical tests was set at $p < 0.05$.

Results

Growth Curves

The goal of Experiment 1 was to measure growth curves at various temperatures in order to identify the duration of the exponential growth phase (Supplemental Figure 1a and 1b).

For cells at 18°C, 22°C, and 26°C, the exponential phase occurred between day 1-5. For these temperatures, the cultures were transferred and measured on day 3 for each transfer.

There was greater variability at 6°C, 10°C, 14°C, and 22°C. Rapid growth was observed between days 1-7 for 14°C and 22°C, while cells at 10°C showed the highest variability, with an exponential phase between day 1-5. Cell abundances at 6°C declined slowly from day 0-7, followed by a constant population size throughout the rest of the experiment. Based on these observations, subsequent transfers and measurements for 6°C, 10°C, 14°C, and 22°C took place on day 4.

Growth rates, C and N_2 fixation rates

Growth rates across three transfers for each temperature treatment were assessed using daily cell counts and chlorophyll concentrations in Experiment 2. Growth rates based on cell counts increased with temperature, peaking at 22°C (μ=0.49 ± 0.10), with slower growth at 26°C (μ=0.40 ± 0.06) and growth at 6°C being indistinguishable from zero (Figure 1a). It is important to note that the growth rates at 22°C, which peaked (μ=0.49 ± 0.10), are representative of the first set of experiments conducted at 18°C, 22°C, and 26°C. This distinction is crucial as the 22°C results from the second set of experiments (featuring 6°C, 10°C, 14°C, and 22°C) were not included due to the loss of symbionts in these conditions. The temperature trends were similar for C and N-specific growth rates, with the highest growth rates occurring at 18°C and 22°C ($\mu_{18°C}$ = 0.29 ± 0.06, $\mu_{22°C}$ = 0.29 ±

0.03) along with a decline at 26°C ($\mu_{26°C}$ = 0.22 ± 0.04). There were positive correlations between growth rates assessed by cell count and C-specific growth rates (slope 1.57, R^2 = 0.94, Figure 2a) and between C-specific and N-specific growth rates (slope 1.33, R^2 = 0.96, Figure 2c).

C and N_2 fixation rates of the UCYN-A/*B.bigelowii* symbiosis were assessed on the day of transfer. The lowest cell-specific C fixation rates were at 6°C and 26°C (6°C: 754 ± 97 fmol C $cell^{-1}$ d^{-1}, 26°C: 767 ± 129 fmol C $cell^{-1}$ d^{-1}). Rates measured in treatments between 10°C and 22°C were significantly higher (mean: 1205 ± 280 fmol C $cell^{-1}$ d^{-1}, Figure 3a) and did not differ among treatments. Similarly, N_2 fixation rates from 10°C to 22°C were not significantly different among temperature treatments (mean: 111 ± 33 fmol C $cell^{-1}$ $d^{-1,}$ Figure 3b). However, when C and N_2 fixation rates are normalized with biomass, both C and N_2 fixation rates per C biomass increased with temperature, reaching their maximum values within the 18°C to 22°C range (Figure 3c and 3d). All rates are higher than the limit of quantification. The C fixation to N_2 fixation ratio (CFR:NFR) and elemental C:N ratios were also examined. While CFR:NFR was highest at 6°C (34.1 ± 8.0) , and remained similar from 10°C to 26°C (11.6 ± 3.4) (Figure 4a), C:N ratios were consistently 8.8 ± 1.1(Figure 4b, Supplemental figure 2).

Cell Sizes

Temperature-driven changes in cell morphology and physiology were investigated by measuring cellular C, N, and chlorophyll fluorescence, cell biovolume, and forward scatter on the flow cytometer as a proxy for cell size. C and N content per cell decreased with temperature, with 6°C cells containing 6-10 times more C and N than cells at the optimum growth temperature (Figure 5a and 5b). Chlorophyll fluorescence per cell, measured by fluorometry, also decreased with increasing temperatures (Figure 5c), following a similar trend with C and N content per cell. These observations were supported by microscopy-based biovolume measurements which showed that both partners (*B. bigelowii* and the UCYN-A symbiont/spheroid body) decreased in biovolume with increasing temperature, with the 6°C and 10°C treatments having significantly larger biovolumes than 14°C to 26°C treatments (Figure 6a and 6b), which was also observed in the microscopy images (Figure 6d). The ratio of sizes of the partners, however, was constant across temperatures (Figure 6c).

Discussion

Temperature impacts on the physiology, morphology, and C:N stoichiometry of the UCYN-A2/*B. bigelowii* symbiosis

This is the first report of growth and activities of the UCYN-A2/*B. bigelowii* symbiosis in culture, which enables the characterization of its stoichiometry and physiology under controlled nutrient and light conditions. The results show that the UCYN-A2/*B. bigelowii* symbiosis had increasing growth rates with increasing temperature from 6°C to 22°C, after which the rates declined, which is consistent with the phytoplankton temperature-growth relationship described by Eppley (1972). According to the model, the rate of growth of phytoplankton should approximately double for every 10°C rise in temperature within a biologically suitable range, followed by a decline as temperatures exceed optimal levels. In our study, this pattern is evident in the growth rates determined through cell counts, C-specific growth rates, and the measurement of chlorophyll content. Increases in growth rate as a function of temperature are attributed to increased rates of cellular processes (Li, 1980) including photosynthesis and respiration. Above the optimal temperature (22°C in this case), growth rate decreases are likely due to heat-induced thermal stress on enzymatic reactions (Ratkowsky et al., 1983).

In contrast to growth rates, there were no statistical differences in C fixation rates between 10°C and 22°C. Other haptophytes such as *Emiliania huxleyii* and *Chrysochromulina* also

maintain comparable C fixation rates across a broad temperature spectrum (Wang et al. 2019). Several hypotheses exist to explain how *E. huxleyii* maintains C fixation rates at a broad range of temperatures, including adjusting membrane fluidity through fatty acid composition changes (Bi et al., 2018) and modifying the relative abundance or activity of C fixation enzymes, like Rubisco, in response to temperature shifts (Dedman et al., 2023). *Chrysochromulina* has been shown to adjust the activity of C-concentrating mechanisms, concentrating C around Rubisco (Hennon et al., 2017). The UCYN-A symbiosis may employ similar mechanisms to maintain C fixation rates across a diverse range of temperatures. Maintaining a constant C fixation rate across a broad temperature range allows the UCYN-A symbiosis to efficiently utilize light for growth and activity, remaining competitive under varying environmental conditions, or ensure a surplus of carbon when the growth rate is low.

N_2 fixation rates were also constant within the temperature range of 10°C to 22°C, with lower rates detectable over the full temperature range tested (6°C to 26°C). N_2 fixation is an energetically expensive process that requires ATP, and synchronization of C fixation and N_2 fixation allows the efficient transfer of energy generated by C fixation to the N_2 fixation process. Our results showed that the temperature for the UCYN-A symbiosis is broader (10°C to 22°C) and peaks at lower temperatures compared to other cyanobacterial N_2-fixers such as *Crocosphaera* (24°C to 32°C, peaking around 28°C to 30°C; Fu et al., 2014) or *Trichodesmium* (18°C to 32°C, maximum in range of 24 – 28°C) (Fu et al., 2014). While the factors contributing to this distinct optimal temperature range are not fully understood,

it could be speculated that living in symbiosis with the haptophyte may influence the optimal temperature range for N_2 fixation. Evolving to synchronize the optimal N_2 fixation temperature within a similar range to the haptophyte growth rate offers an ecological advantage in obtaining the necessary energy and fuel for N_2 fixation.

While the C:N ratio of the symbiosis remained relatively constant, the CFR: NFR ratio decreases with increasing temperature. At 6°C, the CFR: NFR exceeds the C:N ratio, whereas at temperatures between 10°C and 26°C, the ratios are more similar. At lower temperatures, the decrease in N_2 fixation rate is more pronounced than the decrease in C fixation rate. The cells may fix more C relative to N while maintaining the same overall C:N ratio, which could be attributed to C excretion or the reliance on an alternative N source at lower temperatures. This suggests that in colder conditions, the cells might adjust their metabolic strategy to maintain optimal growth and activity.

The results are consistent with smaller cell sizes at higher temperatures that are more efficient in nutrient uptake due to the larger surface area-to-volume ratio (Raven & Geider, 1988; Verberk et al., 2021). This adaptation is not unique to the UCYN-A symbiosis but is also observed in other phytoplankton including haptophytes such as *Prymnesium kappa* and *Calyptrosphaera sp.* (Standeren, 2018). The consistency in C and N_2 fixation rates across a wide temperature range could be a result of the alterations in cell size. This speculation is supported by the observed similar pattern of C and N_2 fixation rates when normalized to biomass and growth rates as determined by cell division (Figure 3c and 3d).

Beyond temperature: multiple factors influencing biogeographical constraints of UCYN-A2/*B. bigelowii* symbiosis

The single-cell N_2 fixation rates for the UCYN-A2/*B. bigelowii* symbiosis at 14 -18°C averaged 114.8 ± 36.3 fmol N $cell^{-1}d^{-1}$, which is consistent with previous field measurements in the Southern California Current system (151.1 ± 112.7 fmol N /cell/d) which were at 14 -18°C (Turk-Kubo et al., 2021). At the most coastal station of this study, measured single cell N_2 fixation was 196 ± 33 fmol N $cell^{-1}d^{-1}$ at 16 -20°C. However, a study by Martínez-Pérez et al. (2016) in the offshore North Atlantic reported a rate of 220 fmol N $cell^{-1}d^{-1}$ at 27°C, which is three times the rate we measured at 26°C. On the other hand, the N_2 fixation rate of UCYN-A2/*B. bigelowii* at 10°C in culture (106.1 ± 38.4 fmol N/cell/day) was observed to be eight times higher than the rates reported in Harding et al. (2018) from the Bering Sea off Nome, Alaska (13.0 ± 7.7 fmol N/cell/day at 10.1°C). At our lowest temperature experiment, 6°C, our lab-measured rate (24.6 ± 7.0 fmol N/cell/day) was also twenty times higher than the 4°C rate that they reported (1.1 ± 2.0 fmol N/cell/day). It is important to note, interpretations of these comparisons must be made with caution, as the rates from field-collected samples require different pre-processing steps to visualize the symbiosis. Harding et al. (2018) estimated the cell-specific N_2 fixation rate using catalyzed reporter deposition (CARD)-FISH coupled to nanoscale secondary ion mass spectrometry (nanoSIMS), likely underestimating rates by up to 12% due to ^{15}N dilution in CARD-FISH (Harding et al., 2022; Meyer et al., 2021). However, our method

measured bulk community rates, determining individual cell N_2 fixation rates by dividing these by cell counts, avoiding isotope dilution challenges encountered in CARD-FISH analyzed samples.

Even after adjusting for the potential underestimation from field samples, our rates at low temperature are higher than the previous measurements in the Bering Sea. This implies factors beyond temperature might constrain the N_2 fixation rate in nature. Light availability could be one such factor. Although daylight hours are extended in the Arctic summer, the region receives sunlight at a lower angle, resulting in generally lower overall irradiance compared to the tropics. Additionally, the light exposure duration in the study by Harding et al. (2018) was longer than the 12/12 light/dark cycle we used in our lab experiments. Another key factor is the nutrient availability in the culture medium versus the natural environment. Our UCYN-A2/*B. bigelowii* cultures were grown in nutrient-replenished F/2 medium, which contains nutrient concentrations (particularly PO_4 and Fe) at least an order of magnitude higher than those in Arctic waters, highlighting a potential variable that could be influencing biogeographical patterns.

Our results suggest that while temperature plays a role, it is not the sole determinant of N_2 fixation rates in colder environments like the Arctic Ocean. Other factors such as nutrient availability and light conditions may also significantly influence these rates. The conclusion contradicts the predictions of the model presented by Wang et al. (2019), which proposed that N_2 fixation rates in the Arctic are minimal and primarily temperature-limited.

Our data imply that given the right or changing ocean conditions, the UCYN-A2 symbiosis has the potential to contribute to higher N_2 fixation rates in such environments.

Our study is the first to characterize the growth kinetics of the UCYN-A2/*B. bigelowii* culture, addressing a critical gap in our understanding. Biogeochemical ocean models, such as the ECCO-Darwin model (Carroll et al., 2020), have previously been constrained by the lack of data on UCYN-A symbiosis due to the absence of controlled lab cultures. For instance, the study by Dugenne et al. (2023) on diazotroph growth rates in mesoscale eddies underscores this limitation: while they could predict growth rates for several diazotrophs based on *in situ* conditions, the growth of UCYN-A could not be modeled due to the lack of culture data and growth parameterization. Our research now offers essential data on how growth and activities of the UCYN-A2/*B. bigelowii* symbiosis vary with temperature in controlled environments. These new findings allow for a more accurate incorporation of the UCYN-A2/*B. bigelowii* symbiosis into models, thereby enhancing our predictions and understanding of marine biogeochemical cycles.

The findings offer insights into how temperature may influence the distribution of the UCYN-A2/*B. bigelowii* symbiosis and hint at potential implications for global N_2 fixation, especially considering the warming trends in most oceanic regions. However, it is important to note that several UCYN-A symbiosis sublineages have different niches, making generalizations challenging. For instance, UCYN-A1, a smaller-sized sublineage, demonstrates higher abundances within subtropical gyres. These regions can have

temperatures reaching 26°C, surpassing the optimal temperature range for the UCYN-A2/*B. bigelowii* symbiosis (Gradoville et al., 2020). This suggests that these two sublineages may have different temperature optima. Similarly, UCYN-A1 is found at higher abundances in colder regions than UCYN-A2 (Harding et al., 2018), hinting that the more widespread UCYN-A1 may be better adapted to colder waters. These subtleties caution against broad generalizations based on our UCYN-A2/*B. bigelowii* study, as it represents only a specific strain in culture. Nonetheless, this work provides a valuable first set of measurements for a UCYN-A strain.

Future research should investigate the temperature sensitivity of other UCYN-A sublineages to obtain a comprehensive understanding of the contribution of this N_2-fixer to biogeochemical cycles. However, such investigations pose challenges, as only a few UCYN-A strains have been successfully cultured. Notably, the UCYN-A2/*B. bigelowii* strain was the first UCYN-A strain brought into culture. Delving into the molecular mechanisms driving cellular biochemical responses could also prove insightful. Our study elucidates the role of the abundant N_2-fixer UCYN-A in biogeochemical cycles in marine environments with differing temperature conditions.

References

Bi, R., Ismar, S. M., Sommer, U., & Zhao, M. (2018). Simultaneous shifts in stoichiometric and fatty acid composition of *Emiliania huxleyi* in response to environmental changes 2.

Bombar, D., Heller, P., Sanchez-Baracaldo, P., Carter, B. J., & Zehr, J. P. (2014). Comparative genomics reveals surprising divergence of two closely related strains of uncultivated UCYN-A cyanobacteria. *8*(12), 2530-2542. https://doi.org/10.1038/ismej.2014.167

Böttjer, D., Dore, J. E., Karl, D. M., Letelier, R. M., Mahaffey, C., Wilson, S. T., Zehr, J., & Church, M. J. (2017). Temporal variability of nitrogen fixation and particulate nitrogen export at Station ALOHA. *Limnology and Oceanography*, *62*(1), 200-216. https://doi.org/10.1002/lno.10386

Breitbarth, E., Oschlies, A., & LaRoche, J. (2007). Physiological constraints on the global distribution of *Trichodesmium* effect of temperature on diazotrophy. *Biogeosciences*, *4*(1), 53-61. https://doi.org/10.5194/bg-4-53-2007

Cabello, A. M., Turk-Kubo, K. A., Hayashi, K., Jacobs, L., Kudela, R. M., & Zehr, J. P. (2020). Unexpected presence of the nitrogen-fixing symbiotic cyanobacterium UCYN-A in Monterey Bay, California. *J Phycol*, *56*(6), 1521-1533. https://doi.org/10.1111/jpy.13045

Capone, D. G., Burns, J. A., Montoya, J. P., Subramaniam, A., Mahaffey, C., Gunderson, T., Michaels, A. F., & Carpenter, E. J. (2005). Nitrogen fixation by *Trichodesmium* spp.: An important source of new nitrogen to the tropical and subtropical North

Atlantic Ocean. *Global Biogeochemical Cycles*, *19*(2), n/a-n/a. https://doi.org/10.1029/2004gb002331

Carroll, D., Menemenlis, D., Adkins, J., Bowman, K., Brix, H., Dutkiewicz, S., Fenty, I., Gierach, M., Hill, C., & Jahn, O. (2020). The ECCO-Darwin data-assimilative global ocean biogeochemistry model: Estimates of seasonal to multidecadal surface ocean pCO2 and air-sea CO_2 flux. *Journal of Advances in Modeling Earth Systems*, *12*(10), e2019MS001888.

Dedman, C. J., Barton, S., Fournier, M., & Rickaby, R. E. (2023). The cellular response to ocean warming in *Emiliania huxleyi*. *Frontiers in Microbiology*, *14*, 1177349.

Dugenne, M., Gradoville, M. R., Church, M. J., Wilson, S. T., Sheyn, U., Harke, M. J., Björkman, K. M., Hawco, N. J., Hynes, A. M., Ribalet, F., Karl, D. M., DeLong, E. F., Dyhrman, S. T., Armbrust, E. V., John, S., Eppley, J. M., Harding, K., Stewart, B., Cabello, A. M., . . . Zehr, J. P. (2023). Nitrogen Fixation in Mesoscale Eddies of the North Pacific Subtropical Gyre: Patterns and Mechanisms. *Global Biogeochemical Cycles*, *37*(4), e2022GB007386. https://doi.org/https://doi.org/10.1029/2022GB007386

Eppley, R. W. (1972). Temperature and phytoplankton growth in the sea. *Fish. bull*, *70*(4), 1063-1085.

Falkowski, Barber, R. T., & Smetacek, V. (1998). Biogeochemical Controls and Feedbacks on Ocean Primary Production. *Science*, *281*(5374), 200-206. https://doi.org/doi:10.1126/science.281.5374.200

Farnelid, H., Turk-Kubo, K., Muñoz-Marín, M., & Zehr, J. (2016). New insights into the ecology of the globally significant uncultured nitrogen-fixing symbiont UCYN-A. *Aquatic Microbial Ecology*, *77*(3), 125-138. https://doi.org/10.3354/ame01794

Ferrón, S., del Valle, D. A., Björkman, K. M., Quay, P. D., Church, M. J., & Karl, D. M. (2016). Application of membrane inlet mass spectrometry to measure aquatic gross primary production by the 18O in vitro method. *Limnology and Oceanography: Methods*, *14*(9), 610-622.

Fu, F.-X., Yu, E., Garcia, N. S., Gale, J., Luo, Y., Webb, E. A., & Hutchins, D. A. (2014). Differing responses of marine N_2 fixers to warming and consequences for future diazotroph community structure. *Aquatic Microbial Ecology*, *72*(1), 33-46.

Gradoville, M. R., Bombar, D., Crump, B. C., Letelier, R. M., Zehr, J. P., & White, A. E. (2017). Diversity and activity of nitrogen-fixing communities across ocean basins. *Limnology and Oceanography*, *62*(5), 1895-1909.

Gradoville, M. R., Farnelid, H., White, A. E., Turk-Kubo, K. A., Stewart, B., Ribalet, F., Ferrón, S., Pinedo-Gonzalez, P., Armbrust, E. V., Karl, D. M., John, S., & Zehr, J. P. (2020). Latitudinal constraints on the abundance and activity of the cyanobacterium UCYN-A and other marine diazotrophs in the North Pacific. *Limnology and Oceanography*. https://doi.org/10.1002/lno.11423

Guillard, R. R., & Ryther, J. H. (1962). Studies of marine planktonic diatoms: I. *Cyclotella nana Hustedt*, and *Detonula confervacea* (Cleve) *Gran*. *Canadian journal of microbiology*, *8*(2), 229-239.

Hagino, K., Onuma, R., Kawachi, M., & Horiguchi, T. (2013). Discovery of an Endosymbiotic Nitrogen-Fixing Cyanobacterium UCYN-A in *Braarudosphaera bigelowii* (*Prymnesiophyceae*). *8*(12), e81749. https://doi.org/10.1371/journal.pone.0081749

Harding, K., Turk-Kubo, K. A., Sipler, R. E., Mills, M. M., Bronk, D. A., & Zehr, J. P. (2018). Symbiotic unicellular cyanobacteria fix nitrogen in the Arctic Ocean. *Proceedings of the National Academy of Sciences*, *115*(52), 13371-13375. https://doi.org/10.1073/pnas.1813658115

Harding, K. J., Turk-Kubo, K. A., Mak, E. W. K., Weber, P. K., Mayali, X., & Zehr, J. P. (2022). Cell-specific measurements show nitrogen fixation by particle-attached putative non-cyanobacterial diazotrophs in the North Pacific Subtropical Gyre. *Nature Communications*, *13*(1), 1-10.

Hennon, G. M., Hernández Limón, M. D., Haley, S. T., Juhl, A. R., & Dyhrman, S. T. (2017). Diverse CO_2-induced responses in physiology and gene expression among eukaryotic phytoplankton. *Frontiers in Microbiology*, *8*, 2547.

Hillebrand, H., Dürselen, C.-D., Kirschtel, D., Pollingher, U., & Zohary, T. (1999). Biovolume Calculation for Pelagic and Benthic Microalgae. *Journal of Phycology*, *35*(2), 403-424. https://doi.org/https://doi.org/10.1046/j.1529-8817.1999.3520403.x

Jickells, T. D., Buitenhuis, E., Altieri, K., Baker, A. R., Capone, D., Duce, R. A., Dentener, F., Fennel, K., Kanakidou, M., LaRoche, J., Lee, K., Liss, P., Middelburg, J. J., Moore, J. K., Okin, G., Oschlies, A., Sarin, M., Seitzinger, S., Sharples, J., . . .

Zamora, L. M. (2017). A reevaluation of the magnitude and impacts of anthropogenic atmospheric nitrogen inputs on the ocean. *Global Biogeochemical Cycles*, *31*(2), 289-305. https://doi.org/https://doi.org/10.1002/2016GB005586

Karl, D., Letelier, R., Tupas, L., Dore, J., Christian, J., & Hebel, D. (1997). The role of nitrogen fixation in biogeochemical cycling in the subtropical North Pacific Ocean. *Nature*, *388*(6642), 533-538. https://doi.org/10.1038/41474

Klawonn, I., Bonaglia, S., Brüchert, V., & Ploug, H. (2015). Aerobic and anaerobic nitrogen transformation processes in N_2-fixing cyanobacterial aggregates. *The ISME journal*, *9*(6), 1456-1466.

Li, W. K. (1980). Temperature adaptation in phytoplankton: cellular and photosynthetic characteristics. *Primary productivity in the sea*, 259-279.

Martínez-Pérez, C., Mohr, W., Löscher, C. R., Dekaezemacker, J., Littmann, S., Yilmaz, P., Lehnen, N., Fuchs, B. M., Lavik, G., Schmitz, R. A., Laroche, J., & Kuypers, M. M. M. (2016). The small unicellular diazotrophic symbiont, UCYN-A, is a key player in the marine nitrogen cycle. *Nature Microbiology*, *1*(11), 16163. https://doi.org/10.1038/nmicrobiol.2016.163

Meyer, N. R., Fortney, J. L., & Dekas, A. E. (2021). NanoSIMS sample preparation decreases isotope enrichment: magnitude, variability and implications for single-cell rates of microbial activity. *Environmental Microbiology*, *23*(1), 81-98.

Mills, M. M., Turk-Kubo, K. A., van Dijken, G. L., Henke, B. A., Harding, K., Wilson, S. T., Arrigo, K. R., & Zehr, J. P. (2020). Unusual marine cyanobacteria/haptophyte

symbiosis relies on N_2 fixation even in N-rich environments. *The ISME journal*, *14*(10), 2395-2406.

Mohr, W., Intermaggio, M. P., & Laroche, J. (2010). Diel rhythm of nitrogen and carbon metabolism in the unicellular, diazotrophic cyanobacterium *Crocosphaera watsonii* WH8501. *12*(2), 412-421. https://doi.org/10.1111/j.1462-2920.2009.02078.x

Montoya, J. P., Voss, M., Kahler, P., & Capone, D. G. (1996). A simple, high-precision, high-sensitivity tracer assay for N_2 fixation. *Applied and Environmental Microbiology*, *62*(3), 986-993.

Moore, C., Mills, M., Arrigo, K., Berman-Frank, I., Bopp, L., Boyd, P., Galbraith, E., Geider, R., Guieu, C., & Jaccard, S. (2013). Processes and patterns of oceanic nutrient limitation. *Nature Geoscience*, *6*(9), 701-710.

Mulholland, M., Bernhardt, P., Blanco-Garcia, J., Mannino, A., Hyde, K., Mondragon, E., Turk, K., Moisander, P., & Zehr, J. (2012). Rates of dinitrogen fixation and the abundance of diazotrophs in North American coastal waters between Cape Hatteras and Georges Bank. *Limnology and Oceanography*, *57*(4), 1067-1083.

Nishimura, T., Uchida, H., Noguchi, R., Oikawa, H., Suzuki, T., Funaki, H., Ihara, C., Hagino, K., Arimitsu, S., Tanii, Y., Abe, S., Hashimoto, K., Mimura, K., Tanaka, K., Yanagida, I., & Adachi, M. (2020). Abundance of the benthic dinoflagellate *Prorocentrum* and the diversity, distribution, and diarrhetic shellfish toxin production of *Prorocentrum lima* complex and *P. caipirignum* in Japan. *Harmful Algae*, *96*, 101687. https://doi.org/https://doi.org/10.1016/j.hal.2019.101687

Ratkowsky, D., Lowry, R., McMeekin, T., Stokes, A., & Chandler, R. (1983). Model for bacterial culture growth rate throughout the entire biokinetic temperature range. *Journal of Bacteriology*, *154*(3), 1222-1226.

Raven, J. A., & Geider, R. J. (1988). Temperature and algal growth. *New phytologist*, *110*(4), 441-461.

Sarkar, D., Landa, M., Bandyopadhyay, A., Pakrasi, H. B., Zehr, J. P., & Maranas, C. D. (2021). Elucidation of trophic interactions in an unusual single-cell nitrogen-fixing symbiosis using metabolic modeling. *PLoS Comput Biol*, *17*(5), e1008983. https://doi.org/10.1371/journal.pcbi.1008983

Schindelin, J., Arganda-Carreras, I., Frise, E., Kaynig, V., Longair, M., Pietzsch, T., Preibisch, S., Rueden, C., Saalfeld, S., Schmid, B., Tinevez, J.-Y., White, D. J., Hartenstein, V., Eliceiri, K., Tomancak, P., & Cardona, A. (2012). Fiji: an open-source platform for biological-image analysis. *Nature methods*, *9*(7), 676-682. https://doi.org/10.1038/nmeth.2019

Schneider, C. A., Rasband, W. S., & Eliceiri, K. W. (2012). NIH Image to ImageJ: 25 years of image analysis. *Nature methods*, *9*(7), 671-675. https://doi.org/10.1038/nmeth.2089

Shiozaki, T., Fujiwara, A., Inomura, K., Hirose, Y., Hashihama, F., & Harada, N. (2020). Biological nitrogen fixation detected under Antarctic sea ice. *Nature geoscience*, *13*(11), 729-732.

Shiozaki, T., Nagata, T., Ijichi, M., & Furuya, K. (2015). Nitrogen fixation and the diazotroph community in the temperate coastal region of the northwestern North Pacific. *Biogeosciences*, *12*(15), 4751-4764.

Standeren, E. (2018). *Cell-and genome size responses to different temperatures in haptophytes*

Tang, W., & Cassar, N. (2019). Data-Driven Modeling of the Distribution of Diazotrophs in the Global Ocean. *Geophysical Research Letters*, *46*(21), 12258-12269. https://doi.org/10.1029/2019GL084376

Thompson, A., Carter, B. J., Turk-Kubo, K., Malfatti, F., Azam, F., & Zehr, J. P. (2014). Genetic diversity of the unicellular nitrogen-fixing cyanobacteria UCYN-A and its prymnesiophyte host. *Environmental Microbiology*, *16*(10), 3238-3249. https://doi.org/10.1111/1462-2920.12490

Thompson, A. W., Foster, R. A., Krupke, A., Carter, B. J., Musat, N., Vaulot, D., Kuypers, M. M. M., & Zehr, J. P. (2012). Unicellular Cyanobacterium Symbiotic with a Single-Celled Eukaryotic Alga. *Science*, *337*(6101), 1546-1550. https://doi.org/10.1126/science.1222700

Tripp, H. J., Bench, S. R., Turk, K. A., Foster, R. A., Desany, B. A., Niazi, F., Affourtit, J. P., & Zehr, J. P. (2010). Metabolic streamlining in an open-ocean nitrogen-fixing cyanobacterium. *464*(7285), 90-94. https://doi.org/10.1038/nature08786

Turk-Kubo, K. A., Farnelid, H. M., Shilova, I. N., Henke, B., & Zehr, J. P. (2017). Distinct ecological niches of marine symbiotic N_2-fixing cyanobacterium *Candidatus*

Atelocyanobacterium thalassa sublineages. *Journal of Phycology*, *53*(2), 451-461. https://doi.org/10.1111/jpy.12505

Turk-Kubo, K. A., Mills, M. M., Arrigo, K. R., van Dijken, G., Henke, B. A., Stewart, B., Wilson, S. T., & Zehr, J. P. (2021). UCYN-A/haptophyte symbioses dominate N_2 fixation in the Southern California Current System. *ISME Communications*, *1*(1), 1-13.

Verberk, W. C., Atkinson, D., Hoefnagel, K. N., Hirst, A. G., Horne, C. R., & Siepel, H. (2021). Shrinking body sizes in response to warming: explanations for the temperature–size rule with special emphasis on the role of oxygen. *Biological Reviews*, *96*(1), 247-268.

Wang, W.-L., Moore, J. K., Martiny, A. C., & Primeau, F. W. (2019). Convergent estimates of marine nitrogen fixation. *Nature*, *566*(7743), 205-211.

Waterbury, & Rippka. (1989). Subsection I. Order *Chroococcaloes*. *Bergey's manual of systematic bacteriology*, *3*, 1728 -1746.

Welschmeyer, N. A. (1994). Fluorometric analysis of chlorophyll a in the presence of chlorophyll b and pheopigments. *Limnology and Oceanography*, *39*(8), 1985-1992. https://doi.org/10.4319/lo.1994.39.8.1985

Wilson, S. T., Böttjer, D., Church, M. J., & Karl, D. M. (2012). Comparative assessment of nitrogen fixation methodologies, conducted in the oligotrophic North Pacific Ocean. *Appl Environ Microbiol*, *78*(18), 6516-6523. https://doi.org/10.1128/aem.01146-12

Zehr, J. P., Bench, S. R., Carter, B. J., Hewson, I., Niazi, F., Shi, T., Tripp, H. J., & Affourtit, J. P. (2008). Globally Distributed Uncultivated Oceanic N_2-Fixing Cyanobacteria Lack Oxygenic Photosystem II. *322*(5904), 1110-1112. https://doi.org/10.1126/science.1165340

Zehr, J. P., & Bombar, D. (2015). Marine nitrogen fixation: organisms, significance, enigmas, and future directions. *Biological Nitrogen Fixation*, 855-872.

Zehr, J. P., Mellon, M. T., & Zani, S. (1998). New nitrogen-fixing microorganisms detected in oligotrophic oceans by amplification of nitrogenase (*nifH*) genes. *Appl. Environ. Microbiol.*, *64*(9), 3444-3450.

Figures

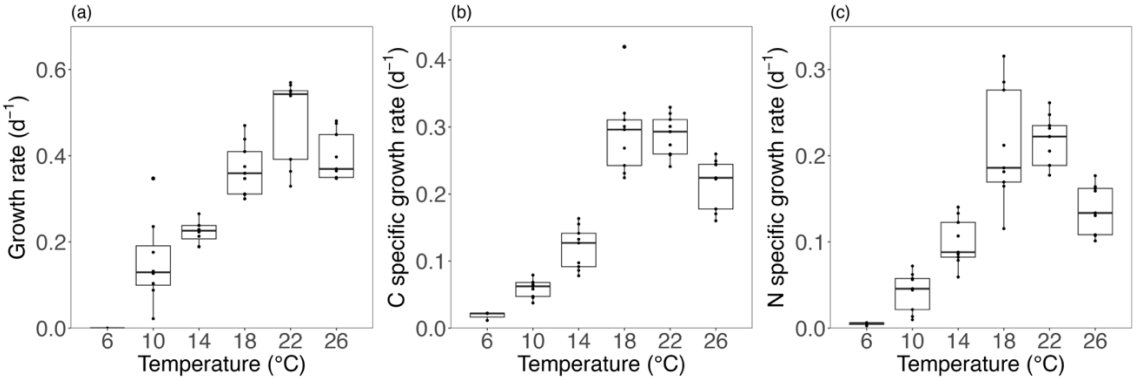

Figure 1. Growth rates of the UCYN-A2/*B. bigelowii* symbiosis as a function of temperature. Growth rates are presented via cell counts (A), C-specific growth rates (B), and N-specific growth rates (C). Boxes represent the interquartile range (IQR), with the median value indicated by the horizontal line in the box. The whiskers extend to the smallest and largest values within 1.5 * IQR from the quartiles. Points beyond the whiskers represent outliers.

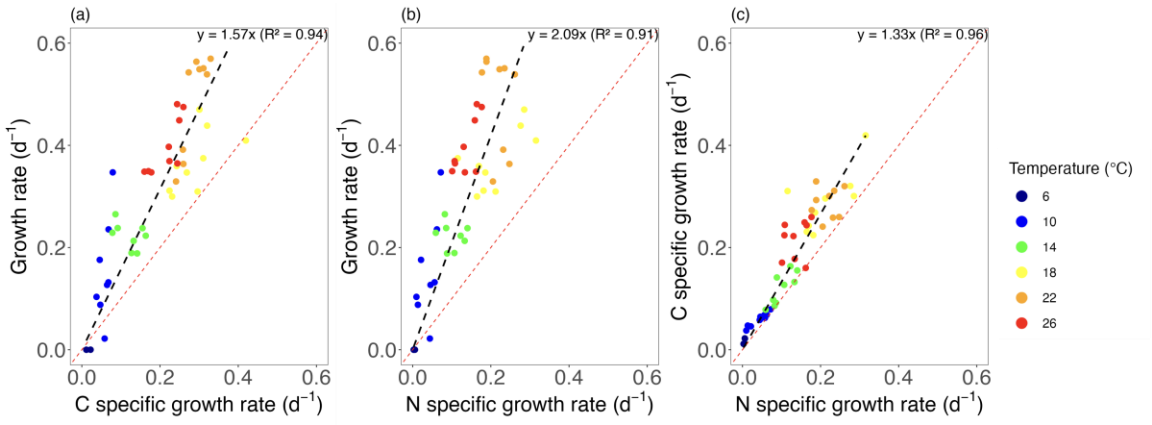

Figure 2. Cell-based growth rate versus C-specific growth rate (A) and N-specific growth rate (B), as well as C-specific growth rate versus N-specific growth rate (C). Colors indicate incubation temperatures of 6°C (dark blue), 10°C (blue), 14°C (green), 18°C (yellow), 22°C (orange), and 26°C (red). Black dashed lines represent the Model I linear regression fit.

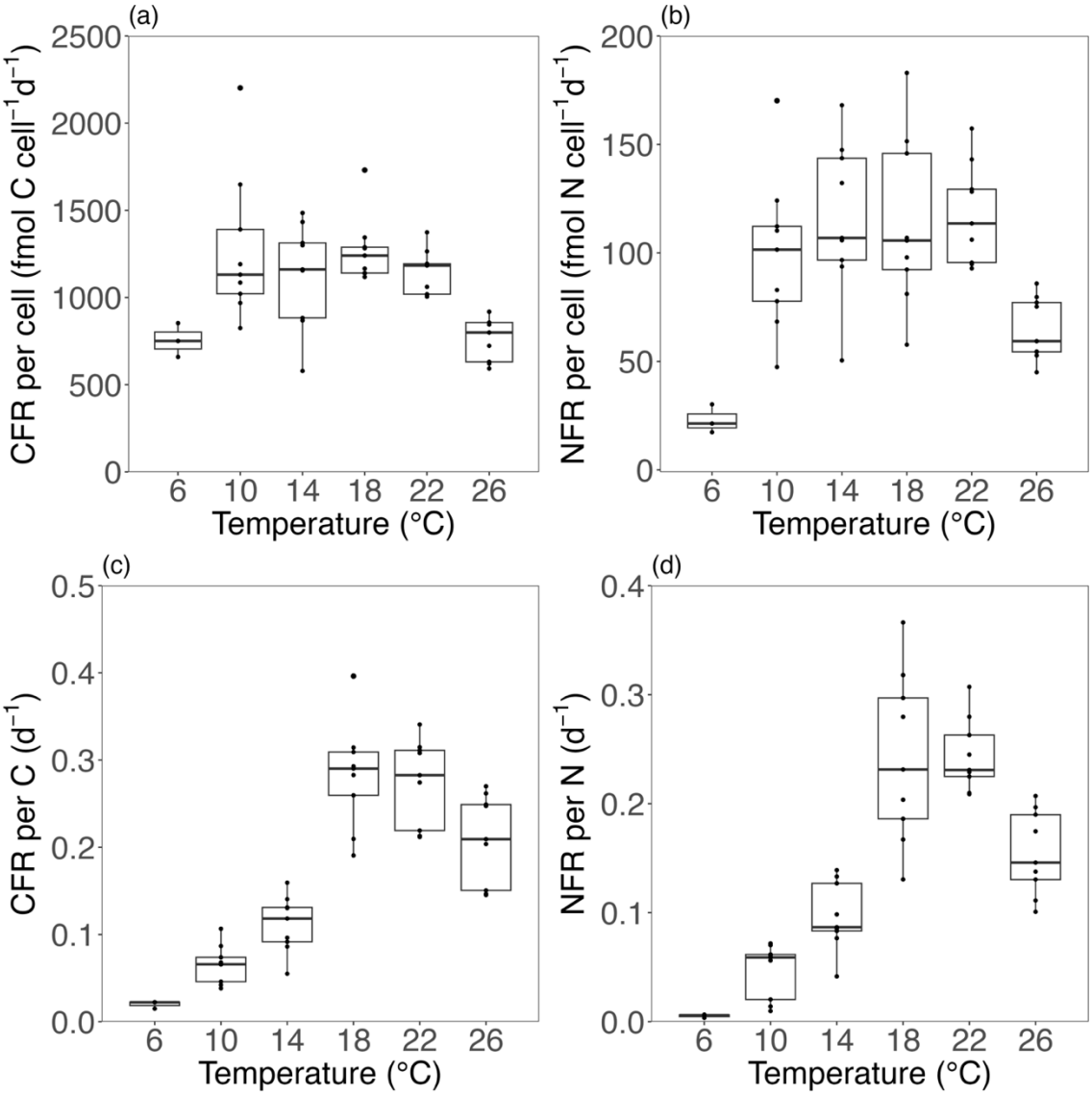

Figure 3. C and N_2 fixation rates as a function of temperature. The figure represents the relationship of C fixation rate (CFR) per cell (A), and N_2 fixation rate (NFR) per cell (B), along with CFR per C content (C), and NFR per N content (D). Each boxplot illustrates the interquartile range (IQR), with the median value represented by the horizontal line within the box. The whiskers extend to the smallest and largest values within 1.5 * IQR from the quartiles, and points beyond the whiskers represent outliers.

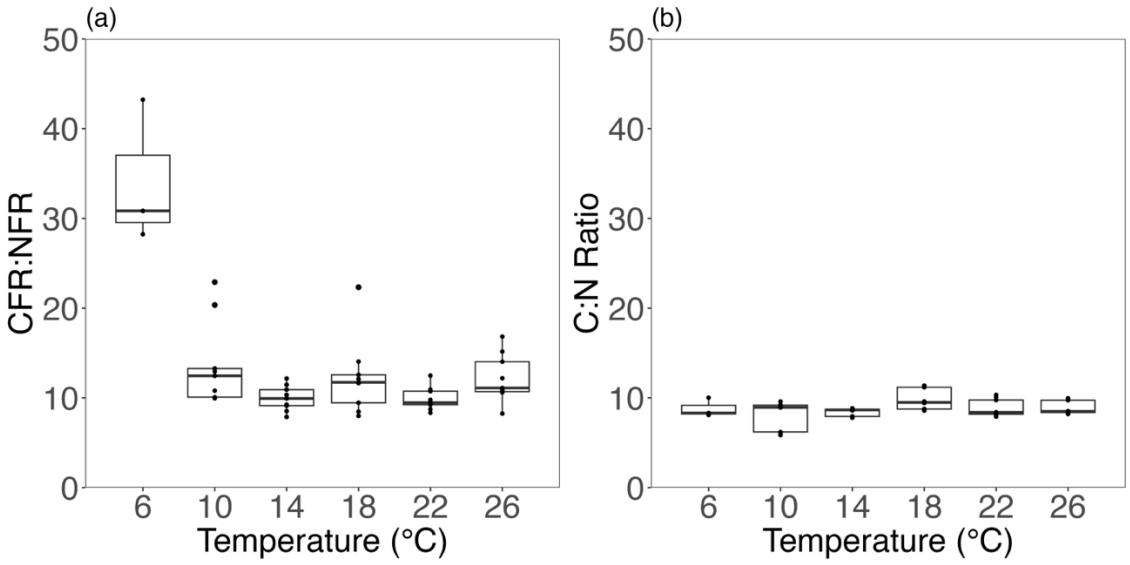

Figure 4. The figure illustrates the ratio of CFR to NFR (A), alongside the ratio of C to N within cells (C:N ratio) (B), each in relation to varying temperatures. The box plots depict the interquartile range (IQR), with a horizontal line representing the median value within each box. The whiskers of the box plots extend to the furthest values within 1.5 times the IQR from the first and third quartiles. Any data points found outside the whiskers are considered as outliers.

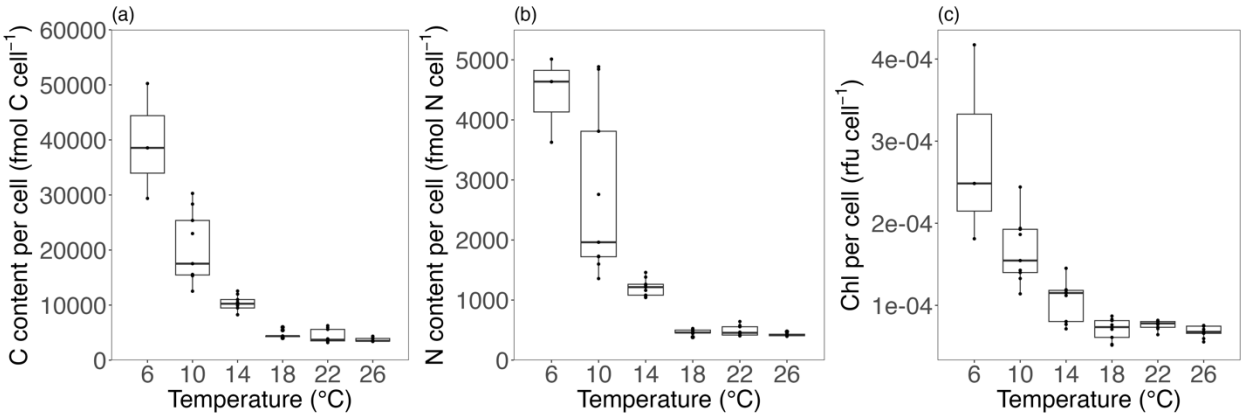

Figure 5. Displayed are comparisons of C content per cell (A), N content per cell (B), and chlorophyll content per cell (C) against varying growth temperatures. The box plots denote the interquartile range (IQR), highlighting the median value with a horizontal line within each box. The whiskers on the box plots reach out to the most distant values within 1.5 times the interquartile range (IQR) from the lower and upper quartiles. Data points located beyond the whiskers are regarded as outliers.

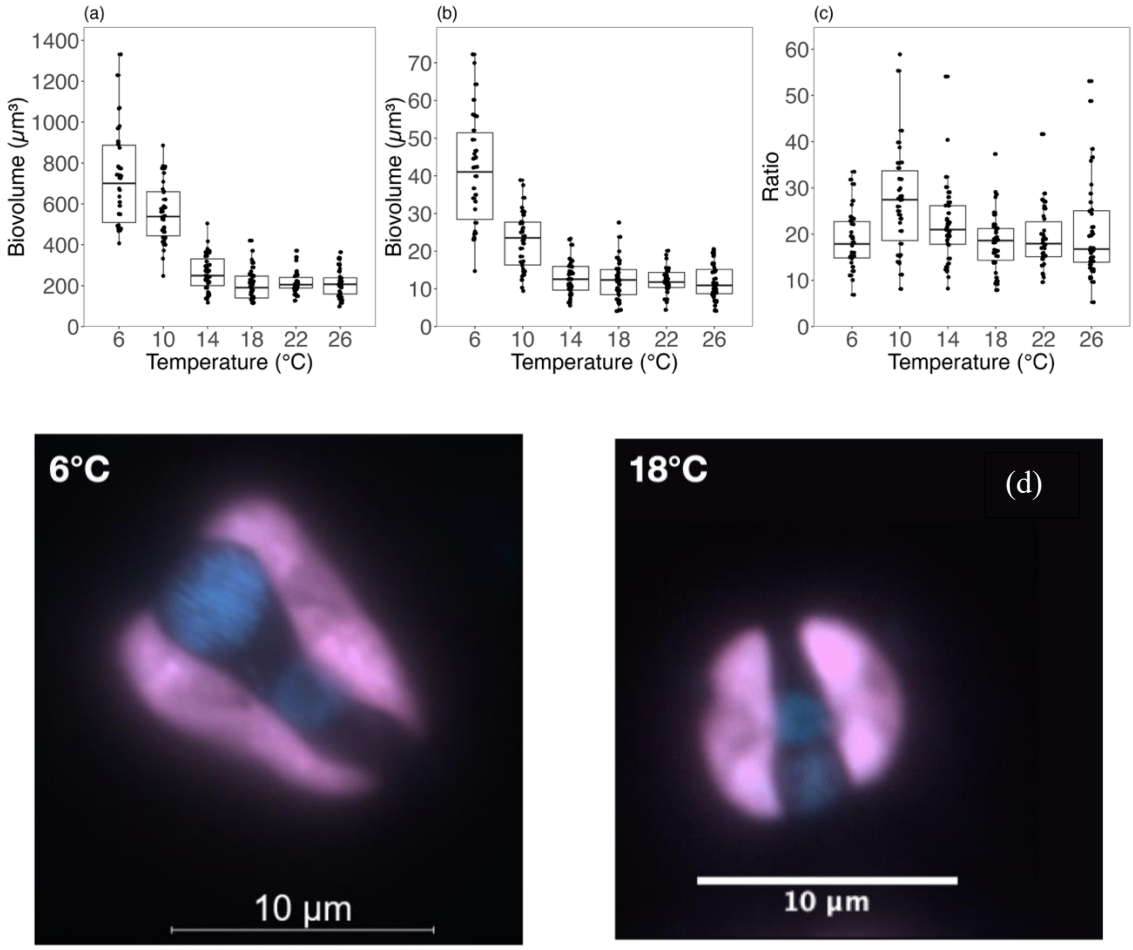

Figure 6a. The figures shows biovolume of the entire UCYN-A2/*B. bigelowii* symbiosis (A), the symbiont (B), and ratio between the entire symbiosis and the symbiont (C) under the microscope plotted versus different temperatures. The box plot whiskers reach up to the most distant values within 1.5 times the interquartile range (IQR) from the lower and upper quartiles. Data points beyond these whiskers are outliers. Thirty cells were counted for each temperature, and the median is represented by the horizontal line in the box plot. The box represents the interquartile range. Figure 6d displays the fluorescent microscopy

images of the symbiosis at 6°C and 18°C. The blue fluorescence signals correspond to the DAPI staining, and the pink fluorescence signals to the chlorophyll fluorescence.

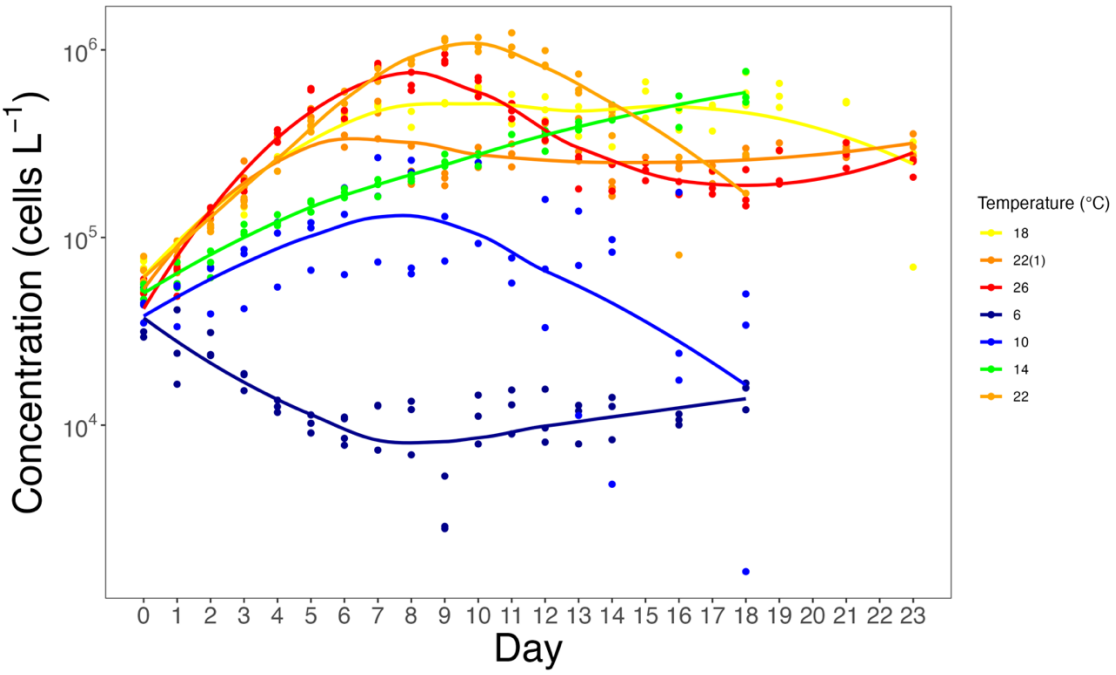

Supplemental Figure 1. Growth curves of the UCYN-A2/B. bigelowii symbiosis under different temperatures. The graph plots the cell concentrations of UCYN-A2/B. bigelowii over time, post-transfer, under various temperatures, each represented by a unique color. Each experimental condition was maintained in three replicates. The temperatures 18, 22(1), and 26 were sourced from the first set of experiments, while 6, 10, 14, and 22 were from the second set.

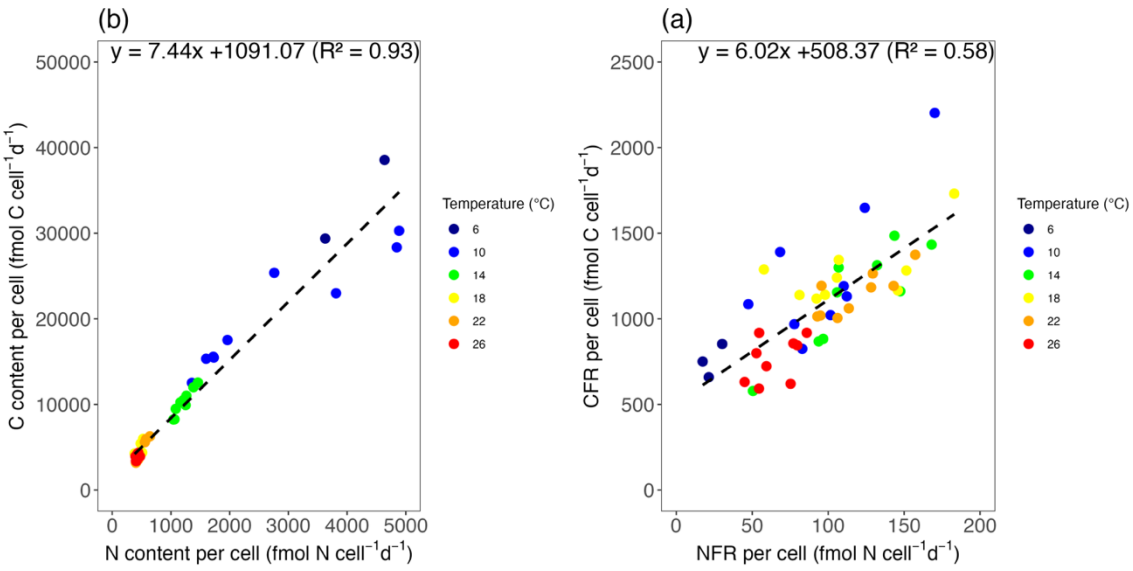

Supplemental Figure 2. C fixation rate plotted against N_2 fixation rate (Figure 4b) and C content per cell plotted against N content per cell (Figure 4c). Different temperatures are indicated by different colors, with 6°C (dark blue), 10°C (blue), 14°C (green), 18°C (yellow), 22°C (orange), and 26°C (red). The black dashed lines represent the model I linear regression fit of the slopes.

Supplemental table 3: Pairwise comparisons of parameters across temperature conditions. The table displays the results of pairwise comparisons of C specific growth rates across various temperature. The adjusted p-value column provides these p-values following Bonferroni correction to account for multiple comparisons.

C specific growth rate

Comparison	Adjusted p-value
10-14	1.00
10-18	0.00
10-22	0.00
10-26	0.02
10-6	1.00
14-18	0.01
14-22	0.01
14-26	0.74
14-6	0.81
18-22	1.00
18-26	1.00
18-6	0.00
22-26	0.64
22-6	0.00
26-6	0.04

N specific growth rate

Comparison	Adjusted p-value
10-14	0.88
10-18	0.00
10-22	0.00
10-26	0.07
10-6	1.00
14-18	0.03
14-22	0.01
14-26	1.00
14-6	0.57
18-22	1.00
18-26	0.52
18-6	0.00
22-26	0.18
22-6	0.00
26-6	0.09

C fixation rate

Comparison	Adjusted p-value
10-14	1.00
10-18	1.00
10-22	1.00
10-26	0.01
10-6	0.15
14-18	1.00
14-22	1.00
14-26	0.02
14-6	0.21
18-22	1.00
18-26	0.00
18-6	0.04
22-26	0.02
22-6	0.20
26-6	1.00

N fixation rate

Comparison	Adjusted p-value
10-14	1.00
10-18	1.00
10-22	1.00
10-26	1.00
10-6	1.00
14-18	1.00
14-22	0.25
14-26	0.02
14-6	0.04
18-22	0.01
18-26	0.10
18-6	0.01
22-26	0.02
22-6	0.01
26-6	1.00

Growth rate

Comparison	Adjusted p-value
10-14	1.00
10-18	0.04
10-22	0.23
10-26	0.00
10-6	0.00

14-18	0.77
14-22	0.00
14-26	0.04
14-6	1.00
18-22	1.00
18-26	1.00
18-6	1.00
22-26	0.03
22-6	0.00
26-6	0.01

CFR:NFR

Comparison	Adjusted p-value
10-14	0.24
10-18	1.00
10-22	1.00
10-26	0.21
10-6	1.00
14-18	1.00
14-22	1.00
14-26	0.56
14-6	1.00
18-22	0.50
18-26	0.53
18-6	0.01
22-26	0.16
22-6	0.01
26-6	0.30

C content per cell

Comparison	Adjusted p-value
10-14	1.00
10-18	0.01
10-22	0.43
10-26	0.00
10-6	0.03
14-18	1.00
14-22	0.00
14-26	0.00
14-6	0.91
18-22	1.00
18-26	1.00
18-6	0.89
22-26	0.03

22-6 0.00
26-6 0.00

N content per cell

Comparison	Adjusted p-value
10-14	1.00
10-18	0.00
10-22	0.16
10-26	0.00
10-6	0.10
14-18	1.00
14-22	0.00
14-26	0.00
14-6	1.00
18-22	1.00
18-26	1.00
18-6	1.00
22-26	0.02
22-6	0.01
26-6	0.00

C:N

Comparison	Adjusted p-value
10-14	1.00
10-18	0.31
10-22	0.06
10-26	1.00
10-6	1.00
14-18	0.30
14-22	1.00
14-26	1.00
14-6	0.50
18-22	1.00
18-26	1.00
18-6	1.00
22-26	0.93
22-6	1.00
26-6	1.00

C fixation rate per C

Comparison	Adjusted p-value
10-14	1.00
10-18	0.00
10-22	0.01
10-26	0.00

10-6	0.01
14-18	1.00
14-22	0.03
14-26	0.50
14-6	1.00
18-22	1.00
18-26	1.00
18-6	0.96
22-26	0.00
22-6	0.00
26-6	0.04

N fixation rate per N

Comparison	Adjusted p-value
10-14	1.00
10-18	0.00
10-22	0.02
10-26	0.00
10-6	0.01
14-18	1.00
14-22	0.05
14-26	1.00
14-6	0.74
18-22	0.34
18-26	1.00
18-6	0.72
22-26	0.00
22-6	0.00
26-6	0.06

Chapter 3: Diazotrophic Assemblages and N_2 Fixation Rates Across Longitudinal and Latitudinal gradients in the North Pacific

Authors: Wing Kwan Esther Mak[1] (wimak@ucsc.edu), Kendra Turk-Kubo[1] (kturk@ucsc.edu), Katie Harding[1,2] (kaharding@ucsd.edu), Mary Rose Gradoville[1,3] (rgradoville@critfc.org), Jonathan P Zehr[1] (zehrj@ucsc.edu)

[1] Department of Ocean Sciences, University of California, Santa Cruz, CA, USA

[2] Marine Biology Research Division, Scripps Institute of Oceanography, San Diego, CA, USA

[3] Columbia River Inter-Tribal Fish Commission, Portland, OR, USA

Abstract

Biological dinitrogen (N_2) fixation is an important source of new N in the euphotic zone of oligotrophic ocean gyres. Microorganisms capable of N_2 fixation (diazotrophs) are diverse, including multiple species of cyanobacteria and non-cyanobacterial diazotrophs (NCDs). Although much is known about diazotrophs in the North Pacific Subtropical Gyre (NPSG), less is known about the spatial variability across the ocean basin including the transition zones at the edges of the gyre. In this study, the spatial variability of N_2 fixation and of major diazotroph groups was determined along a southwest to northeast transect across the North Pacific from Guam to San Francisco, during November 2019. The shifts observed in diazotrophs in these regions followed four distinct hydrographically-defined regions. N_2 fixation was generally low across the transect, and at a minimum in the vicinity of the transition zone chlorophyl front, but detectable at 20 out of 23 stations in surface waters (0.36 ±0.28 nmol N $L^{-1}d^{-1}$) and at the deep chlorophyll maximum (0.50 ±0.72 nmol N $L^{-1}d^{-1}$) at 18 out of 19 stations. In the western region of the transect, where sea-surface temperatures (SST) were the warmest (ca. 29°C), two strains of *Crocosphaera, C. watsonii and C. waterburyi* were the dominant diazotrophs. As SST decreased to below 26°C, UCYN-A symbiosis became dominant. An unexpected dominance of the UCYN-A3 subgroup in the central region was also detected. Throughout the transect, NCDs were also present, especially the well-studied NCD, Gamma A. In summary, findings from this study support a latitudinal boundary for N_2 fixation and cyanobacterial diazotrophs in the North Pacific, and contributes to filling the existing data gap in the western NPSG.

Introduction

In the oligotrophic open oceans such as the North Pacific Subtropical Gyre (NPSG), nitrogen (N), essential for phytoplankton growth, is often present in low concentrations that limit primary production (Moore et al., 2013). One important source of bioavailable N in the NPSG is biological dinitrogen (N_2) fixation (BNF) (Karl et al., 1997), a process carried out by certain microorganisms (diazotrophs) that convert N_2 gas into ammonium. The fixed N is then supplied to phytoplankton through excretion, cell lysis induced by viral infections, and grazing (Mulholland, 2007). BNF contributes up to 50% of the NPSG and is a significant N source in these regions (Böttjer et al., 2017; Capone et al., 2005; Jickells et al., 2017; Karl et al., 1997).

Diverse diazotrophs inhabit the NPSG. Among the dominant diazotrophs in these warm oligotrophic waters are cyanobacterial diazotrophs such as *Trichodesmium*, a bloom-forming filamentous cyanobacteria (Capone et al., 1997), diazotroph diatom associations (Scharek et al., 1999), *Crocosphaera*, a free-living unicellular cyanobacterium (Webb et al., 2009), and UCYN-A, a haptophyte symbiont (Thompson et al., 2012) present throughout the global ocean. Additionally, non-cyanobacterial diazotrophs (NCDs) that are likely heterotrophic, including Gamma A (Langlois et al., 2015), are also observed in the NPSG (Cheung et al., 2020; Harding et al., 2022; Shao & Luo, 2022; Tang & Cassar, 2019; Turk-Kubo et al., 2023).

Despite the importance of BNF in the NPSG, the spatial and temporal distribution and activity of diazotrophs are not fully understood. This is largely because most previous data have been obtained from studies conducted near Station ALOHA (A Long-term Oligotrophic Habitat Assessment, 22° 45'N, 158° 00'W). However, the NPSG is characterized by dynamic and diverse seascapes, suggesting distinct biogeochemical provinces with unique hydrological characteristics as well as phytoplankton communities (Hofmann Elizondo et al., 2021; Kavanaugh et al., 2014; Reygondeau et al., 2013). Consequently, this inherent heterogeneity challenges the extrapolation of findings from a single location, like Station ALOHA, to the wider Pacific environment. Notably, most ALOHA-centric diazotrophy studies are concentrated in the spring and summer, signifying higher N_2 fixation rates in warmer months (Böttjer et al., 2017; Dore et al., 2002). The applicability of these findings to the broader NPSG region, especially during winter, remains largely unexplored. Moreover, data availability is especially limited in the western Pacific and transition zones (Cheung et al., 2020; Shao & Luo, 2022; Zehr & Bombar, 2015) where significant variations in hydrologic (e.g., temperature, salinity) and chemical properties (e.g., nutrient availability) have been observed, which influence the distributions of diazotroph as well as general phytoplankton populations. This highlights a significant gap in the understanding of the complex spatial and temporal dynamics across the larger basin, including in the transitional zones and the under-researched western Pacific region.

Further north, the North Pacific Transition Zone (NPTZ) marks the transition between the cool, relatively fresh waters from the subarctic gyre and the warm, salty waters of the

NPSG. It also marks higher nutrient concentration and chlorophyll. Previous studies have demonstrated that although diazotrophs, such as UCYN-A, are detectable, their abundance is substantially lower in the southern front of the NPTZ compared to the NPSG (Cheung et al., 2020; Church et al., 2008; Gradoville et al., 2020). There are instances where diazotrophs such as UCYN-B and certain non-cyanobacterial diazotrophs (NCDs) are found in relatively higher numbers, though these numbers are generally low (Cheung et al., 2020; Church et al., 2008). This underscores a consistent trend of lower diazotroph abundance in the NPTZ compared to the NPSG.

By conducting a study along a transect across the full North Pacific basin, from Guam to San Francisco, transitioning through the NPSG and NPTZ, the spatial variability of diazotrophs and associated N_2 fixation rates across four hydrographically distinct regions were determined. This study aims to identify and enumerate key diazotrophs in the region, quantify N_2 fixation rates, and analyze the key environmental factors that contribute to the dynamics of diazotroph populations.

Methods

Sample collection and analysis

Samples were collected during a cruise in the North Pacific aboard the R/V Sally Ride from Apra, Guam (13.42°N, 144.65°E) to San Francisco, CA, USA (37.77°N, 122.24°W) in November 2019. Seawater samples were obtained from 6-8 depths at 25 different stations along the transect using a Niskin rosette outfitted with a conductivity, temperature, and depth (CTD) profiler. The seawater was pre-filtered through 210 μm pore-size nylon mesh to eliminate large grazers. Following this, the samples were transferred to duplicate, triple acid-washed, and Milli-Q rinsed 2.4 L polycarbonate (PC) bottles. Each sample was then subsampled for DNA (~2 L), chlorophyll (500 mL), and nutrient analyses (50 mL).

DNA samples were filtered through 0.2 μm pore-size membrane Supor filters (Pall Corp, Port Washington, NY, United States) using a peristaltic pump. Post filtration, the filters were stored in microcentrifuge tubes containing sterile 0.5 mm and 0.1mm diameter glass beads (Biospec Products, Bartlesville). The tubes were flash frozen with liquid nitrogen and preserved at -80°C until further processing. For the collection of chlorophyll samples, 500 mL of seawater was filtered through GF/F filters. These filters were flash frozen in liquid nitrogen and stored at -80°C pending further processing. The chlorophyll extraction process started with submerging the filter in 7 mL of 90% acetone (v/v), ensuring the complete coverage of the filter material to facilitate the release of chlorophyll into the solvent. The acetone-filters mixture was placed in a dark, cool environment overnight to allow for complete extraction of chlorophyll. The chlorophyll-a concentration in the

acetone solution was analyzed using a Turner TD-700 fluorometer. Finally, nutrient samples were collected and frozen at -20°C. The analysis was conducted for nitrite (NO_2) + nitrate (NO_3), and phosphate (PO_4) concentrations following the guidelines outlined in 40 CFR Part 136 Appendix B by the Environmental Protection Agency (EPA), which establishes test procedures for the analysis of these pollutants. The method limits of detection were 0.01 μM and 0.02 μM, respectively.

Regions defined by hydrography and biochemical properties

Temperature, salinity, and oxygen and chlorophyll concentrations were measured with the Niskin attached CTD during the sampling. Stations along the transect were classified into distinct regions based on parameters including temperature, salinity, oxygen, chlorophyll, latitude, and longitude. A hierarchical clustering approach using these parameters, along with the Gower distance metric, was implemented in the cluster package in R 4.3.0. The optimal number of clusters was determined using the silhouette method, which computes a measure of how similar an object is to its own cluster compared to other clusters. Silhouette scores were analyzed for several potential values of k, with the highest scores being found at k=4. A hierarchical clustering tree was then constructed using the Ward.D2 method, and the transect was partitioned into four clusters: western, central, central eastern, and eastern regions.

Modeled environmental parameters

Environmental data was extracted from the Mercator-Pisces Biogeochemistry Daily Forecast (Pisces model) from the Collaborative Marine Atlas Project (CMAP) (Ashkezari et al., 2021; Aumont et al., 2015). The corresponding data from the days of the cruise were downloaded. Each station corresponds to the closest quarter degree of latitude and longitude in the Pisces model, and the station depths were mapped to the closest available depth in the Pisces model. The environmental parameters that were extracted were chl (chlorophyll-a), Fe (dissolved iron), NO_3 (nitrate), PO_4 (phosphate), phyc (concentration of phytoplankton expressed as carbon in seawater), Si (silicate), nppv (net primary production of biomass expressed as carbon), pH (pH level), and spCO2 (surface partial pressure of carbon dioxide).

Bulk N_2 fixation rates

Bulk N_2 fixation rates were measured using the $^{15}N_2$ uptake method (Mohr et al., 2010; Montoya et al., 1996), with a modification to allow for $^{15}N_2$ bubble dissolution (Klawonn et al., 2015). Incubations were conducted using seawater from 15 m depth and the deep chlorophyll maximum (DCM, 62 m– 131 m). Seawater was sampled from Niskin bottles and transferred into triplicate 4 L polycarbonate bottles. The bottles were filled to capacity, capped, and a $^{15}N_2$ gas bubble (bubble size, manufacturer, lot number) was injected. This was followed by 20 minutes of agitation by rolling the bottles back and forth at ~25 rpm to allow for better dissolution of the bubble, before bubble release (Klawonn et al., 2015).

Then ^{13}C -bicarbonate (60 μM, 99%, Cambridge Isotopes) was added. Bottles were then incubated for 24 hours in a surface seawater-cooled incubators shaded to light intensity at 15 m depth. Dark bottle treatments were set up by separate sets of triplicate bottles that were incubated in complete darkness using black plastic bags and duct tape and followed the incubation steps described above for 24 hours. The agitation step for dark bottles was performed in low-light conditions. Although the incubations were initiated at different times of the day, the duration of all experiments was 24 hours to cover one full diel cycle. Time zero $\delta^{15}PN$ natural abundance samples were also collected at each station to serve as controls and establish baseline values for N_2 fixation rates.

After 24h, the incubation bottles were opened, and samples were siphoned into 15 mL glass vials after three volumes of overflow and stored at 4°C to determine the initial atom percent (At%) of N_2. This sample was later measured via membrane inlet mass spectrometry (MIMS) (2.8 At% ± 0.4) in Lawrence Livermore National Laboratory according to Ferrón et al. (2016). The remaining seawater (~4 L) was vacuum-filtered through combusted GF/F filters and flash frozen before being stored at -80°C.

The filters were desiccated at 60°C for 24 hours before being compressed into tin capsules for combustion. Particulate carbon, particulate nitrogen and isotopic composition (δ13C, δ15N) was measured with a Carlo-Erba EA NC2500 coupled with Thermo Finnigan DeltaPlus XP at the University of Hawaii Stable Isotope Facility. N_2 fixation rates were calculated using the equation provided by Montoya et al. (1996):

$$N_2\ fixation\ rate\ (fmol\ cell^{-1}d^{-1}) = \frac{A_{PN} - A_{PN_0}}{A_{N_2} - A_{PN_0}} \times \frac{[PN]}{\Delta t}$$

where A_{PN} and A_{PN0} are the fractional ^{15}N enrichment (atom %) after and prior to the incubation, respectively. [PN] is the particulate nitrogen concentration at the conclusion of the incubation period, Δt is incubation time (days), AN_2 is the fractional ^{15}N-enrichment of the N_2 source pool, as determined by MIMS.

Diazotroph diversity and abundance

To assess diazotroph diversity and abundance, DNA was extracted with the DNeasy Plant Mini kit (Qiagen, Hilden, Germany). The protocol was modified to increased cell lysis by incorporating 3x freeze-thaw, bead-beating, and proteinase K digestion, as outlined by Moisander et al. (2008). Five diazotroph groups, UCYN-A1, UCYN-A2/3, UCYN-B, UCYN-C, *Trichodesmium*, and Gamma A, were quantified by digital droplet PCR (ddPCR) using commonly used primer/probe sets (Church, Jenkins, et al., 2005; Church, Short, et al., 2005; Foster et al., 2007; Langlois et al., 2008; Moisander et al., 2010; Thompson et al., 2014). Gradoville et al. (2021) comprehensively described the ddPCR protocols used, including reaction settings, droplet formation, thermocycling variables, threshold establishment and the limits of detection.

Amplification of the *nifH* gene was performed by nested PCR using degenerate universal *nifH* primers nifH3/nifH4 and nifH1/nifH2 (Zehr & McReynolds, 1989). A targeted

amplicon sequencing approach was used to create barcoded libraries as described in Green et al. (2015), using 5' common sequence linkers (Moonsamy et al., 2013) on second round primers, nifH1/nifH2. The resulting PCR products were subsequently sequenced utilizing the Illumina MiSeq sequencing technique (2 × 300 bp, aiming for a sequencing depth of 20,000 for each sample) at the Genome Research Core Facility at the University of Illinois. Amplicon sequence variants (ASVs) were determined using a custom DADA2-based pipeline (https://github.com/jdmagasin/nifH-ASV-workflow) that has been optimized for *nifH* amplicon analyses. ASVs were taxonomically annotated via BLAST against two custom databases, one containing 879 sequenced diazotroph genomes ("genome879", https://www.jzehrlab.com/nifh), and the second containing UCYN-A oligotypes (Turk-Kubo et al., 2017) and a recent NCD *nifH* gene catalog (Turk-Kubo et al., 2022) was used to identify specific marine cyanobacterial and NCD sequence types. Raw sequence data can be found in the SRA database at NCBI under Bioproject X.

Correlation of Diazotroph Abundance with Environmental Parameters

To elucidate the relationships between the abundance of diazotrophs (by ddPCR) and various environmental parameters, either measured from the CTD or output from the Pisces model), correlations were calculated using the cor function in conjunction with the Spearman's rank correlation method in R (R Core team, 2022). Specifically, the parameters chl (chlorophyll-a), Fe, NO_3, PO_4, phyc, Si (silicate), nppv, and spCO2. were derived from the Pisces model, while temperature, salinity, oxygen, and chlorophyll were directly

measured from the CTD. The significance level of each correlation was determined by calculating p-values for each pair of variables using the cor.test function. These were adjusted using the Benjamini-Hochberg correction to reduce the false discovery rate. Following this, a heatmap visualization of the correlation matrix was generated using the heatmaply package (Galili et al., 2018), displaying only those results where $p < 0.05$.

Grazing Rates

Microzooplankton grazing rates on *Crocosphaera* and other diazotrophs were measured using the dilution approach measured using the dilution approach (Landry et al., 1995) at 5 m depth and the DCM. Seawater was transferred from Niskin bottles into 20 L polycarbonate carboys. The diluent was prepared by gravity-filtering seawater from the same location through 0.2 μm pore-size Polycaps (Whatman GmbH, Dassel, Germany). Triplicate 2 L bottles were rinsed with the 0.2 μm filtered diluent, then filled with seawater and diluent at ratios of 20%, 60%, and 100%. The bottles were amended with N, P and Fe at final concentrations of 2.0 μM NO_3^-, 0.2 μM NH_4^+, 0.5 μM PO_4^{3-}, and 0.1 μM Fe (Turk-Kubo et al., 2018). The bottles were incubated for 24 hours at light levels mimicking 5 m and DCM in a flow-through incubator on deck. Initial (T_0) DNA, chlorophyll, and flow cytometry samples were collected from the carboys in triplicate. At t = 24h (T_{24}), DNA samples (2L) were collected from each bottle and filtered through 0.2 μm pore-size Supor membranes (Pall Corp., Washington Port, NY, USA), flash frozen and stored at -80 °C. Microzooplankton grazing rates for each group were determined using cell count estimates

determined by ddPCR. The DNA extraction protocol and ddPCR methods are detailed in the preceding sections.

The growth rates for each treatment were calculated as follows:

$$\mu = \ln (T_{24}/(T_0 \text{ x fraction of whole water}))$$

where μ represents the growth rate, T_0 and T_{24} represent the initial and final abundance of the targeted diazotrophs, measured at the start and after 24 hours, respectively.

Mortality (m) for each group was calculated by plotting the growth rate against dilution levels and fitting a line with a linear regression model. The negative slope is the grazing rate for the targeted group, while the y-intercept represents the theoretical growth rate in the absence of grazers (Landry & Hassett, 1982).

Results and Discussion

Four distinct hydrographic regions

This study spanned a region from Guam to the west coast of California (San Francisco), traversing several distinct regions in the NPSG and the transition zone to investigate diazotroph distributions and abundances. The NPSG is recognized as a diazotroph habitat, primarily due to its well-defined thermocline that hinders vertical mixing or nutrient upwelling to the surface layer, thereby creating an oligotrophic environment which would favor diazotrophic growth (Church et al., 2009; Karl, 1999).

The longitudinal transect across the Pacific Ocean from Apra, Guam to San Francisco sampled a broad array of oceanographic conditions, capturing the biogeochemical diversity from the oligotrophic West to the East Pacific Ocean, including the nutrient-rich coastal area of California (Figure 1a). The transect was categorized into four regions based on variations in temperature, salinity, oxygen, and chlorophyll. These were the western (Station 1–8), central (Station 9-16), central eastern (Station 17–19), and eastern regions (Station 20–25), classified via a hierarchical clustering method (Figure 1).

The western region (Station 1–8), characterized by elevated sea surface temperatures (28.5–29.6°C) and a pronounced subsurface salinity maximum (~35.1 ppt at 100–150 m), exhibited deeper DCM depths of 104–130 m, reflective of its oligotrophic nature with low chlorophyll concentrations. Transitioning to the Central region, a decrease in sea surface temperatures (21.5–27.3°C) was noted, accompanied by a shoaling of the DCM at 75–102

m, indicating a shift in the thermal and nutrient profiles with a marginally higher surface salinity of 34.9 to 35.1. Advancing eastward, the central eastern region was defined by the transition zone chlorophyll front (TZCF) near 34°N, marking a zone of enriched surface chlorophyll, colder dense waters, and intermediate salinity. The shallower DCM (64–100 m) with heightened chlorophyll fluorescence (0.10–0.12) showed an elevated phytoplankton biomass. Lastly, the eastern region was characterized by a transition to cooler (around 19°C), fresher waters with intermediate chlorophyll concentrations, marking the entry into a distinct biogeochemical realm influenced by the eastern boundary California current ecosystem.

This spatial segregation not only delineates the hydrographic heterogeneity across the Pacific but also sets the stage for a deeper exploration into how such environmental gradients influence diazotroph distributions and their functional roles within these distinct oceanic domains.

Two strains of *Crocosphaera* dominate the western region

The western region contained the highest observed abundances of *Crocosphaera*. *Crocosphaera watsonii (C. watsonii)*, the dominant tropical open ocean species of *Crocosphaera* (Zehr et al., 2022), had high abundance in the western stations (Station 1–8) determined by ddPCR analysis, revealing an average abundance of 1.7 x 10^5 *nifH* copies L^{-1} at 15 m (Figure 2). *C. watsonii* abundance measurements by this study provide one of

the few detailed measurements in this region. While some abundance data for *C. watsonii* is available for the West NPSG, particularly closer to the coast, this sampling across the open ocean delivers a more complete dataset, addressing considerable gaps in current knowledge (Shao et al., 2023; Tang & Cassar, 2019).

C. watsonii nifH gene abundance was positively correlated with temperature (R^2= 0.89, p-value < 0.05, Supplemental table 1). The temperature-abundance graph indicates that the highest abundance peaks at 29°C and decreased at approximately 27°C (Figure 4b). Interestingly, this finding deviates from prior research which suggests that *C. watsonii* in laboratory cultures grows at temperatures ranging from 24-32°C (Fu et al., 2014). This discrepancy particularly at 27°C, may not be solely attributed to temperature variations but could be influenced by other external factors, such as grazing. Notably, at two easternmost stations within the western region (Station 6 and 8), significant grazing rates on *C. watsonii* were measured, at 1.28 d^{-1} and 1.14^{-1} respectively (Supplementary Table 2). These rates surpass the previously recorded rates at Station ALOHA, which ranged between 0.4-0.8 d^{-1} (Dugenne et al., 2020; Turk-Kubo et al., 2018; Wilson et al., 2017). It is known that in the NPSG, *C. watsonii* can be grazed by various dinoflagellates and ciliates, as documented using an Imaging FlowCytobot (Dugenne et al., 2020). However, the absence of positive grazing rates at Station 7 indicates more factors than temperature and grazing contribute to *C. watsonii* abundances and distributions.

Using *nifH* amplicon sequencing revealed sequences sharing high nucleotide identity with *Crocosphaera waterburyi* (97.5%-100% similarity), which is a newly defined *Crocosphaera* species known to be distinct from *C. watsonii* in terms of morphology, phylogeny, and physiology (Cleveland et al., 2023), and is not targeted by the UCYN-B ddPCR primer (Cleveland et al., 2023). This alignment suggests the possible presence of a strain from the genus *Crocosphaera*, resembling *C. waterburyi*, The *C. waterburyi* sequences were found predominantly in the western stations (Figure 5), and appear to be present across a broader temperature spectrum (28-34°C) compared to *C. watsonii*. *C. waterburyi* was previously reported in the North Pacific and identified as the novel, uncultured Croco-OTU3. This species was primarily observed during spring and summer at Station ALOHA (Turk-Kubo et al., 2023). The results from this study showed its presence during the fall/winter, albeit in a region warmer than the winter conditions at Station ALOHA. *Crocosphaera* likely contributed to part of the NFRs observed in the western regions (0.56 ± 0.27 nmol N L^{-1} d^{-1}). Moreover, they most certainly play a role in the observed dark rate (0.23 ± 0.19 nmol N N L^{-1} d^{-1}), as they fix N_2 predominantly at night (Dron et al., 2012; Mohr et al., 2010; Tuit et al., 2004).

Emergence of UCYN-A sublineages in the central and eastern region

UCYN-A1 was found to be absent in most western stations based on ddPCR quantification but began to appear in the eastern portion of the transect, surpassing *Crocosphaera* abundances around Station 9. UCYN-A1 depth-integrated abundances (5.7×10^5 *nifH*

copies L^{-1}) peaked between Stations 9-15, followed by a decrease to 6.8×10^3 *nifH* copies L^{-1} between Stations 16-17 near the TZCF. Leaving the TZCF, UCYN-A1 resurged to 10^5 *nifH* copies L^{-1} from Station 20-23. UCYN-A2/A3 were not detected in any of the stations using ddPCR across the transect, with the exception of Station 13 at a depth of 5 m, where they were present at a low abundance (2.7×10^5 *nifH* copies L^{-1}).

UCYN-A emerged as the dominant diazotroph as temperatures decreased below 27°C around Station 10 in the transect (Figure 2). UCYN-A, a diazotroph that forms symbiosis with a haptophyte host (Thompson et al., 2012), consists of several sublineages varying in size that inhabit different habitat of the ocean. UCYN-A1, the open-ocean sublineage, reached abundances of 10^5 *nifH* copies L^{-1} in the central region (Stations 9-15), with a prevalent distribution between 5 m to 75 m depths. Typically, UCYN-A are found in cooler temperatures than *Crocosphaera* (Tang & Cassar, 2019), which may explain their absence in the western region.

Beyond quantification of UCYN-A1, the *nifH* amplicon study identified the presence of other UCYN-A sublineages, UCYN-A3 and UCYN-A5 (Figure 5). UCYN-A3 was detected in the central region in the *nifH* amplicon dataset (Stations 10-16), while in the eastern region UCYN-A5 coexisted with UCYN-A3. Interestingly, despite UCYN-A3 being undetectable in ddPCR analyses for these regions, it had a higher relative abundance in *nifH* sequencing compared to UCYN-A1, suggesting a potential bias in PCR amplification that is worth noting, given that currently UCYN-A3 cannot be differentiated

from UCYN-A2 and UCYN-A4 with existing ddPCR assays (Farnelid et al., 2016). While it is well-established that UCYN-A1 and UCYN-A3 mainly inhabit open ocean areas (Henke et al., 2018; Turk-Kubo et al., 2017), very little is known about the biogeography of UCYN-A5, nor has the host been identified. While sequencing data suggests a prominence of UCYN-A3 in certain regions, ddPCR data indicate a lower abundance. This discrepancy highlights the importance of cross-validating techniques and considering potential biases or limitations in each method.

Distribution of NCDs across the transect

Aside from cyanobacterial diazotrophs, NCDs were found throughout the transect. Among the NCDs, Gamma A, one of the most extensively studied NCD, was the most prevalent. It was detected in 74 out of 106 samples, spanning the west, central, and eastern regions, at an average abundance of 10^3 *nifH* copies L^{-1} (Figure 2). However, Gamma A was absent at the TZCF, consistent with its known preference for warm, oxygen-rich, oligotrophic waters (Langlois et al., 2015; Shao & Luo, 2022; Turk-Kubo et al., 2022). Considering vertical distribution, Gamma A was largely found within the top 100 m of the water column, rarely extending below this depth. This distribution resonates with prior research, suggesting Gamma A may rely on photosynthetic activity of phytoplankton in surface waters or possibly even be photoheterotrophic, and their own light-dependent strategies (Cornejo-Castillo & Zehr, 2021; Langlois et al., 2015; Moisander et al., 2008).

A detailed analysis of relationships with the environmental parameters, shows that the abundance of Gamma A is positively correlated with temperature (correlation = 0.71, p-value < 0.005, Supplemental table 1), with a maximum at 27.9°C. This contrasts with results of Shao and Luo (2022) which revealed temperature was not an important factor in determining the abundances of Gamma A. While this study revealed a correlation between Gamma A and temperature, especially in the under-sampled region of the Northwest Pacific Ocean that Shao and Luo (2022) did not sample, these generalizations need to be interpreted with caution. This study primarily focused on warmer regions (20-30°C), potentially biasing the correlation, while Shao and Luo (2022) includes data from cooler environments.

Alpha1, another prominent NCD, had a distinct distribution pattern across the transect. Notably, the maximum relative abundance of Alpha1 appears to mirror the depth of the DCM, hinting at its preference or adaptation for a specific niche in the open ocean. The distribution of Alpha1 has been found to extend down to depths of 1000 m in regions such as the South China Sea (Chen et al., 2019), which underscores its affinity for regions marked by elevated nutrient concentrations and little to no light. Conversely, previous studies have noted a correlation between chlorophyll-a and the presence of Alpha1 (Chen et al., 2014; Chen et al., 2016), suggesting its reliance on photosynthate from primary producers.

Low but quantifiable N_2 fixation rates were detected in the transition zone chlorophyll front

Stations 17-19 were characterized by elevated surface chlorophyll, a decrease in salinity, and a shift to denser and colder water (Figure 1). These hydrographic factors are indicative of the transition from the oligotrophic gyre to the transition zone (Polovina et al., 2001). The distinct hydrographic features suggest a low mixing rate between these two water masses, leading to the observed changes. The pronounced chlorophyll increases further indicates the proximity to the TZCF (Polovina et al., 2001).

Along with these hydrographic shifts, changes in the diazotrophic assemblages associated with the TZCF were observed. At Station 17, the ddPCR analysis showed depth-related variations: UCYN-A1 was undetectable at 5 m and 15 m but was present at deeper depths of 64 m and 150 m as depicted in Figure 2 (ddPCR analysis of UCYN-A1 across various depths). Gamma A was absent at this station. Unfortunately, the abundance of UCYN-A1 at Stations 18 and 19 could not be ascertained due to unavailable ddPCR samples (Figure 2). In contrast, Figure 5 (amplicon sequencing data across Stations 17-19) highlighted the absence of Gamma A. Instead, it showed sporadic signals of Gamma 3 (originally described by (Halm et al., 2012), g-ETSP2 (Turk-Kubo et al., 2014), and SCCS-Turk-Kubo3 (Turk-Kubo et al., 2022) along with additional sequences affiliating with groups 1B and 1G. Additionally, Station 18 at 80 m was dominated by *Trichodesmium*, although it remained below the ddPCR detection threshold. Although a temperature decline was recorded, the

physiological responses of these poorly characterized diazotrophs to such changes remain elusive.

Despite the presence of diazotrophs, NFR were low in the transition zone (average = 0.07 ± 0.03 nmol N L^{-1} d^{-1}, Figure 3). Gradoville et al., (2020) reported sporadic detection of NFR in the vicinity of the transition zone during spring/summer, with no NFR detected in April 2016, followed by low but detectable rates the following year (June 2017, 1.35–5.52 nmol N L^{-1} d^{-1}). Gradoville et al. (2020) suggested that the detectable NFR in 2017 may have been due to shifts in macronutrient concentrations later in the season or enhanced aeolian dust deposition and iron concentrations. This expedition took place in winter 2019, a period characterized by a north-south shift of the TZCF (Polovina et al., 2001). Although NFR were lower than the previously reported rate from the June 2017 survey, the trend aligns with their survey, where NPTZ has generally lower NFR than NPSG. However, the NFR cannot be ascribed solely to nutrient alterations since no significant change in nutrients was observed at depths hosting detectable diazotrophs.

Conclusion and Future Directions

Despite the recognized significance of NPSG as a diazotroph habitat, it remains largely under-sampled, with many research surveys concentrated at or near Station ALOHA. Notably, there is a pronounced data deficiency from the western NPSG, especially at sub-surface depths inhabited by diazotrophs, as pointed out by Shao et al. (2023). This study, conducted in the under-sampled fall/winter season, fills this knowledge gap by showing that there is a consistent presence of various diazotroph populations and that there is low but quantifiable NFR, including the detection of two *Crocosphaera* strains in the warmer western regions, the emergence of different UCYN-A strains across the transect, and distinct NCD distribution patterns. Looking ahead, it's imperative that future research delves into the factors that influence the observable NFR in the transition zone.

Acknowledgements

We gratefully acknowledge the captain and crew of the R/V Sally Ride for their support, Bruce Appelgate and the Scripps Institute of Oceanography Ship Fund Program for awarding us ship time, the SCOPE technical team. This work was supported by a grant from the Simons Foundation (SCOPE Award ID 329108).

References

Ashkezari, M. D., Hagen, N. R., Denholtz, M., Neang, A., Burns, T. C., Morales, R. L., Lee, C. P., Hill, C. N., & Armbrust, E. V. (2021). Simons Collaborative Marine Atlas Project (Simons CMAP): An open-source portal to share, visualize, and analyze ocean data. *Limnology and Oceanography: Methods*, *19*(7), 488-496. https://doi.org/https://doi.org/10.1002/lom3.10439

Aumont, O., Ethé, C., Tagliabue, A., Bopp, L., & Gehlen, M. (2015). PISCES-v2: an ocean biogeochemical model for carbon and ecosystem studies. *Geosci. Model Dev.*, *8*(8), 2465-2513. https://doi.org/10.5194/gmd-8-2465-2015

Baas-Becking, L. (1934). Geobiologie of inleiding tot de milieukunde. WP van Stockum and Zoon NV, The Hague, The Netherlands. *Cited from*, 14-24.

Behrenfeld, M. J., & Kolber, Z. S. (1999). Widespread Iron Limitation of Phytoplankton in the South Pacific Ocean. *science*, *283*(5403), 840-843. https://doi.org/doi:10.1126/science.283.5403.840

Benavides, M., Shoemaker, K. M., Moisander, P. H., Niggemann, J., Dittmar, T., Duhamel, S., Grosso, O., Pujo-Pay, M., Hélias-Nunige, S., Fumenia, A., & Bonnet, S. (2018). Aphotic N_2 fixation along an oligotrophic to ultraoligotrophic transect in the western tropical South Pacific Ocean. *Biogeosciences*, *15*(10), 3107-3119. https://doi.org/10.5194/bg-15-3107-2018

Bentzon-Tilia, M., Traving, S. J., Mantikci, M., Knudsen-Leerbeck, H., Hansen, J. L. S., Markager, S., & Riemann, L. (2015). Significant N_2 fixation by heterotrophs,

photoheterotrophs and heterocystous cyanobacteria in two temperate estuaries. *The ISME journal*, *9*(2), 273-285. https://doi.org/10.1038/ismej.2014.119

Bergman, B., Gallon, J. R., Rai, A. N., & Stal, L. J. (1997). N2 Fixation by non-heterocystous cyanobacteria. *FEMS Microbiology Reviews*, *19*(3), 139-185. https://doi.org/https://doi.org/10.1016/S0168-6445(96)00028-9

Berman-Frank, I., Lundgren, P., & Falkowski, P. (2003). Nitrogen fixation and photosynthetic oxygen evolution in cyanobacteria. *Research in microbiology*, *154*(3), 157-164.

Bi, R., Ismar, S. M., Sommer, U., & Zhao, M. (2018). Simultaneous shifts in stoichiometric and fatty acid composition of *Emiliania huxleyi* in response to environmental changes 2.

Björkman, K. M., & Karl, D. M. (2003). Bioavailability of dissolved organic phosphorus in the euphotic zone at Station ALOHA, North Pacific Subtropical Gyre. *Limnology and Oceanography*, *48*(3), 1049-1057. https://doi.org/https://doi.org/10.4319/lo.2003.48.3.1049

Bombar, D., Heller, P., Sanchez-Baracaldo, P., Carter, B. J., & Zehr, J. P. (2014). Comparative genomics reveals surprising divergence of two closely related strains of uncultivated UCYN-A cyanobacteria. *8*(12), 2530-2542. https://doi.org/10.1038/ismej.2014.167

Bombar, D., Paerl, R. W., & Riemann, L. (2016). Marine non-cyanobacterial diazotrophs: moving beyond molecular detection. *Trends in Microbiology*, *24*(11), 916-927.

Böttjer, D., Dore, J. E., Karl, D. M., Letelier, R. M., Mahaffey, C., Wilson, S. T., Zehr, J., & Church, M. J. (2017). Temporal variability of nitrogen fixation and particulate nitrogen export at Station ALOHA. *Limnology and Oceanography*, *62*(1), 200-216. https://doi.org/https://doi.org/10.1002/lno.10386

Boyd, P. W., Rynearson, T. A., Armstrong, E. A., Fu, F., Hayashi, K., Hu, Z., Hutchins, D. A., Kudela, R. M., Litchman, E., & Mulholland, M. R. (2013). Marine phytoplankton temperature versus growth responses from polar to tropical waters–outcome of a scientific community-wide study. *PLoS ONE*, *8*(5), e63091.

Brauer, V. S., Stomp, M., Rosso, C., van Beusekom, S. A., Emmerich, B., Stal, L. J., & Huisman, J. (2013). Low temperature delays timing and enhances the cost of nitrogen fixation in the unicellular cyanobacterium *Cyanothece*. *The ISME journal*, *7*(11), 2105-2115.

Breitbarth, E., Oschlies, A., & LaRoche, J. (2007). Physiological constraints on the global distribution of *Trichodesmium* effect of temperature on diazotrophy. *Biogeosciences*, *4*(1), 53-61. https://doi.org/10.5194/bg-4-53-2007

Brown, S. M., & Jenkins, B. D. (2014). Profiling gene expression to distinguish the likely active diazotrophs from a sea of genetic potential in marine sediments. *Environmental Microbiology*, *16*(10), 3128-3142. https://doi.org/https://doi.org/10.1111/1462-2920.12403

Burns, J. A., Pittis, A. A., & Kim, E. (2018). Gene-based predictive models of trophic modes suggest Asgard archaea are not phagocytotic. *Nature Ecology & Evolution*, *2*(4), 697-704. https://doi.org/10.1038/s41559-018-0477-7

Cabello, A. M., Turk-Kubo, K. A., Hayashi, K., Jacobs, L., Kudela, R. M., & Zehr, J. P. (2020). Unexpected presence of the nitrogen-fixing symbiotic cyanobacterium UCYN-A in Monterey Bay, California. *J Phycol*, *56*(6), 1521-1533. https://doi.org/10.1111/jpy.13045

Callahan, B. J., McMurdie, P. J., Rosen, M. J., Han, A. W., Johnson, A. J. A., & Holmes, S. P. (2016). DADA2: High-resolution sample inference from Illumina amplicon data. *Nature methods*, *13*(7), 581-583.

Canfield, D. E., Glazer, A. N., & Falkowski, P. G. (2010). The Evolution and Future of Earth's Nitrogen Cycle. *Science*, *330*(6001), 192-196. https://doi.org/doi:10.1126/science.1186120

Capone, D. G., Burns, J. A., Montoya, J. P., Subramaniam, A., Mahaffey, C., Gunderson, T., Michaels, A. F., & Carpenter, E. J. (2005). Nitrogen fixation by *Trichodesmium* spp.: An important source of new nitrogen to the tropical and subtropical North Atlantic Ocean. *Global Biogeochemical Cycles*, *19*(2), n/a-n/a. https://doi.org/10.1029/2004gb002331

Capone, D. G., Zehr, J. P., Paerl, H. W., Bergman, B., & Carpenter, E. J. (1997). *Trichodesmium*, a Globally Significant Marine Cyanobacterium. *Science*, *276*(5316), 1221-1229. https://doi.org/doi:10.1126/science.276.5316.1221

Carpenter, E. J., & Capone, D. G. (1992). Nitrogen fixation in Trichodesmium blooms. In *Marine pelagic cyanobacteria: Trichodesmium and other diazotrophs* (pp. 211-217). Springer.

Carpenter, E. J., Montoya, J. P., Burns, J., Mulholland, M. R., Subramaniam, A., & Capone, D. G. (1999). Extensive bloom of a N_2-fixing diatom/cyanobacterial association in the tropical Atlantic Ocean. *Marine Ecology Progress Series*, *185*, 273-283.

Carroll, D., Menemenlis, D., Adkins, J., Bowman, K., Brix, H., Dutkiewicz, S., Fenty, I., Gierach, M., Hill, C., & Jahn, O. (2020). The ECCO-Darwin data-assimilative global ocean biogeochemistry model: Estimates of seasonal to multidecadal surface ocean pCO_2 and air-sea CO_2 flux. *Journal of Advances in Modeling Earth Systems*, *12*(10), e2019MS001888.

Cermak, N., Becker, J. W., Knudsen, S. M., Chisholm, S. W., Manalis, S. R., & Polz, M. F. (2017). Direct single-cell biomass estimates for marine bacteria via Archimedes' principle. *The ISME journal*, *11*(3), 825-828.

Chen, T.-Y., Chen, Y.-l. L., Sheu, D.-S., Chen, H.-Y., Lin, Y.-H., & Shiozaki, T. (2019). Community and abundance of heterotrophic diazotrophs in the northern South China Sea: Revealing the potential importance of a new alphaproteobacterium in N_2 fixation. *Deep Sea Research Part I: Oceanographic Research Papers*, *143*, 104-114. https://doi.org/https://doi.org/10.1016/j.dsr.2018.11.006

Cheung, S., Nitanai, R., Tsurumoto, C., Endo, H., Nakaoka, S. i., Cheah, W., Lorda, J. F., Xia, X., Liu, H., & Suzuki, K. (2020). Physical forcing controls the basin-scale occurrence of nitrogen-fixing organisms in the North Pacific Ocean. *Global Biogeochemical Cycles*, *34*(9), e2019GB006452.

Cheung, S., Suzuki, K., Saito, H., Umezawa, Y., Xia, X., & Liu, H. (2017). Highly heterogeneous diazotroph communities in the Kuroshio Current and the Tokara Strait, Japan. *PLoS ONE*, *12*(10), e0186875.

Chin, K. J., Liesack, W., & Janssen, P. H. (2001). *Opitutus terrae* gen. nov., sp. nov., to accommodate novel strains of the division 'Verrucomicrobia' isolated from rice paddy soil. *International Journal of Systematic and Evolutionary Microbiology*, *51*(6), 1965-1968. https://doi.org/https://doi.org/10.1099/00207713-51-6-1965

Church, Jenkins, B., Karl, D., & Zehr, J. (2005). Vertical distributions of nitrogen-fixing phylotypes at Stn Aloha in the oligotrophic North Pacific Ocean. *Aquatic Microbial Ecology*, *38*, 3-14. https://doi.org/10.3354/ame038003

Church, Short, C. M., Jenkins, B. D., Karl, D. M., & Zehr, J. P. (2005). Temporal Patterns of Nitrogenase Gene (*nifH*) Expression in the Oligotrophic North Pacific Ocean. *71*(9), 5362-5370. https://doi.org/10.1128/aem.71.9.5362-5370.2005

Church, M. J., Björkman, K. M., Karl, D. M., Saito, M. A., & Zehr, J. P. (2008). Regional distributions of nitrogen-fixing bacteria in the Pacific Ocean. *Limnology and Oceanography*, *53*(1), 63-77. https://doi.org/https://doi.org/10.4319/lo.2008.53.1.0063

Church, M. J., Mahaffey, C., Letelier, R. M., Lukas, R., Zehr, J. P., & Karl, D. M. (2009). Physical forcing of nitrogen fixation and diazotroph community structure in the North Pacific subtropical gyre. *23*(2), n/a-n/a. https://doi.org/10.1029/2008gb003418

Cleveland, C. S., Turk-Kubo, K. A., Zhao, Y., Zehr, J. P., & Webb, E. A. (2023). A novel, N_2-fixing cyanobacterium present and active in the global oceans. *bioRxiv*, 2023.2008.2027.555023. https://doi.org/10.1101/2023.08.27.555023

Codispoti, L. (2007). An oceanic fixed nitrogen sink exceeding 400 Tg N a^{-1} vs the concept of homeostasis in the fixed-nitrogen inventory. *Biogeosciences*, *4*(2), 233-253.

Colón-López, M. S., Sherman, D. M., & Sherman, L. A. (1997). Transcriptional and translational regulation of nitrogenase in light-dark-and continuous-light-grown cultures of the unicellular cyanobacterium *Cyanothece* sp. strain ATCC 51142. *Journal of Bacteriology*, *179*(13), 4319-4327.

Cornejo-Castillo, F. M., & Zehr, J. P. (2019). Hopanoid lipids may facilitate aerobic nitrogen fixation in the ocean. *Proc Natl Acad Sci U S A*, *116*(37), 18269-18271. https://doi.org/10.1073/pnas.1908165116

Cornejo-Castillo, F. M., & Zehr, J. P. (2021). Intriguing size distribution of the uncultured and globally widespread marine non-cyanobacterial diazotroph Gamma-A. *The ISME journal*, *15*(1), 124-128.

Dedman, C. J., Barton, S., Fournier, M., & Rickaby, R. E. (2023). The cellular response to ocean warming in *Emiliania huxleyi*. *Frontiers in Microbiology*, *14*, 1177349.

Dixon, R., & Kahn, D. (2004). Genetic regulation of biological nitrogen fixation. *Nat Rev Microbiol*, *2*(8), 621-631. https://doi.org/10.1038/nrmicro954

Dore, J. E., Brum, J. R., Tupas, L. M., & Karl, D. M. (2002). Seasonal and interannual variability in sources of nitrogen supporting export in the oligotrophic subtropical

North Pacific Ocean. *Limnology and Oceanography*, *47*(6), 1595-1607. https://doi.org/https://doi.org/10.4319/lo.2002.47.6.1595

Dron, A., Rabouille, S., Claquin, P., Le Roy, B., Talec, A., & Sciandra, A. (2012). Light-dark (12:12) cycle of carbon and nitrogen metabolism in *Crocosphaera watsonii* WH8501: relation to the cell cycle. *14*(4), 967-981. https://doi.org/10.1111/j.1462-2920.2011.02675.x

Dugdale, R. C., & Goering, J. J. (1967). Uptake of new and regenerated forms of nitrogen in primary productivity. *Limnology and Oceanography*, *12*(2), 196-206. https://doi.org/https://doi.org/10.4319/lo.1967.12.2.0196

Dugenne, M., Gradoville, M. R., Church, M. J., Wilson, S. T., Sheyn, U., Harke, M. J., Björkman, K. M., Hawco, N. J., Hynes, A. M., Ribalet, F., Karl, D. M., DeLong, E. F., Dyhrman, S. T., Armbrust, E. V., John, S., Eppley, J. M., Harding, K., Stewart, B., Cabello, A. M., . . . Zehr, J. P. (2023). Nitrogen Fixation in Mesoscale Eddies of the North Pacific Subtropical Gyre: Patterns and Mechanisms. *Global Biogeochemical Cycles*, *37*(4), e2022GB007386. https://doi.org/https://doi.org/10.1029/2022GB007386

Dugenne, M., Henderikx Freitas, F., Wilson, S. T., Karl, D. M., & White, A. E. (2020). Life and death of *Crocosphaera* sp. in the Pacific Ocean: Fine scale predator–prey dynamics. *Limnology and Oceanography*, *65*(11), 2603-2617. https://doi.org/https://doi.org/10.1002/lno.11473

Dyhrman, S. T., Chappell, P. D., Haley, S. T., Moffett, J. W., Orchard, E. D., Waterbury, J. B., & Webb, E. A. (2006). Phosphonate utilization by the globally important

marine diazotroph *Trichodesmium*. *Nature*, *439*(7072), 68-71. https://doi.org/10.1038/nature04203

Dyhrman, S. T., & Haley, S. T. (2006a). Phosphorus Scavenging in the Unicellular Marine Diazotroph *Crocosphaera watsonii*. *Applied and Environmental Microbiology*, *72*(2), 1452-1458. https://doi.org/10.1128/aem.72.2.1452-1458.2006

Dyhrman, S. T., & Haley, S. T. (2006b). Phosphorus scavenging in the unicellular marine diazotroph *Crocosphaera watsonii*. *Appl Environ Microbiol*, *72*(2), 1452-1458. https://doi.org/10.1128/aem.72.2.1452-1458.2006

Edwards, K. F. (2019). Mixotrophy in nanoflagellates across environmental gradients in the ocean. *Proceedings of the National Academy of Sciences*, *116*(13), 6211-6220. https://doi.org/10.1073/pnas.1814860116

Eppley, R. W. (1972). Temperature and phytoplankton growth in the sea. *Fish. bull*, *70*(4), 1063-1085.

Falkowski, Barber, R. T., & Smetacek, V. (1998). Biogeochemical Controls and Feedbacks on Ocean Primary Production. *Science*, *281*(5374), 200-206. https://doi.org/doi:10.1126/science.281.5374.200

Farnelid, H., Andersson, A. F., Bertilsson, S., Al-Soud, W. A., Hansen, L. H., Sørensen, S., Steward, G. F., Hagström, Å., & Riemann, L. (2011). Nitrogenase gene amplicons from global marine surface waters are dominated by genes of non-cyanobacteria. *PLoS ONE*, *6*(4), e19223.

Farnelid, H., Turk-Kubo, K., Muñoz-Marín, M., & Zehr, J. (2016). New insights into the ecology of the globally significant uncultured nitrogen-fixing symbiont UCYN-A. *Aquatic Microbial Ecology*, *77*(3), 125-138. https://doi.org/10.3354/ame01794

Fay, P. (1992). Oxygen relations of nitrogen fixation in cyanobacteria. *Microbiol Rev*, *56*(2), 340-373. https://doi.org/10.1128/mr.56.2.340-373.1992

Ferrón, S., del Valle, D. A., Björkman, K. M., Quay, P. D., Church, M. J., & Karl, D. M. (2016). Application of membrane inlet mass spectrometry to measure aquatic gross primary production by the ^{18}O in vitro method. *Limnology and Oceanography: Methods*, *14*(9), 610-622.

Field, C. B., Behrenfeld, M. J., Randerson, J. T., & Falkowski, P. (1998). Primary Production of the Biosphere: Integrating Terrestrial and Oceanic Components. *Science*, *281*(5374), 237-240. https://doi.org/doi:10.1126/science.281.5374.237

Fischer, R., Giebel, H. A., Hillebrand, H., & Ptacnik, R. (2017). Importance of mixotrophic bacterivory can be predicted by light and loss rates. *Oikos*, *126*(5), 713-722.

Foster, R. A., Subramaniam, A., Mahaffey, C., Carpenter, E. J., Capone, D. G., & Zehr, J. P. (2007). Influence of the Amazon River plume on distributions of free-living and symbiotic cyanobacteria in the western tropical north Atlantic Ocean. *Limnology and Oceanography*, *52*(2), 517-532. https://doi.org/https://doi.org/10.4319/lo.2007.52.2.0517

Foster, R. A., Villareal, T. A., Lundin, D., Waterbury, J. B., Webb, E. A., & Zehr, J. P. (2022). *Richelia*. In *Bergey's Manual of Systematics of Archaea and Bacteria* (pp. 1-17). https://doi.org/https://doi.org/10.1002/9781118960608.gbm01520

Frias-Lopez, J., Thompson, A., Waldbauer, J., & Chisholm, S. W. (2009). Use of stable isotope-labelled cells to identify active grazers of picocyanobacteria in ocean surface waters. *Environmental Microbiology*, *11*(2), 512-525.

Fu, F.-X., Yu, E., Garcia, N. S., Gale, J., Luo, Y., Webb, E. A., & Hutchins, D. A. (2014). Differing responses of marine N_2 fixers to warming and consequences for future diazotroph community structure. *Aquatic Microbial Ecology*, *72*(1), 33-46.

Galili, T., O'Callaghan, A., Sidi, J., & Sievert, C. (2018). heatmaply: an R package for creating interactive cluster heatmaps for online publishing. *Bioinformatics*, *34*(9), 1600-1602. https://doi.org/10.1093/bioinformatics/btx657

Gallon, J. (1992). Reconciling the incompatible: nitrogen fixation and oxygen. *New phytologist*, *122*, 571-609.

Galloway, J. N., Dentener, F. J., Capone, D. G., Boyer, E. W., Howarth, R. W., Seitzinger, S. P., Asner, G. P., Cleveland, C. C., Green, P., & Holland, E. A. (2004). Nitrogen cycles: past, present, and future. *Biogeochemistry*, *70*, 153-226.

Garcia, N. S., Fu, F., Sedwick, P. N., & Hutchins, D. A. (2015). Iron deficiency increases growth and nitrogen-fixation rates of phosphorus-deficient marine cyanobacteria. *ISME*, *9*(1), 238-245. https://doi.org/10.1038/ismej.2014.104

Goebel, N. L., Edwards, C. A., Church, M. J., & Zehr, J. P. (2007). Modeled contributions of three types of diazotrophs to nitrogen fixation at Station ALOHA. *The ISME journal*, *1*(7), 606-619. https://doi.org/10.1038/ismej.2007.80

Gradoville, M. R., Bombar, D., Crump, B. C., Letelier, R. M., Zehr, J. P., & White, A. E. (2017). Diversity and activity of nitrogen-fixing communities across ocean basins. *Limnology and Oceanography*, *62*(5), 1895-1909.

Gradoville, M. R., Cabello, A. M., Wilson, S. T., Turk-Kubo, K. A., Karl, D. M., & Zehr, J. P. (2021). Light and depth dependency of nitrogen fixation by the non-photosynthetic, symbiotic cyanobacterium UCYN-A. *Environmental Microbiology*, *23*(8), 4518-4531.

Gradoville, M. R., Farnelid, H., White, A. E., Turk-Kubo, K. A., Stewart, B., Ribalet, F., Ferrón, S., Pinedo-Gonzalez, P., Armbrust, E. V., Karl, D. M., John, S., & Zehr, J. P. (2020). Latitudinal constraints on the abundance and activity of the cyanobacterium UCYN-A and other marine diazotrophs in the North Pacific. *Limnology and Oceanography*. https://doi.org/10.1002/lno.11423

Green, S. J., Venkatramanan, R., & Naqib, A. (2015). Deconstructing the polymerase chain reaction: understanding and correcting bias associated with primer degeneracies and primer-template mismatches. *PLoS ONE*, *10*(5), e0128122.

Gruber, N., & Galloway, J. N. (2008). An Earth-system perspective of the global nitrogen cycle. *Nature*, *451*(7176), 293-296. https://doi.org/10.1038/nature06592

Gruber, N., & Sarmiento, J. L. (1997). Global patterns of marine nitrogen fixation and denitrification. *Global Biogeochemical Cycles*, *11*(2), 235-266. https://doi.org/https://doi.org/10.1029/97GB00077

Guillard, R. R., & Ryther, J. H. (1962). Studies of marine planktonic diatoms: I. *Cyclotella nana Hustedt*, and *Detonula confervacea* (Cleve) *Gran*. *Canadian journal of microbiology*, *8*(2), 229-239.

Hagino, K., Onuma, R., Kawachi, M., & Horiguchi, T. (2013). Discovery of an Endosymbiotic Nitrogen-Fixing Cyanobacterium UCYN-A in *Braarudosphaera bigelowii* (*Prymnesiophyceae*). *8*(12), e81749. https://doi.org/10.1371/journal.pone.0081749

Halm, H., Lam, P., Ferdelman, T. G., Lavik, G., Dittmar, T., LaRoche, J., D'Hondt, S., & Kuypers, M. M. (2012). Heterotrophic organisms dominate nitrogen fixation in the South Pacific Gyre. *ISME*, *6*(6), 1238-1249. https://doi.org/10.1038/ismej.2011.182

Hansen, P., & Hjorth, M. (2002). Growth and grazing responses of *Chrysochromulina ericina* (*Prymnesiophyceae*): the role of irradiance, prey concentration and pH. *Marine Biology*, *141*, 975-983.

Harding, K., Turk-Kubo, K. A., Sipler, R. E., Mills, M. M., Bronk, D. A., & Zehr, J. P. (2018). Symbiotic unicellular cyanobacteria fix nitrogen in the Arctic Ocean. *Proceedings of the National Academy of Sciences*, *115*(52), 13371-13375. https://doi.org/10.1073/pnas.1813658115

Harding, K. J., Turk-Kubo, K. A., Mak, E. W. K., Weber, P. K., Mayali, X., & Zehr, J. P. (2022). Cell-specific measurements show nitrogen fixation by particle-attached putative non-cyanobacterial diazotrophs in the North Pacific Subtropical Gyre. *Nature Communications*, *13*(1), 1-10.

Henke, B. A., Turk-Kubo, K. A., Bonnet, S., & Zehr, J. P. (2018). Distributions and Abundances of Sublineages of the N_2-Fixing Cyanobacterium *Candidatus Atelocyanobacterium thalassa* (UCYN-A) in the New Caledonian Coral Lagoon. *Front Microbiol*, *9*, 554. https://doi.org/10.3389/fmicb.2018.00554

Hennon, G. M., Hernández Limón, M. D., Haley, S. T., Juhl, A. R., & Dyhrman, S. T. (2017). Diverse CO_2-induced responses in physiology and gene expression among eukaryotic phytoplankton. *Frontiers in Microbiology*, *8*, 2547.

Herlemann, D. P., Labrenz, M., Jürgens, K., Bertilsson, S., Waniek, J. J., & Andersson, A. F. (2011). Transitions in bacterial communities along the 2000 km salinity gradient of the Baltic Sea. *The ISME journal*, *5*(10), 1571-1579.

Hillebrand, H., Dürselen, C.-D., Kirschtel, D., Pollingher, U., & Zohary, T. (1999). Biovolume Calculation for Pelagic and Benthic Microalgae. *Journal of Phycology*, *35*(2), 403-424. https://doi.org/https://doi.org/10.1046/j.1529-8817.1999.3520403.x

Hofmann Elizondo, U., Righetti, D., Benedetti, F., & Vogt, M. (2021). Biome partitioning of the global ocean based on phytoplankton biogeography. *Progress in Oceanography*, *194*, 102530. https://doi.org/https://doi.org/10.1016/j.pocean.2021.102530

Howard, J. B., & Rees, D. C. (1996). Structural Basis of Biological Nitrogen Fixation. *Chem Rev*, *96*(7), 2965-2982. https://doi.org/10.1021/cr9500545

Inomura, K., Bragg, J., & Follows, M. J. (2017). A quantitative analysis of the direct and indirect costs of nitrogen fixation: a model based on *Azotobacter vinelandii*. *The ISME journal*, *11*(1), 166-175.

Jickells, T. D., Buitenhuis, E., Altieri, K., Baker, A. R., Capone, D., Duce, R. A., Dentener, F., Fennel, K., Kanakidou, M., LaRoche, J., Lee, K., Liss, P., Middelburg, J. J., Moore, J. K., Okin, G., Oschlies, A., Sarin, M., Seitzinger, S., Sharples, J., . . . Zamora, L. M. (2017). A reevaluation of the magnitude and impacts of anthropogenic atmospheric nitrogen inputs on the ocean. *Global Biogeochemical Cycles*, *31*(2), 289-305. https://doi.org/https://doi.org/10.1002/2016GB005586

Jones, H. (1997). A classification of mixotrophic protists based on their behaviour. *Freshwater Biology*, *37*(1), 35-43.

Karl, D., Letelier, R., Tupas, L., Dore, J., Christian, J., & Hebel, D. (1997). The role of nitrogen fixation in biogeochemical cycling in the subtropical North Pacific Ocean. *Nature*, *388*(6642), 533-538. https://doi.org/10.1038/41474

Karl, D. M. (1999). A sea of change: biogeochemical variability in the North Pacific Subtropical Gyre. *Ecosystems*, *2*, 181-214.

Kavanaugh, M. T., Hales, B., Saraceno, M., Spitz, Y. H., White, A. E., & Letelier, R. M. (2014). Hierarchical and dynamic seascapes: A quantitative framework for scaling

pelagic biogeochemistry and ecology. *Progress in Oceanography*, *120*, 291-304. https://doi.org/https://doi.org/10.1016/j.pocean.2013.10.013

Kawachi, M., Inouye, I., Maeda, O., & Chihara, M. (1991). The haptonema as a food-capturing device: observations on *Chrysochromulina hirta* (*Prymnesiophyceae*). *Phycologia*, *30*(6), 563-573. https://doi.org/10.2216/i0031-8884-30-6-563.1

Kitajima, S., Furuya, K., Hashihama, F., Takeda, S., & Kanda, J. (2009). Latitudinal distribution of diazotrophs and their nitrogen fixation in the tropical and subtropical western North Pacific. *Limnology and Oceanography*, *54*(2), 537-547.

Klawonn, I., Bonaglia, S., Brüchert, V., & Ploug, H. (2015). Aerobic and anaerobic nitrogen transformation processes in N_2-fixing cyanobacterial aggregates. *The ISME journal*, *9*(6), 1456-1466.

Kong, L., Jing, H., Kataoka, T., Sun, J., & Liu, H. (2011). Phylogenetic diversity and spatio-temporal distribution of nitrogenase genes (*nifH*) in the northern South China Sea. *Aquatic Microbial Ecology*, *65*(1), 15-27.

Krupke, A., Mohr, W., Laroche, J., Fuchs, B. M., Amann, R. I., & Kuypers, M. M. (2015). The effect of nutrients on carbon and nitrogen fixation by the UCYN-A–haptophyte symbiosis. *The ISME journal*, *9*(7), 1635-1647. https://doi.org/10.1038/ismej.2014.253

Landa, M., Turk-Kubo, K. A., Cornejo-Castillo, F. M., Henke, B. A., & Zehr, J. P. (2021). Critical Role of Light in the Growth and Activity of the Marine N_2-Fixing UCYN-A Symbiosis [Original Research]. *Frontiers in Microbiology*, *12*. https://doi.org/10.3389/fmicb.2021.666739

Landry, M., & Hassett, R. (1982). Estimating the grazing impact of marine micro-zooplankton. *Marine Biology*, *67*(3), 283-288.

Landry, M., Kirshtein, J., & Constantinou, J. (1995). A refined dilution technique for measuring the community grazing impact of microzooplankton, with experimental tests in the central equatorial Pacific. *Marine ecology progress series. Oldendorf*, *120*(1), 53-63.

Landry, M. R., Brown, S. L., Campbell, L., Constantinou, J., & Liu, H. (1998). Spatial patterns in phytoplankton growth and microzooplankton grazing in the Arabian Sea during monsoon forcing. *Deep Sea Research Part II: Topical Studies in Oceanography*, *45*(10-11), 2353-2368.

Langlois, R., Großkopf, T., Mills, M., Takeda, S., & LaRoche, J. (2015). Widespread Distribution and Expression of Gamma A (UMB), an Uncultured, Diazotrophic, γ-Proteobacterial *nifH* Phylotype. *PLoS ONE*, *10*(6), e0128912. https://doi.org/10.1371/journal.pone.0128912

Langlois, R. J., Hummer, D., & Laroche, J. (2008). Abundances and Distributions of the Dominant *nifH* Phylotypes in the Northern Atlantic Ocean. *Applied and Environmental Microbiology*, *74*(6), 1922-1931. https://doi.org/10.1128/aem.01720-07

Leigh, G. J. (2002). *Nitrogen fixation at the millennium*. Elsevier.

Li, W. K. (1980). Temperature adaptation in phytoplankton: cellular and photosynthetic characteristics. *Primary productivity in the sea*, 259-279.

Liu, X., & Millero, F. J. (2002). The solubility of iron in seawater. *Marine Chemistry*, *77*(1), 43-54. https://doi.org/https://doi.org/10.1016/S0304-4203(01)00074-3

Love, M. I., Huber, W., & Anders, S. (2014). Moderated estimation of fold change and dispersion for RNA-seq data with DESeq2. *Genome biology*, *15*(12), 1-21.

Marie, D., Partensky, F., Vaulot, D., & Brussaard, C. (1999). Enumeration of Phytoplankton, Bacteria, and Viruses in Marine Samples. *Current Protocols in Cytometry*, *10*(1), 11.11.11-11.11.15. https://doi.org/https://doi.org/10.1002/0471142956.cy1111s10

Martínez-Pérez, C., Mohr, W., Löscher, C. R., Dekaezemacker, J., Littmann, S., Yilmaz, P., Lehnen, N., Fuchs, B. M., Lavik, G., Schmitz, R. A., Laroche, J., & Kuypers, M. M. M. (2016). The small unicellular diazotrophic symbiont, UCYN-A, is a key player in the marine nitrogen cycle. *Nature Microbiology*, *1*(11), 16163. https://doi.org/10.1038/nmicrobiol.2016.163

McMurdie, P. J., & Holmes, S. (2013). phyloseq: an R package for reproducible interactive analysis and graphics of microbiome census data. *PLoS ONE*, *8*(4), e61217.

Meyer, N. R., Fortney, J. L., & Dekas, A. E. (2021). NanoSIMS sample preparation decreases isotope enrichment: magnitude, variability and implications for single-cell rates of microbial activity. *Environmental Microbiology*, *23*(1), 81-98.

Michaels, A. F., Olson, D., Sarmiento, J. L., Ammerman, J. W., Fanning, K., Jahnke, R., Knap, A. H., Lipschultz, F., & Prospero, J. M. (1996). Inputs, losses and

transformations of nitrogen and phosphorus in the pelagic North Atlantic Ocean. *Biogeochemistry*, *35*(1), 181-226. https://doi.org/10.1007/BF02179827

Mills, M. M., Ridame, C., Davey, M., La Roche, J., & Geider, R. J. (2004). Iron and phosphorus co-limit nitrogen fixation in the eastern tropical North Atlantic. *Nature*, *429*(6989), 292-294. https://doi.org/10.1038/nature02550

Mills, M. M., Turk-Kubo, K. A., van Dijken, G. L., Henke, B. A., Harding, K., Wilson, S. T., Arrigo, K. R., & Zehr, J. P. (2020). Unusual marine cyanobacteria/haptophyte symbiosis relies on N_2 fixation even in N-rich environments. *The ISME journal*, *14*(10), 2395-2406.

Mitra, A., Flynn, K. J., Burkholder, J. M., Berge, T., Calbet, A., Raven, J. A., Granéli, E., Glibert, P. M., Hansen, P. J., Stoecker, D. K., Thingstad, F., Tillmann, U., Våge, S., Wilken, S., & Zubkov, M. V. (2014). The role of mixotrophic protists in the biological carbon pump. *Biogeosciences*, *11*(4), 995-1005. https://doi.org/10.5194/bg-11-995-2014

Mohr, W., Intermaggio, M. P., & Laroche, J. (2010). Diel rhythm of nitrogen and carbon metabolism in the unicellular, diazotrophic cyanobacterium *Crocosphaera watsonii* WH8501. *12*(2), 412-421. https://doi.org/10.1111/j.1462-2920.2009.02078.x

Moisander, P. H., Beinart, R. A., Hewson, I., White, A. E., Johnson, K. S., Carlson, C. A., Montoya, J. P., & Zehr, J. P. (2010). Unicellular Cyanobacterial Distributions Broaden the Oceanic N_2 Fixation Domain. *Science*, *327*(5972), 1512-1514. https://doi.org/10.1126/science.1185468

Moisander, P. H., Beinart, R. A., Voss, M., & Zehr, J. P. (2008). Diversity and abundance of diazotrophic microorganisms in the South China Sea during intermonsoon. *The ISME Journal*, *2*(9), 954-967.

Montoya, J. P., Holl, C. M., Zehr, J. P., Hansen, A., Villareal, T. A., & Capone, D. G. (2004). High rates of N_2 fixation by unicellular diazotrophs in the oligotrophic Pacific Ocean. *Nature*, *430*(7003), 1027-1032. https://doi.org/10.1038/nature02824

Montoya, J. P., Voss, M., Kahler, P., & Capone, D. G. (1996). A simple, high-precision, high-sensitivity tracer assay for N_2 fixation. *Applied and Environmental Microbiology*, *62*(3), 986-993.

Moonsamy, P., Williams, T., Bonella, P., Holcomb, C., Höglund, B., Hillman, G., Goodridge, D., Turenchalk, G., Blake, L., & Daigle, D. (2013). High throughput HLA genotyping using 454 sequencing and the Fluidigm Access Array™ system for simplified amplicon library preparation. *Tissue antigens*, *81*(3), 141-149.

Moore, C., Mills, M., Arrigo, K., Berman-Frank, I., Bopp, L., Boyd, P., Galbraith, E., Geider, R., Guieu, C., & Jaccard, S. (2013). Processes and patterns of oceanic nutrient limitation. *Nature Geoscience*, *6*(9), 701-710.

Mulholland, M., Bernhardt, P., Blanco-Garcia, J., Mannino, A., Hyde, K., Mondragon, E., Turk, K., Moisander, P., & Zehr, J. (2012). Rates of dinitrogen fixation and the abundance of diazotrophs in North American coastal waters between Cape Hatteras and Georges Bank. *Limnology and Oceanography*, *57*(4), 1067-1083.

Mulholland, M. R. (2007). The fate of nitrogen fixed by diazotrophs in the ocean.

Newton, W. E. (2015). Recent Advances in Understanding Nitrogenases and How They Work. In *Biological Nitrogen Fixation* (pp. 5-20). https://doi.org/https://doi.org/10.1002/9781119053095.ch2

Nishimura, T., Uchida, H., Noguchi, R., Oikawa, H., Suzuki, T., Funaki, H., Ihara, C., Hagino, K., Arimitsu, S., Tanii, Y., Abe, S., Hashimoto, K., Mimura, K., Tanaka, K., Yanagida, I., & Adachi, M. (2020). Abundance of the benthic dinoflagellate *Prorocentrum* and the diversity, distribution, and diarrhetic shellfish toxin production of *Prorocentrum lima* complex and *P. caipirignum* in Japan. *Harmful Algae*, *96*, 101687. https://doi.org/https://doi.org/10.1016/j.hal.2019.101687

Nygaard, K., & Tobiesen, A. (1993). Bacterivory in algae: A survival strategy during nutrient limitation. *38*(2), 273-279. https://doi.org/10.4319/lo.1993.38.2.0273

Offre, P., Spang, A., & Schleper, C. (2013). Archaea in biogeochemical cycles. *Annual Review of Microbiology*, *67*, 437-457.

Ohki, K., & Fujita, Y. (1988). Aerobic nitrogenase activity measured as acetylene reduction in the marine non-heterocystous cyanobacterium *Trichodesmium* spp. grown under artificial conditions. *Marine Biology*, *98*, 111-114.

Paerl, R. W., Hansen, T. N., Henriksen, N. N., Olesen, A. K., & Riemann, L. (2018). N-fixation and related O_2 constraints on model marine diazotroph *Pseudomonas stutzeri* BAL361. *Aquatic Microbial Ecology*, *81*(2), 125-136.

Pereira, N., Shilova, I. N., & Zehr, J. P. (2019). Use of the high-affinity phosphate transporter gene, *pstS*, as an indicator for phosphorus stress in the marine

diazotroph *Crocosphaera watsonii* (Chroococcales, Cyanobacteria). *J Phycol*, *55*(4), 752-761. https://doi.org/10.1111/jpy.12863

Polovina, J. J., Howell, E., Kobayashi, D. R., & Seki, M. P. (2001). The transition zone chlorophyll front, a dynamic global feature defining migration and forage habitat for marine resources. *Progress in Oceanography*, *49*(1-4), 469-483.

Postgate, J. (1998). *Nitrogen fixation*. Cambridge University Press.

Postgate, J. R., Stewart, W. D. P., & Rosswall, T. (1982). Biological nitrogen fixation: fundamentals. *Philosophical Transactions of the Royal Society of London. B, Biological Sciences*, *296*(1082), 375-385. https://doi.org/doi:10.1098/rstb.1982.0013

Priyadarshi, A., Smith, S. L., Mandal, S., Tanaka, M., & Yamazaki, H. (2019). Micro-scale patchiness enhances trophic transfer efficiency and potential plankton biodiversity. *Scientific Reports*, *9*(1), 17243. https://doi.org/10.1038/s41598-019-53592-6

Quast, C., Pruesse, E., Yilmaz, P., Gerken, J., Schweer, T., Yarza, P., Peplies, J., & Glöckner, F. O. (2012). The SILVA ribosomal RNA gene database project: improved data processing and web-based tools. *Nucleic acids research*, *41*(D1), D590-D596.

Ratkowsky, D., Lowry, R., McMeekin, T., Stokes, A., & Chandler, R. (1983). Model for bacterial culture growth rate throughout the entire biokinetic temperature range. *Journal of Bacteriology*, *154*(3), 1222-1226.

Raven, J. A., & Geider, R. J. (1988). Temperature and algal growth. *New phytologist*, *110*(4), 441-461.

Reygondeau, G., Longhurst, A., Martinez, E., Beaugrand, G., Antoine, D., & Maury, O. (2013). Dynamic biogeochemical provinces in the global ocean. *Global Biogeochemical Cycles*, *27*(4), 1046-1058.

Riemann, L., Farnelid, H., & Steward, G. F. (2010). Nitrogenase genes in non-cyanobacterial plankton: prevalence, diversity and regulation in marine waters. *Aquatic Microbial Ecology*, *61*(3), 235-247. https://www.int-res.com/abstracts/ame/v61/n3/p235-247/

Robson, R. L., & Postgate, J. R. (1980). Oxygen and hydrogen in biological nitrogen fixation. *Annual Reviews in Microbiology*, *34*(1), 183-207.

Rosenberg, E., DeLong, E. F., Lory, S., Stackebrandt, E., & Thompson, F. (2014). The prokaryotes: other major lineages of Bacteria and the Archaea.

Rothhaupt, K. O. (1996). Laboratorary Experiments with a Mixotrophic *Chrysophyte* and Obligately Phagotrophic and Photographic Competitors. *77*(3), 716. https://doi.org/10.2307/2265496

Saito, M. A., Bertrand, E. M., Dutkiewicz, S., Bulygin, V. V., Moran, D. M., Monteiro, F. M., Follows, M. J., Valois, F. W., & Waterbury, J. B. (2011). Iron conservation by reduction of metalloenzyme inventories in the marine diazotroph *Crocosphaera watsonii*. *Proceedings of the National Academy of Sciences*, *108*(6), 2184-2189. https://doi.org/doi:10.1073/pnas.1006943108

Sañudo-Wilhelmy, S. A., Kustka, A. B., Gobler, C. J., Hutchins, D. A., Yang, M., Lwiza, K., Burns, J., Capone, D. G., Raven, J. A., & Carpenter, E. J. (2001). Phosphorus limitation of nitrogen fixation by *Trichodesmium* in the central Atlantic Ocean. *Nature*, *411*(6833), 66-69. https://doi.org/10.1038/35075041

Sarkar, D., Landa, M., Bandyopadhyay, A., Pakrasi, H. B., Zehr, J. P., & Maranas, C. D. (2021). Elucidation of trophic interactions in an unusual single-cell nitrogen-fixing symbiosis using metabolic modeling. *PLoS Comput Biol*, *17*(5), e1008983. https://doi.org/10.1371/journal.pcbi.1008983

Scharek, R., Tupas, L. M., & Karl, D. M. (1999). Diatom fluxes to the deep sea in the oligotrophic North Pacific gyre at Station ALOHA. *Marine Ecology Progress Series*, *182*, 55-67.

Schindelin, J., Arganda-Carreras, I., Frise, E., Kaynig, V., Longair, M., Pietzsch, T., Preibisch, S., Rueden, C., Saalfeld, S., Schmid, B., Tinevez, J.-Y., White, D. J., Hartenstein, V., Eliceiri, K., Tomancak, P., & Cardona, A. (2012). Fiji: an open-source platform for biological-image analysis. *Nature methods*, *9*(7), 676-682. https://doi.org/10.1038/nmeth.2019

Schneider, C. A., Rasband, W. S., & Eliceiri, K. W. (2012). NIH Image to ImageJ: 25 years of image analysis. *Nature methods*, *9*(7), 671-675. https://doi.org/10.1038/nmeth.2089

Seefeldt, L. C., Hoffman, B. M., & Dean, D. R. (2009). Mechanism of Mo-Dependent Nitrogenase. *Annual Review of Biochemistry*, *78*(1), 701-722. https://doi.org/10.1146/annurev.biochem.78.070907.103812

Shao, Z., & Luo, Y. W. (2022). Controlling factors on the global distribution of a representative marine non-cyanobacterial diazotroph phylotype (Gamma A). *Biogeosciences*, *19*(11), 2939-2952. https://doi.org/10.5194/bg-19-2939-2022

Shao, Z., Xu, Y., Wang, H., Luo, W., Wang, L., Huang, Y., Agawin, N. S. R., Ahmed, A., Benavides, M., Bentzon-Tilia, M., Berman-Frank, I., Berthelot, H., Biegala, I. C., Bif, M. B., Bode, A., Bonnet, S., Bronk, D. A., Brown, M. V., Campbell, L., . . . Luo, Y. W. (2023). Global oceanic diazotroph database version 2 and elevated estimate of global oceanic N_2 fixation. *Earth Syst. Sci. Data*, *15*(8), 3673-3709. https://doi.org/10.5194/essd-15-3673-2023

Shi, T., Ilikchyan, I., Rabouille, S., & Zehr, J. P. (2010). Genome-wide analysis of diel gene expression in the unicellular N_2-fixing cyanobacterium *Crocosphaera watsonii* WH 8501. *The ISME journal*, *4*(5), 621-632.

Shiozaki, T., Bombar, D., Riemann, L., Hashihama, F., Takeda, S., Yamaguchi, T., Ehama, M., Hamasaki, K., & Furuya, K. (2017). Basin scale variability of active diazotrophs and nitrogen fixation in the North Pacific, from the tropics to the subarctic Bering Sea. *Global Biogeochemical Cycles*, *31*(6), 996-1009.

Shiozaki, T., Fujiwara, A., Inomura, K., Hirose, Y., Hashihama, F., & Harada, N. (2020). Biological nitrogen fixation detected under Antarctic sea ice. *Nature geoscience*, *13*(11), 729-732.

Shiozaki, T., Kondo, Y., Yuasa, D., & Takeda, S. (2018). Distribution of major diazotrophs in the surface water of the Kuroshio from northeastern Taiwan to

south of mainland Japan. *Journal of Plankton Research*, *40*(4), 407-419. https://doi.org/10.1093/plankt/fby027

Shiozaki, T., Nagata, T., Ijichi, M., & Furuya, K. (2015). Nitrogen fixation and the diazotroph community in the temperate coastal region of the northwestern North Pacific. *Biogeosciences*, *12*(15), 4751-4764.

Sintes, E., & Del Giorgio, P. A. (2010). Community heterogeneity and single-cell digestive activity of estuarine heterotrophic nanoflagellates assessed using lysotracker and flow cytometry. *Environmental Microbiology*, *12*(7), 1913-1925.

Stal, L. J. (2009). Is the distribution of nitrogen-fixing cyanobacteria in the oceans related to temperature? *Environ Microbiol*, *11*(7), 1632-1645. https://doi.org/10.1111/j.1758-2229.2009.00016.x

Standeren, E. (2018). *Cell-and genome size responses to different temperatures in haptophytes*

Stoecker, D. K., Hansen, P. J., Caron, D. A., & Mitra, A. (2017). Mixotrophy in the marine plankton. *Annual Review of Marine Science*, *9*, 311-335.

Strock, J. (2008). Ammonification. In *Encyclopedia of ecology, five-volume set* (pp. 162-165). Elsevier Inc.

Suzuki, S., Kawachi, M., Tsukakoshi, C., Nakamura, A., Hagino, K., Inouye, I., & Ishida, K. I. (2021). Unstable Relationship Between *Braarudosphaera bigelowii* (= *Chrysochromulina parkeae*) and Its Nitrogen-Fixing Endosymbiont. *Front Plant Sci*, *12*, 749895. https://doi.org/10.3389/fpls.2021.749895

Tang, W., & Cassar, N. (2019). Data-driven modeling of the distribution of diazotrophs in the global ocean. *Geophysical Research Letters*, *46*(21), 12258-12269.

Team, R. C. (2022). *R: A Language and Environment for Statistical Computing. R Foundation for Statistical Computing, Vienna. https://www.R-project.org*. In

Thamdrup, B. (2012). New pathways and processes in the global nitrogen cycle. *Annual Review of Ecology, Evolution, and Systematics*, *43*, 407-428.

Thompson, A., Carter, B. J., Turk-Kubo, K., Malfatti, F., Azam, F., & Zehr, J. P. (2014). Genetic diversity of the unicellular nitrogen-fixing cyanobacteria UCYN-A and its prymnesiophyte host. *Environmental Microbiology*, *16*(10), 3238-3249. https://doi.org/10.1111/1462-2920.12490

Thompson, A. W., Foster, R. A., Krupke, A., Carter, B. J., Musat, N., Vaulot, D., Kuypers, M. M. M., & Zehr, J. P. (2012). Unicellular Cyanobacterium Symbiotic with a Single-Celled Eukaryotic Alga. *Science*, *337*(6101), 1546-1550. https://doi.org/10.1126/science.1222700

Tripp, H. J., Bench, S. R., Turk, K. A., Foster, R. A., Desany, B. A., Niazi, F., Affourtit, J. P., & Zehr, J. P. (2010). Metabolic streamlining in an open-ocean nitrogen-fixing cyanobacterium. *464*(7285), 90-94. https://doi.org/10.1038/nature08786

Tuit, C., Waterbury, J., & Ravizza, G. (2004). Diel variation of molybdenum and iron in marine diazotrophic cyanobacteria. *Limnology and Oceanography*, *49*(4), 978-990. https://doi.org/10.4319/lo.2004.49.4.0978

Turk, K., Rees, A. P., Zehr, J. P., Pereira, N., Swift, P., Shelley, R., Lohan, M., Woodward, E. M. S., & Gilbert, J. (2011). Nitrogen fixation and nitrogenase (*nifH*) expression

in tropical waters of the eastern North Atlantic. *The ISME journal*, *5*(7), 1201-1212. https://doi.org/10.1038/ismej.2010.205

Turk-Kubo, K. A., Connell, P., Caron, D., Hogan, M. E., Farnelid, H. M., & Zehr, J. P. (2018). In situ diazotroph population dynamics under different resource ratios in the North Pacific Subtropical Gyre. *Frontiers in Microbiology*, *9*, 1616.

Turk-Kubo, K. A., Farnelid, H. M., Shilova, I. N., Henke, B., & Zehr, J. P. (2017). Distinct ecological niches of marine symbiotic N_2-fixing cyanobacterium *Candidatus Atelocyanobacterium thalassa* sublineages. *Journal of Phycology*, *53*(2), 451-461. https://doi.org/10.1111/jpy.12505

Turk-Kubo, K. A., Gradoville, M. R., Cheung, S., Cornejo-Castillo, F., Harding, K. J., Morando, M., Mills, M., & Zehr, J. P. (2022). Non-cyanobacterial diazotrophs: Global diversity, distribution, ecophysiology, and activity in marine waters. *FEMS Microbiol Rev*. https://doi.org/10.1093/femsre/fuac046

Turk-Kubo, K. A., Henke, B. A., Gradoville, M. R., Magasin, J. D., Church, M. J., & Zehr, J. P. (2023). Seasonal and spatial patterns in diazotroph community composition at Station ALOHA. *Frontiers in Marine Science*, *10*, 1130158.

Turk-Kubo, K. A., Mills, M. M., Arrigo, K. R., van Dijken, G., Henke, B. A., Stewart, B., Wilson, S. T., & Zehr, J. P. (2021). UCYN-A/haptophyte symbioses dominate N_2 fixation in the Southern California Current System. *ISME Communications*, *1*(1), 1-13.

Unrein, F., Gasol, J. M., Not, F., Forn, I., & Massana, R. (2014). Mixotrophic haptophytes are key bacterial grazers in oligotrophic coastal waters. *The ISME journal*, *8*(1), 164.

Van de Graaf, A. A., Mulder, A., de Bruijn, P., Jetten, M., Robertson, L. A., & Kuenen, J. G. (1995). Anaerobic oxidation of ammonium is a biologically mediated process. *Applied and Environmental Microbiology*, *61*(4), 1246-1251.

Van Mooy, B. A. S., Fredricks, H. F., Pedler, B. E., Dyhrman, S. T., Karl, D. M., Koblížek, M., Lomas, M. W., Mincer, T. J., Moore, L. R., Moutin, T., Rappé, M. S., & Webb, E. A. (2009). Phytoplankton in the ocean use non-phosphorus lipids in response to phosphorus scarcity. *458*(7234), 69-72. https://doi.org/10.1038/nature07659

Verberk, W. C., Atkinson, D., Hoefnagel, K. N., Hirst, A. G., Horne, C. R., & Siepel, H. (2021). Shrinking body sizes in response to warming: explanations for the temperature–size rule with special emphasis on the role of oxygen. *Biological Reviews*, *96*(1), 247-268.

Vitousek, P. M., Cassman, K., Cleveland, C., Crews, T., Field, C. B., Grimm, N. B., Howarth, R. W., Marino, R., Martinelli, L., Rastetter, E. B., & Sprent, J. I. (2002). Towards an ecological understanding of biological nitrogen fixation. *Biogeochemistry*, *57*(1), 1-45. https://doi.org/10.1023/A:1015798428743

Wang, W.-L., Moore, J. K., Martiny, A. C., & Primeau, F. W. (2019). Convergent estimates of marine nitrogen fixation. *Nature*, *566*(7743), 205-211.

Ward, B. (2012). The global nitrogen cycle. *Fundamentals of geobiology*, 36-48.

Ward, B. A., Dutkiewicz, S., Moore, C. M., & Follows, M. J. (2013). Iron, phosphorus, and nitrogen supply ratios define the biogeography of nitrogen fixation. *Limnology and Oceanography*, *58*(6), 2059-2075.

Ward, B. A., & Follows, M. J. (2016). Marine mixotrophy increases trophic transfer efficiency, mean organism size, and vertical carbon flux. *Proceedings of the National Academy of Sciences*, *113*(11), 2958-2963. https://doi.org/10.1073/pnas.1517118113

Ward, B. B., Arp, D. J., & Klotz, M. G. (2011). *Nitrification*. American Society for Microbiology Press.

Waterbury, & Rippka. (1989). Subsection I. Order *Chroococcaloes*. *Bergey's manual of systematic bacteriology*, *3*, 1728 -1746.

Webb, E. A., Ehrenreich, I. M., Brown, S. L., Valois, F. W., & Waterbury, J. B. (2009). Phenotypic and genotypic characterization of multiple strains of the diazotrophic cyanobacterium, *Crocosphaera watsonii*, isolated from the open ocean. *11*(2), 338-348. https://doi.org/10.1111/j.1462-2920.2008.01771.x

Webb, E. A., Foster, R. A., Villareal, T., Waterbury, J. B., & Zehr, J. P. (2022). *Trichodesmium*. In *Bergey's Manual of Systematics of Archaea and Bacteria* (pp. 1-12). https://doi.org/https://doi.org/10.1002/9781118960608.gbm00448.pub2

Welschmeyer, N. A. (1994). Fluorometric analysis of chlorophyll a in the presence of chlorophyll b and pheopigments. *Limnology and Oceanography*, *39*(8), 1985-1992. https://doi.org/10.4319/lo.1994.39.8.1985

Whittaker, S., Bidle, K. D., Kustka, A. B., & Falkowski, P. G. (2011). Quantification of nitrogenase in *Trichodesmium* IMS 101: implications for iron limitation of nitrogen fixation in the ocean. *Environ Microbiol Rep*, *3*(1), 54-58. https://doi.org/10.1111/j.1758-2229.2010.00187.x

Wilson, Foster, R. A., Zehr, J. P., & Karl, D. M. (2010). Hydrogen production by *Trichodesmium erythraeum Cyanothece* sp. and *Crocosphaera watsonii*. *Aquatic Microbial Ecology*, *59*(2), 197-206.

Wilson, Tozzi, S., Foster, R. A., Ilikchyan, I., Kolber, Z. S., Zehr, J. P., & Karl, D. M. (2010). Hydrogen Cycling by the Unicellular Marine Diazotroph *Crocosphaera watsonii* Strain WH8501. *76*(20), 6797-6803. https://doi.org/10.1128/aem.01202-10

Wilson, S. T., Aylward, F. O., Ribalet, F., Barone, B., Casey, J. R., Connell, P. E., Eppley, J. M., Ferrón, S., Fitzsimmons, J. N., Hayes, C. T., Romano, A. E., Turk-Kubo, K. A., Vislova, A., Armbrust, E. V., Caron, D. A., Church, M. J., Zehr, J. P., Karl, D. M., & Delong, E. F. (2017). Coordinated regulation of growth, activity and transcription in natural populations of the unicellular nitrogen-fixing cyanobacterium *Crocosphaera*. *Nature Microbiology*, *2*(9), 17118. https://doi.org/10.1038/nmicrobiol.2017.118

Wilson, S. T., Böttjer, D., Church, M. J., & Karl, D. M. (2012). Comparative assessment of nitrogen fixation methodologies, conducted in the oligotrophic North Pacific Ocean. *Appl Environ Microbiol*, *78*(18), 6516-6523. https://doi.org/10.1128/aem.01146-12

Zehr, J. P., Bench, S. R., Carter, B. J., Hewson, I., Niazi, F., Shi, T., Tripp, H. J., & Affourtit, J. P. (2008). Globally Distributed Uncultivated Oceanic N_2-Fixing Cyanobacteria Lack Oxygenic Photosystem II. *322*(5904), 1110-1112. https://doi.org/10.1126/science.1165340

Zehr, J. P., Bench, S. R., Mondragon, E. A., McCarren, J., & DeLong, E. F. (2007). Low genomic diversity in tropical oceanic N_2-fixing cyanobacteria. *Proceedings of the National Academy of Sciences*, *104*(45), 17807-17812. https://doi.org/doi:10.1073/pnas.0701017104

Zehr, J. P., & Bombar, D. (2015). Marine nitrogen fixation: organisms, significance, enigmas, and future directions. *Biological Nitrogen Fixation*, 855-872.

Zehr, J. P., & Capone, D. G. (2023). Unsolved mysteries in marine nitrogen fixation. *Trends Microbiol*. https://doi.org/10.1016/j.tim.2023.08.004

Zehr, J. P., Foster, R. A., Waterbury, J., & Webb, E. A. (2022). *Crocosphaera*. In *Bergey's Manual of Systematics of Archaea and Bacteria* (pp. 1-9). https://doi.org/https://doi.org/10.1002/9781118960608.gbm01517

Zehr, J. P., & Kudela, R. M. (2011). Nitrogen Cycle of the Open Ocean: From Genes to Ecosystems. *Annual Review of Marine Science*, *3*(1), 197-225. https://doi.org/10.1146/annurev-marine-120709-142819

Zehr, J. P., & McReynolds, L. A. (1989). Use of degenerate oligonucleotides for amplification of the *nifH* gene from the marine cyanobacterium *Trichodesmium thiebautii*. *Appl Environ Microbiol*, *55*(10), 2522-2526. https://doi.org/10.1128/aem.55.10.2522-2526.1989

Zehr, J. P., Mellon, M. T., & Zani, S. (1998). New nitrogen-fixing microorganisms detected in oligotrophic oceans by amplification of nitrogenase (*nifH*) genes. *Appl. Environ. Microbiol.*, *64*(9), 3444-3450.

Zehr, J. P., Shilova, I. N., Farnelid, H. M., Muñoz-Marín, M. D. C., & Turk-Kubo, K. A. (2017). Unusual marine unicellular symbiosis with the nitrogen-fixing cyanobacterium UCYN-A. *Nature Microbiology*, *2*(1), 16214. https://doi.org/10.1038/nmicrobiol.2016.214

Zehr, J. P., Waterbury, J. B., Turner, P. J., Montoya, J. P., Omoregie, E., Steward, G. F., Hansen, A., & Karl, D. M. (2001). Unicellular cyanobacteria fix N_2 in the subtropical North Pacific Ocean. *Nature*, *412*(6847), 635-638. https://doi.org/10.1038/35088063

Zhang, R., Zhang, D., Chen, M., Jiang, Z., Wang, C., Zheng, M., Qiu, Y., & Huang, J. (2019). N_2 fixation rate and diazotroph community structure in the western tropical North Pacific Ocean. *Acta Oceanologica Sinica*, *38*(12), 26-34. https://doi.org/10.1007/s13131-019-1513-4

Figures

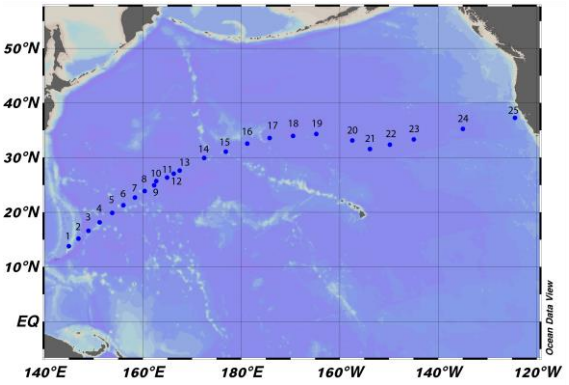

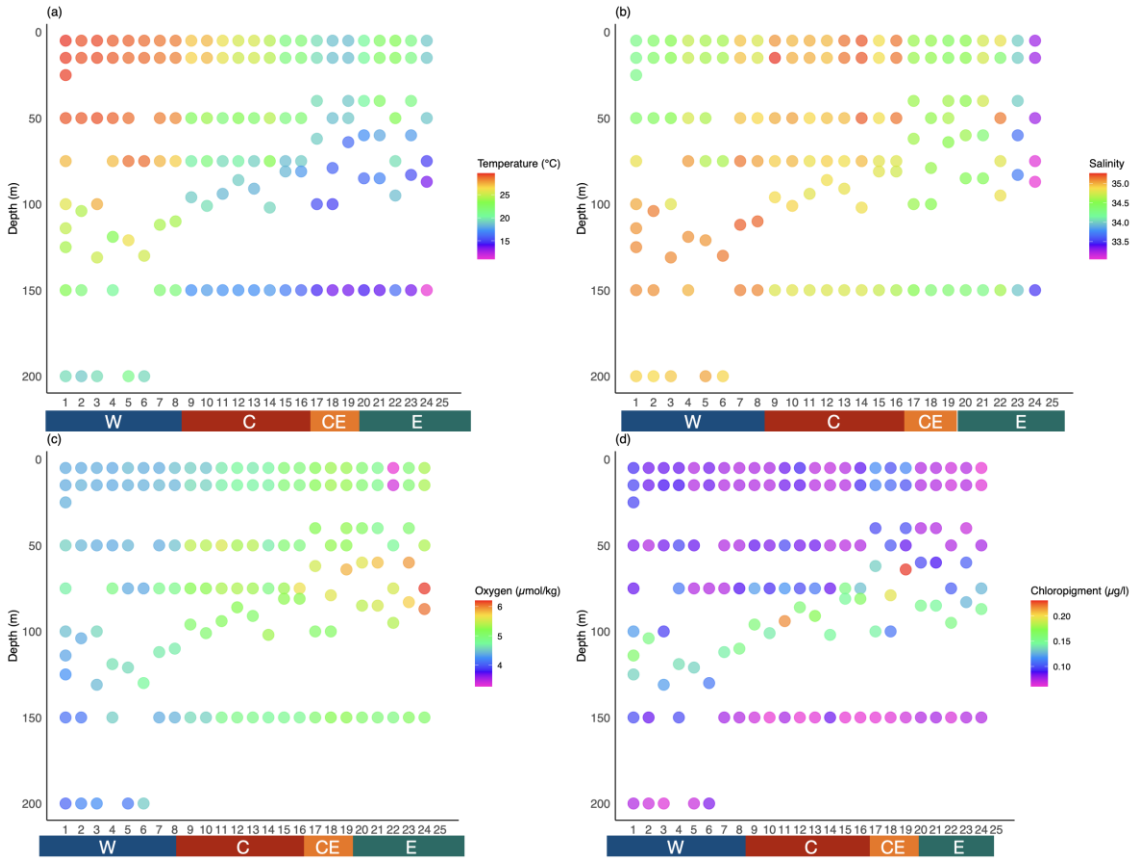

Figure 1. (a) Station map of the transect. (b), (c), (d), and (e) temperature, salinity, oxygen, and chlorophyll at each station and depth; warmer colors denote higher values, while colder

colors indicate lower values. Bars below panels delineate hydrographic regions of the transect, defined based on hydrography: W represents the western region (stations 1–8), C represents the central region (stations 9–16), CE represents the central east region (stations 17-19), and E represents the eastern region (stations 20–24). The delineation of hydrographic regions along the transect was achieved through a hierarchical clustering approach based on measured parameters, with the optimal number of clusters determined using the silhouette method as detailed in the methodology section.

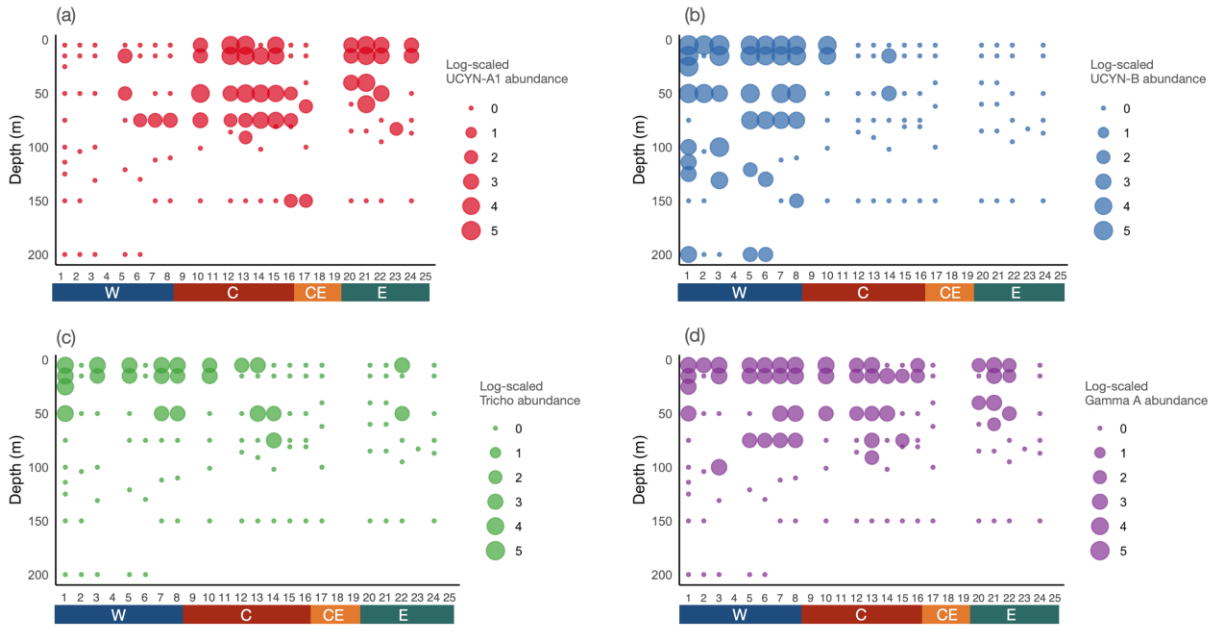

Figure 2. *nifH* gene abundance of (a) UCYN-A1, (b) UCYN-B, (c) *Trichodesmium*, and (d) gamma A at all stations/depths. The log abundances are represented by the size of the bubbles, with 0 denoting samples below detection limits. The bars below the figure indicate different regions of the transect, defined based on hydrography, as explained in Figure 1.

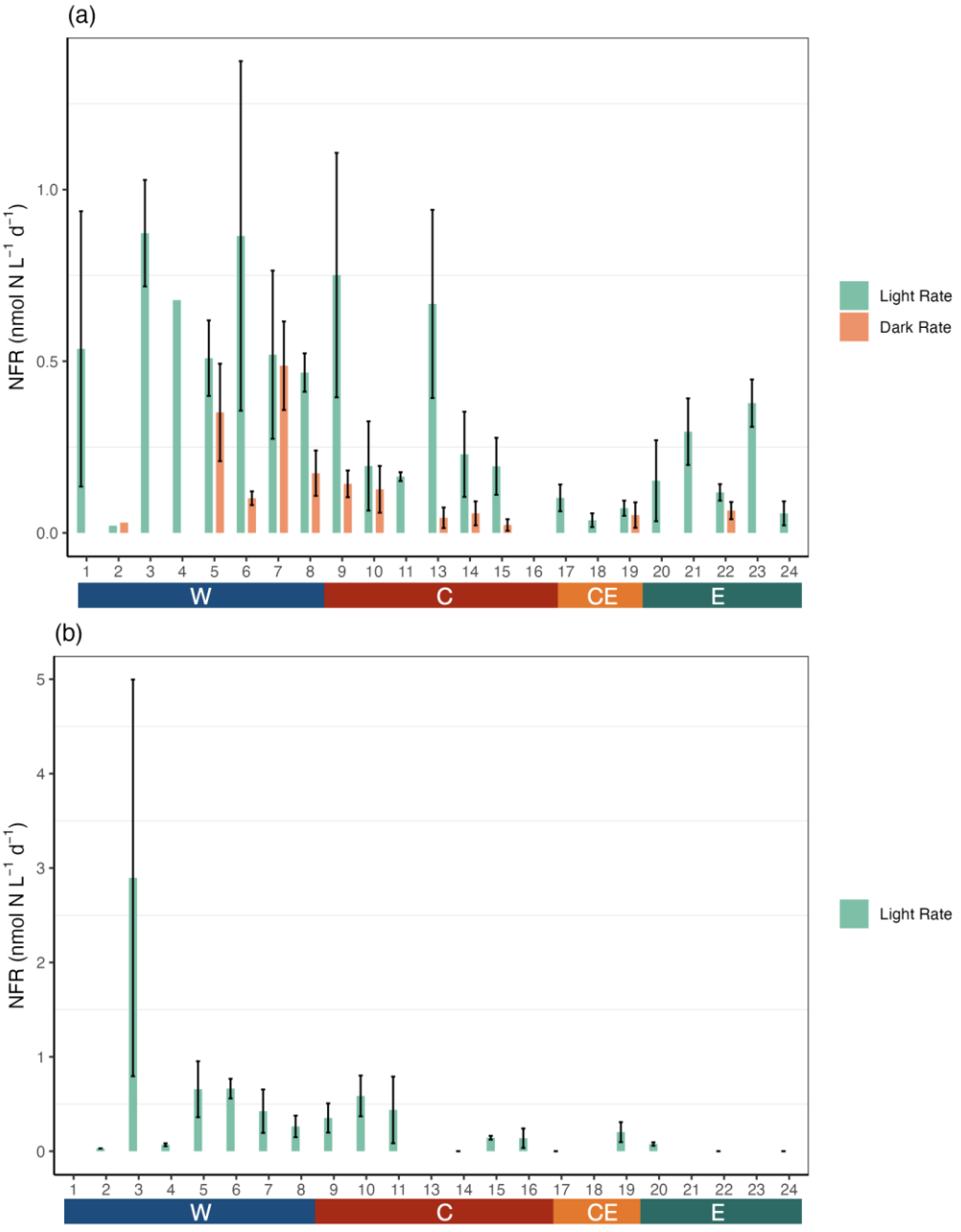

Figure 3. Nitrogen fixation rates (NFR) measured at each station at (a) 15 m and (b) the deep chlorophyll maximum (DCM). Each bar represents the mean NFR, with error bars indicating standard deviation. Green bars denote the 24-hour NFR incubated under a light/dark cycle, referred to as “light”, while orange bars represent the 24-hour dark rates

(determined for 15m samples only). W represents the western region (stations 1–8), C represents the central region (stations 9–16), CE represents the central east region (stations 17-19), and E represents the eastern region (stations 20–24).

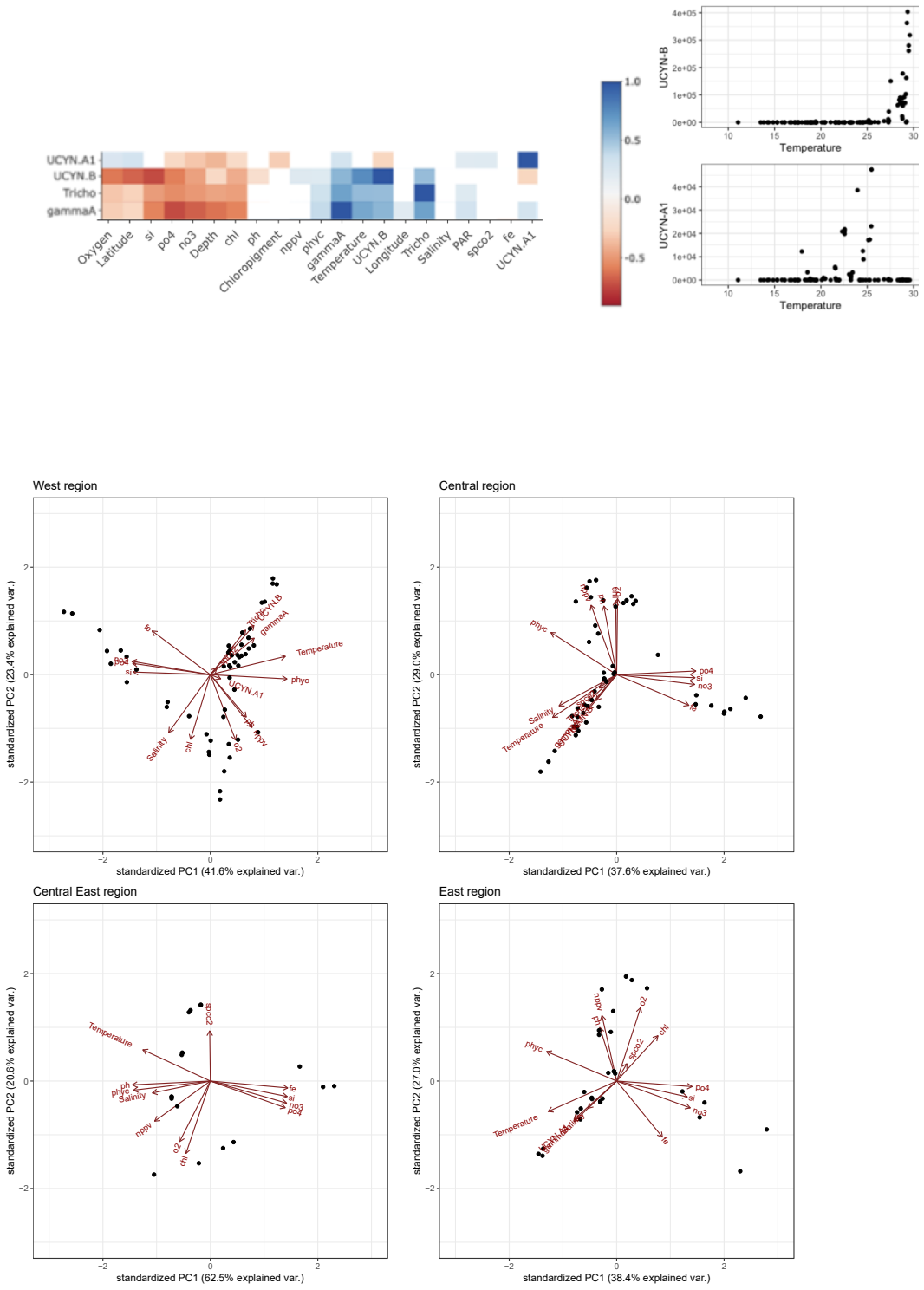

Figure 4. (a) Correlations between diazotroph *nifH* gene abundances and environmental factors across all samples. Blue indicates a positive correlation, while red signifies a

negative correlation, and darker shades represent stronger correlations. This heatmap only includes correlations with p-values < 0.05. (b) *nifH* gene abundance of *Crocosphaera* and UCYN-A1 as a function of temperature. (c) Principal component analysis of environmental influences, grouped by region, with a focus on the UCYN-A1, UCYN-B, *Trichodesmium*, and gamma A. Each panel corresponds to a distinct region, with the axes representing the two principal components that capture the most significant variations in the dataset. Arrows denote the environmental factors; their direction and length indicate the influence of each variable on the principal components.

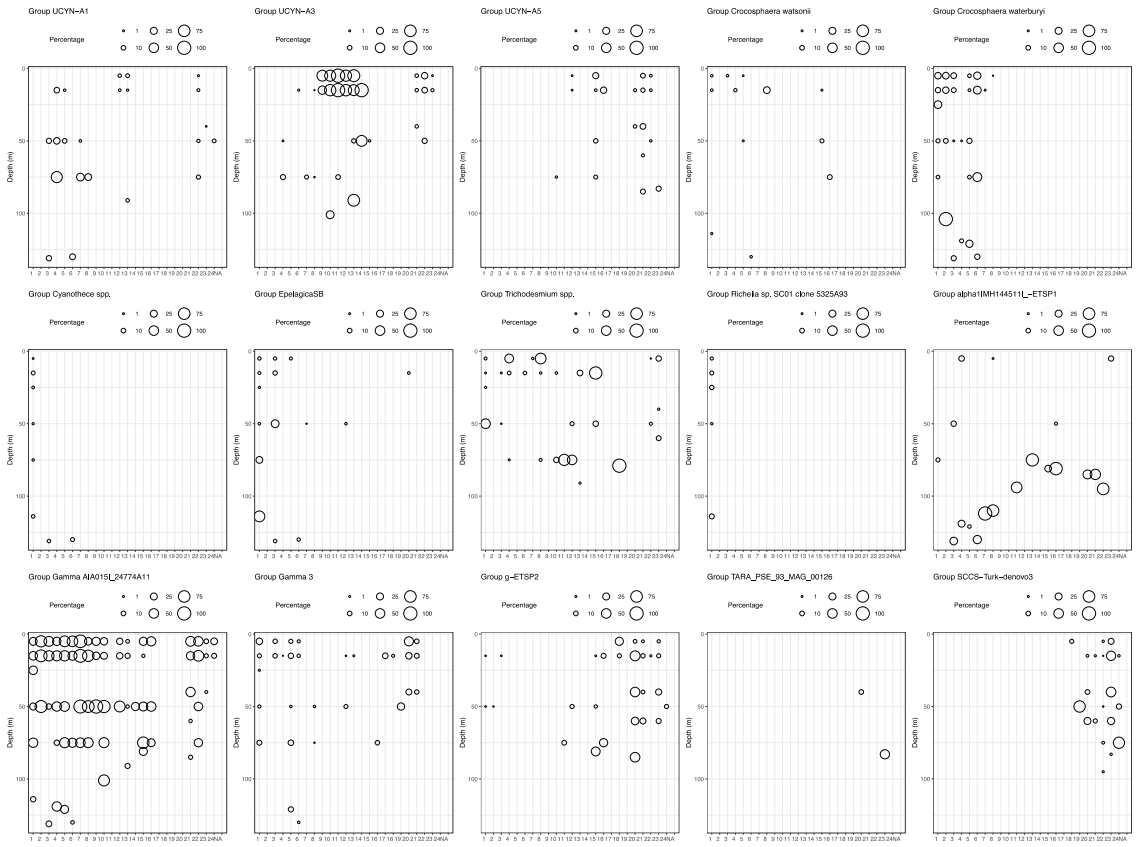

Figure 5. Relative abundances of the top 20 most abundant *nifH* groups based on ASV classifications, along with *Crocosphaera watsonii*, across different stations and depths. Bubble size indicates the percentage of *nifH* gene sequences in each sample assigned to each taxon.

Supplemental Table 1. Correlations between ddPCR-based diazotroph nifH gene abundance and selected environmental variables, as determined using the Spearman rank correlation method. Only correlations with a coefficient greater than 0.5 and adjusted p-values less than 0.05 are displayed. In the table, “Tricho” is *Trichodesmium*, "chl" refers to Chlorophyll-a, "Fe" indicates dissolved iron, "PO_4" represents phosphate, "phyc" is the concentration of phytoplankton expressed as carbon in seawater, "Si" indicates silicate, "nppv" denotes the net primary production of biomass expressed as carbon, and "spCO2" represents the surface partial pressure of carbon dioxide. The environmental data was sourced from the Mercator-Pisces Biogeochemistry Daily Forecast (Pisces model) from the Simons Collaborative Marine Atlas Project (CMAP) as detailed in Ashkezari et al., 2021 and Aumont et al., 2015.

	Variable 1	Variable 2	Correlation	p-value	Adjusted p-value
rho189	gammaA	nppv	0.57584325	0.01556213	0.03734911
rho2	gammaA	Oxygen	-0.5647456	0.01817824	0.04251859
rho51	gammaA	phyc	0.77806658	0.00023523	0.00094092
rho204	gammaA	PO_4	-0.856983	1.11E-05	5.79E-05
rho13	gammaA	Si	-0.6991502	0.00178923	0.00609664
rho166	gammaA	Latitude	-0.660925	0.00386987	0.01186761
rho95	gammaA	Temperature	0.71641312	0.00121487	0.00435459
rho21	Tricho	Temperature	0.61039102	0.0092601	0.02530482

rho203	UCYN-B	Temperature	0.89044915	1.67E-06	1.52E-05
rho50	Tricho	Oxygen	-0.5652752	0.01804607	0.04251859
rho177	Tricho	PO_4	-0.7085844	0.00145283	0.0050757
rho4	Tricho	gammaA	0.69427448	0.00198665	0.00668679
rho99	UCYN-A1	nppv	-0.5652752	0.01804607	0.04251859
rho44	UCYN-A1	spco2	0.62631426	0.007146	0.02076101
rho169	UCYN-A1	UCYN-B	-0.6254419	0.00725074	0.02084587
rho208	UCYN-B	chl	-0.7751984	0.00025668	0.00101206
rho52	UCYN-B	nppv	0.71482898	0.00126022	0.00445925
rho33	UCYN-B	Oxygen	-0.6860163	0.00236158	0.00766819
rho133	UCYN-B	phyc	0.59546214	0.01166897	0.03067272
rho256	UCYN-B	PO_4	-0.5858579	0.01346444	0.03397337
rho146	UCYN-B	Si	-0.8383119	2.64E-05	0.00012552
rho103	UCYN-B	gammaA	0.61985246	0.0079514	0.02216754
rho90	UCYN-B	Latitude	-0.8877051	1.99E-06	1.52E-05

Supplementary Table 2. Grazing and Growth Rates of Crocosphaera at Stations 2, 4, 6, 7, 8, and 10.Rates were determined using the classical dilution method. The table showcases the measured grazing rate, growth rate, and the associated p-value for statistical significance. Significant grazing rates ($p<0.05$) are observed at Stations 6 and 8, as indicated by their p-values. At other stations, grazing rates were not found to be statistically significant (n.s.).

Station	Grazing rate	Growth rate	p-value
2	0.26 ± 0.39	0.49 ± 0.27	n.s
4	0.08 ± 0.16	0.49 ± 0.11	n.s
6	1.29 ± 0.45	-0.99 ± 0.31	0.03
7	0.15 ± 0.75	-0.37 ± 0.51	n.s
8	1.15 ± 0.39	1.45 ± 0.27	0.02
10	-0.9 ± 0.33	0.51 ± 0.21	n.s